



Calhoun: The NPS Institutional Archive

Theses and Dissertations

Thesis Collection

2005-09

Modeling, simulation and performance analysis of multiple-input multiple-output (MIMO) systems with multicarrier time delay diversity modulation



Calhoun is a project of the Dudley Knox Library at NPS, furthering the precepts and goals of open government and government transparency. All information contained herein has been approved for release by the NPS Public Affairs Officer.

Dudley Knox Library / Naval Postgraduate School
411 Dyer Road / 1 University Circle
Monterey, California USA 93943

<http://www.nps.edu/library>



NAVAL POSTGRADUATE SCHOOL

MONTEREY, CALIFORNIA

THESIS

**MODELING, SIMULATION AND PERFORMANCE
ANALYSIS OF MULTIPLE-INPUT MULTIPLE-OUTPUT
(MIMO) SYSTEMS WITH MULTICARRIER TIME DELAY
DIVERSITY MODULATION**

by

Muhammad Shahid

September 2005

Thesis Advisor:

Second Reader:

Frank Kragh

Tri Ha

Approved for public release; distribution is unlimited

THIS PAGE INTENTIONALLY LEFT BLANK

REPORT DOCUMENTATION PAGE		Form Approved OMB No. 0704-0188	
Public reporting burden for this collection of information is estimated to average 1 hour per response, including the time for reviewing instruction, searching existing data sources, gathering and maintaining the data needed, and completing and reviewing the collection of information. Send comments regarding this burden estimate or any other aspect of this collection of information, including suggestions for reducing this burden, to Washington headquarters Services, Directorate for Information Operations and Reports, 1215 Jefferson Davis Highway, Suite 1204, Arlington, VA 22202-4302, and to the Office of Management and Budget, Paperwork Reduction Project (0704-0188) Washington DC 20503.			
1. AGENCY USE ONLY (Leave blank)	2. REPORT DATE September 2005	1. AGENCY USE ONLY (Leave blank)	
4. TITLE AND SUBTITLE: Modeling, Simulation and Performance Analysis of Multiple-Input Multiple-Output (MIMO) Systems with Multicarrier Time Delay Diversity Modulation		5. FUNDING NUMBERS	
6. AUTHOR(S) Muhammad Shahid			
7. PERFORMING ORGANIZATION NAME(S) AND ADDRESS(ES) Naval Postgraduate School Monterey, CA 93943-5000		8. PERFORMING ORGANIZATION REPORT NUMBER	
9. SPONSORING / MONITORING AGENCY NAME(S) AND ADDRESS(ES) N/A		10. SPONSORING/MONITORING AGENCY REPORT NUMBER	
11. SUPPLEMENTARY NOTES The views expressed in this thesis are those of the author and do not reflect the official policy or position of the Department of Defense or the U.S. Government.			
12a. DISTRIBUTION / AVAILABILITY STATEMENT Approved for public release; distribution is unlimited		12b. DISTRIBUTION CODE	
13. ABSTRACT (maximum 200 words) This thesis investigates the fundamentals of multiple-input single-output (MISO) and multiple-input multiple-output (MIMO) radio communication systems with space-time codes. A MISO system and MIMO systems were designed using multicarrier delay diversity modulation (MDDM). MDDM was incorporated with orthogonal frequency division multiplexing (OFDM). The design was implemented with binary phase shift keying (BPSK). Matlab was used to simulate the design, which was tested in both an additive white Gaussian noise (AWGN) channel and in a slow fading frequency nonselective multipath channel with AWGN. The receiver design was incorporated with the maximal ratio combiner (MRC) receiving technique with perfect knowledge of channel state information (CSI). The theoretical performance was derived for both channels and was compared with the simulated results.			
14. SUBJECT TERMS Multiple-input Single-output (MISO), Multiple-input Multiple-output (MIMO), Orthogonal Frequency Division Multiplexing (OFDM), Binary Phase Shift Keying, Rayleigh Fading Channel, Maximal Ratio Combining (MRC), Spatial Diversity		15. NUMBER OF PAGES 119	
		16. PRICE CODE	
17. SECURITY CLASSIFICATION OF REPORT Unclassified	18. SECURITY CLASSIFICATION OF THIS PAGE Unclassified	17. SECURITY CLASSIFICATION OF REPORT Unclassified	18. SECURITY CLASSIFICATION OF THIS PAGE UL

NSN 7540-01-280-5500

Standard Form 298 (Rev. 2-89)
Prescribed by ANSI Std. Z39-18

THIS PAGE INTENTIONALLY LEFT BLANK

Approved for public release; distribution is unlimited

**MODELING, SIMULATION AND PERFORMANCE ANALYSIS OF
MULTIPLE-INPUT MULTIPLE-OUTPUT (MIMO) SYSTEMS WITH
MULTICARRIER DELAY DIVERSITY MODULATION (MDDM)**

Muhammad Shahid
Squadron Leader, Pakistan Air Force
B.S., NED University Karachi, Pakistan, 1993

Submitted in partial fulfillment of the
requirements for the degree of

MASTER OF SCIENCE IN ELECTRICAL ENGINEERING

from the

**NAVAL POSTGRADUATE SCHOOL
September 2005**

Author: Muhammad Shahid

Approved by: Frank Kragh
Thesis Advisor

Tri Ha
Second Reader

Jeffrey B. Knorr
Chairman, Department of Electrical and Computer Engineering

THIS PAGE INTENTIONALLY LEFT BLANK

ABSTRACT

This thesis investigates the fundamentals of multiple-input single-output (MISO) and multiple-input multiple-output (MIMO) radio communication systems with space-time codes. A MISO system and MIMO systems were designed using multicarrier delay diversity modulation (MDDM). MDDM was incorporated with orthogonal frequency division multiplexing (OFDM). The design was implemented with binary phase shift keying (BPSK). Matlab was used to simulate the design, which was tested in both an additive white Gaussian noise (AWGN) channel and in a slow fading frequency nonselective multipath channel with AWGN. The receiver design was incorporated with the maximal ratio combiner (MRC) receiving technique with perfect knowledge of channel state information (CSI). The theoretical performance was derived for both channels and was compared with the simulated results.

THIS PAGE INTENTIONALLY LEFT BLANK

TABLE OF CONTENTS

I.	INTRODUCTION.....	1
A.	BACKGROUND	1
B.	OBJECTIVE AND METHODOLOGY.....	2
C.	RELATED RESEARCH.....	2
D.	THESIS ORGANIZATION.....	2
II.	MIMO SYSTEMS AND MULTICARRIER DELAY DIVERSITY	5
A.	MULTIPLE-INPUT MULTIPLE-OUTPUT (MIMO) SYSTEMS.....	5
1.	Single-Input Single-Output System.....	5
2.	Single-Input Multiple-Output System.....	6
3.	Multiple-Input Single-Output System.....	7
4.	Multiple-Input Multiple-Output System	8
B.	SPACE TIME CODING	12
C.	MULTICARRIER DELAY DIVERSITY IN MIMO SYSTEMS.....	13
D.	ORTHOGONAL FREQUENCY DIVISION MULTIPLEXING	15
1.	Generation of OFDM.....	19
2.	Cyclic Guard Interval.....	20
E.	THE MULTIPATH AND FADING CHANNEL	21
1.	Flat Rayleigh Fading Channel	23
2.	Maximal-Ratio Combining	29
F.	SUMMARY	37
III.	MULTICARRIER DELAY DIVERSITY MODULATION TRANSMITTER AND RECEIVER MODELS	39
A.	THE MULTICARRIER DELAY DIVERSITY MODULATION SCHEME	39
B.	MDDM TRANSMITTER	40
1.	Binary Information Source and M PSK Modulator	40
2.	OFDM Modulator	40
3.	Cyclic Delay Addition	42
4.	Guard Interval (Cyclic Prefix) Addition.....	42
5.	Digital to Analog Conversion and RF Modulation	43
C.	MDDM RECEIVER	43
D.	SUMMARY	47
IV.	ANALYSIS AND SIMULATION OF MULTICARRIER DELAY DIVERSITY MODULATION SCHEME.....	49
A.	SIMULATION OF MDDM TRANSMITTER.....	51
B.	SIMULATION OF MDDM RECIVER.....	52
C.	SIMULATION AND PERFORMANCE ANALYSIS OF MDDM IN AWGN.....	53
1.	Performance Analysis of MISO System with Two Transmit and One Receive Antenna	54

2.	Performance Analysis of MIMO System with Two Transmit and Two Receive Antennas	60
3.	Performance Analysis of MIMO System with Two Transmit and Three Receive Antennas.....	62
D.	SIMULATION AND PERFORMANCE ANALYSIS OF MDDM IN A MULTIPATH FADING CHANNEL	65
1.	Performance Analysis of MISO System with Two Transmit and One Receive Antenna	67
2.	Performance Analysis of MIMO System with Two Transmit and Two Receive Antennas	72
3.	Performance Analysis of MIMO System with Two Transmit and Three Receive Antennas.....	77
E.	SUMMARY	82
V.	CONCLUSION	83
A.	RESULTS	83
B.	RECOMMENDATION FOR FUTURE RESEARCH.....	83
APPENDIX	MATLAB CODES	85
A.	SIMULATION OF THE MDDM IN AN AWGN CHANNEL.....	85
B.	COMPUTING THEORETICAL BER OF THE MDDM IN AN AWGN CHANNEL.....	87
C.	SIMULATION OF THE MDDM IN FREQUENCY NONSELECTIVE SLOW FADING RAYLEIGH CHANNEL	88
D.	COMPUTING THEORETICAL BER OF THE MDDM IN FREQUENCY NONSLECECTIVE SLOW FADING RAYLEIGH CHANNEL.....	92
E.	FUNCTIONS TO INTERPOLATE PROBABILITY DISTRIBUTION FUNCTIONS	93
	LIST OF REFERENCES.....	95
	INITIAL DISTRIBUTION LIST	99

LIST OF FIGURES

Figure 1	SISO System (After Ref. [7]).....	6
Figure 2	SIMO System (After Ref. [7])	6
Figure 3	MISO System (After Ref. [7])	8
Figure 4	MIMO System (After Ref. [7]).....	8
Figure 5	Frequency Spectrum of (a) FDM vs (b) OFDM (After Ref. [14]).....	16
Figure 6	OFDM Symbols with Guard Intervals.....	21
Figure 7	MRC for BPSK with Time Diversity (After Ref. [8, 15])	31
Figure 8	MRC for BPSK for Space Diversity (After Ref. [8, 15])	37
Figure 9	Block Diagram of MDDM Transmitter (After Ref. [2]).....	40
Figure 10	Orthogonal Frequency Division Multiplexing Modulator.....	41
Figure 11	Assignment of Subcarriers at the Input of IFFT Block (After Ref. [20])	42
Figure 12	Block Diagram of MDDM Receiver.....	44
Figure 13	Orthogonal Frequency Division Multiplexing Demodulator.....	45
Figure 14	BPSK Correlation Demodulator for MIMO System with MDDM	53
Figure 15	Simulation of MDDM MIMO System in AWGN	54
Figure 16	Results of MDDM MISO System in AWGN	59
Figure 17	Results of MDDM MIMO System in AWGN.....	62
Figure 18	Results of MDDM MIMO System in AWGN.....	65
Figure 19	Simulation of MDDM MIMO System in Multipath.....	66
Figure 20	Simulation of Channel Response.....	66
Figure 21	Results of MDDM MISO System in Slow Rayleigh Fading Channel.....	72
Figure 22	Results of MDDM MIMO System in Slow Rayleigh Fading Channel	77
Figure 23	Results of MDDM MIMO System in Slow Rayleigh Fading Channel	82

THIS PAGE INTENTIONALLY LEFT BLANK

LIST OF TABLES

Table 1	Assignment of OFDM Subcarriers (After IEEE 802.16a standard, Ref. [20]).....	41
Table 2	BPSK Modulation Scheme (After Ref. [8]).....	49
Table 3	Demodulation of BPSK Signal (After Ref. [8]).....	53

THIS PAGE INTENTIONALLY LEFT BLANK

LIST OF ACRONYMS

AWGN	Additive White Gaussian Noise
BER	Bit Error Rate
BPSK	Binary Phase–Shift Keying
CSI	Channel State Information
DFT	Discrete Fourier Transform
FECC	Forward Error Correction Coding
FFT	Fast Fourier Transform
IDFT	Inverse Discrete Fourier Transform
IFFT	Inverse Fast Fourier Transform
IID	Independent Identically Distributed
LOS	Line of Sight
MDDM	Multicarrier Delay Diversity Modulation
MIMO	Multiple–Input Multiple–Output
MISO	Multiple-Input Single-Output
MRC	Maximal-Ratio Combining
OFDM	Orthogonal Frequency Division Multiplexing
SISO	Single–Input Single–Output
SNR	Signal-to-Noise Ratio
STBC	Space Time Block Code
STTC	Space Time Trellis Code

THIS PAGE INTENTIONALLY LEFT BLANK

ACKNOWLEDGMENTS

I would like to express my sincere thanks to my advisor Professor Frank Kragh for his support, professional guidance and patience during this research. Without his help, this thesis would not have been possible.

I thank my wife Shazia for the sacrifice, love and support that she has made during the course of my studies at the Naval Postgraduate School.

THIS PAGE INTENTIONALLY LEFT BLANK

EXECUTIVE SUMMARY

In modern military and commercial wireless communications, the demand for high speed and reliable communication within the constraints of limited radio frequency spectrum and power, are the prime technical criteria for communication systems. To obtain a higher data rate at an acceptable bit error rate, larger bandwidth is required. To mitigate severe fading channel conditions, a higher transmitted power level is required. Multiple-input multiple-output (MIMO) communication systems have the potential to provide increased capacity and reliability without increasing the bandwidth or transmitted power. MIMO systems exploit time and spatial diversities by employing multiple antennas at the transmitter and receiver. MIMO systems may help to enhance the robustness of military communication systems under the worst operating conditions.

Multicarrier communication in the form of orthogonal frequency division multiplexing (OFDM) has been adopted in several wireless communications standards due to its ability to mitigate severe multipath conditions, its bandwidth efficiency and its simplicity of implementation. The combination of OFDM and MIMO technologies holds the promise of increasing future communications demands.

The main objective of this thesis was to investigate the fundamentals of MIMO systems with a multicarrier delay diversity modulation (MDDM) technique. A simple model was designed to incorporate MDDM in multiple-input single-output (MISO) and MIMO systems. This design was simulated and analyzed to demonstrate its performance. The system was implemented with binary phase shift keying (BPSK) in Matlab and was tested in both an additive white Gaussian noise (AWGN) channel with no fading and a slow multipath fading channel with AWGN. The receiver design was based on the maximal ratio combining (MRC) technique with the assumption of perfect knowledge of channel state information (CSI) at the receiver end. The simulated performance results and theoretical analysis results were compared with the conventional single-input single-output (SISO) system results. The performance metric of bit error probability versus

E_b / N_0 (energy per bit to noise power spectral density ratio) was used. To establish a fair comparison, the transmitted power for the SISO, MISO and MIMO systems was maintained equal.

The results showed that the designed MISO and MIMO system performed within expected parameters of the theoretical analysis in both the AWGN channel with no fading and the multipath fading channel with AWGN. The comparison of performances in the AWGN channel with no fading showed that the MISO system performed better than the SISO system for low E_b / N_0 values up to 6.5 dB and the performance of the MISO system was poorer for higher E_b / N_0 values. The performances of the MIMO systems were better than that of the SISO system for all values of E_b / N_0 and all systems studies herein. The MIMO systems with two receive antennas and three receive antennas outperformed a SISO system by 1.7 dB and 3.4 dB less transmit power required respectively for equal performance. For the multipath fading channel with AWGN, the MISO and MIMO systems were able to achieve significant advantage over a SISO system.

I. INTRODUCTION

A. BACKGROUND

One of the major challenges facing modern communications is to satisfy the ever increasing demand of high speed reliable communications with the constraints of extremely limited frequency spectrum and limited power. Wireless communications systems like cellular mobile communications, internet and multimedia services require very high capacity to fulfill the demand of high data rates. These systems must achieve the desired reliability within the limits of power and frequency spectrum availability, often in severe channel environments. They need to overcome signal scattering and multipath effects, especially in densely populated urban areas. For many military communication systems, reliable communication is to be achieved with low probability of detection and interception even in hostile jamming environments.

The solutions to achieve high capacity with reliability could include time, frequency and space diversity. Wireless communication systems with multiple transmit and multiple receive antennas can provide high capacity at low probability of bit error with extremely low power, even in dense scattering and multipath environments. These multiple-input multiple-output (MIMO) systems with appropriate space-time codes have been an area of recent research as they hold the promise of ever increasing data rates. The capacity of a MIMO system can be increased linearly by increasing the number of transmit and receive antennas. The applications of MIMO systems in a frequency selective channel require equalization and other techniques to compensate for frequency selectivity of the channel, which add to the complexity of these systems. In recent years, orthogonal frequency division multiplexing (OFDM) has been widely used in communications systems to operate in frequency selective channels including several wireless communication standards. Communication systems with a MIMO-OFDM combination can significantly improve capacity and reliability by exploiting the robustness of OFDM to fading, enhanced by adding more diversity gain via space time codes. In this research, delay diversity in combination with a MIMO-OFDM system is the primary focus and is referred to as multicarrier delay diversity modulation (MDDM).

[1, 2]

B. OBJECTIVE AND METHODOLOGY

The main objective of this research was to investigate MIMO-OFDM systems by using a cyclic delay diversity technique as a space time code and compare its performance to conventional single-input single-output (SISO) systems. The first step to achieve the objective was to study the fundamentals of OFDM systems. Then, the OFDM technique was applied to a multiple-input single-output (MISO) system and MIMO systems with cyclic delay diversity. A MISO system and two MIMO systems, using a MDDM scheme with two transmit antennas, were simulated in Matlab with one, two and three receive antennas, respectively. Multicarrier delay diversity was implemented with binary phase shift keying (BPSK) and was realized in equivalent baseband form to facilitate comparison with published theory. The design was simulated both with an additive white Gaussian noise (AWGN) channel with no fading and then with a multipath faded channel with AWGN. Theoretical performance and simulated system performance were compared with reference to the single-input single-output (SISO) system.

C. RELATED RESEARCH

MIMO systems promise high efficiency in providing low probability of bit error without increasing the transmitted power or the bandwidth [1]. Therefore, research in this area has been very active during recent years. The performance of MIMO systems applying techniques such as delay diversity, space-time block codes (STBC) and space-time trellis codes (STTC) has led to the development of several practical systems [1, 2]. Numerous studies have been performed to realize and investigate the performance of these systems. Space time codes were originally developed for flat fading channels. Later, incorporation of OFDM in these systems has provided a solution to communications in the frequency selective channel [1]. Delay diversity was the first diversity technique introduced for MIMO systems and was described in [3] and [4]. The use of delay diversity with OFDM was proposed in [5] for a flat fading channel and a cyclic delay diversity approach with OFDM was recommended for the frequency selective fading channel in [6] which has been further investigated in [2].

D. THESIS ORGANIZATION

This thesis is organized in five chapters. Chapter II introduces the fundamentals of MIMO systems and the multicarrier delay diversity modulation scheme. It discusses

the capacity of MIMO systems, space time coding and use of time delay diversity as a space time coding technique in MIMO systems. Chapter III describes the modeling and simulation of the MDDM transmitter and receiver. Chapter IV analyzes the performance of this modulation technique both in an AWGN channel with no fading and in a slow fading multipath channel with AWGN. Chapter V reviews the summary of the work done with results and includes recommendations for future study. Matlab code is attached as an Appendix.

THIS PAGE INTENTIONALLY LEFT BLANK

II. MIMO SYSTEMS AND MULTICARRIER DELAY DIVERSITY

The objective of this chapter is to establish the basic understanding of MIMO systems, space time coding and the application of MDDM in MIMO systems. An overview of the MIMO model is presented. The fundamentals of OFDM and its implementations with the discrete Fourier transform (DFT) are discussed. Then, the implementation of cyclic delay diversity with OFDM within the context of MIMO systems is presented. Finally, the multipath flat fading channel and the maximum ratio combining receiver are discussed.

A. MULTIPLE-INPUT MULTIPLE-OUTPUT (MIMO) SYSTEMS

In order to facilitate the understanding of multiple-input multiple-output systems, single-input single-output (SISO) systems, single-input multiple-output (SIMO) systems and multiple-input single-output (MISO) systems models are discussed briefly. In this thesis, all signals and models are represented in complex baseband equivalent form to facilitate analysis.

1. Single-Input Single-Output System

The SISO system model is shown in Figure 1. The signal transmitted from the antenna is denoted as $x(t)$. The signal received at the receiving end, $r(t)$, passes through the channel with impulse response $h(t)$ in an additive white Gaussian noise (AWGN) environment. It is assumed that the bandwidth of the signal is small enough such that the frequency response of the channel is flat and the channel response can be given as

$$h = |h|e^{i\phi} \quad (2.1)$$

where $i = \sqrt{-1}$. The relationship between the transmitted signal and receive signal is given by

$$\begin{aligned} r(t) &= \int_{-\infty}^{\infty} x(\tau)h(t-\tau)d\tau + n(t) \\ &= \int_{-\infty}^{\infty} x(\tau)|h|e^{i\phi}\delta(t-\tau)d\tau + n(t) \\ &= x(t)h + n(t) \end{aligned} \quad (2.2)$$

where $\delta(t)$ is the Dirac delta function and $n(t)$ is the AWGN. The received signal is the transmitted signal convolved with the channel impulse response plus added noise. [7]

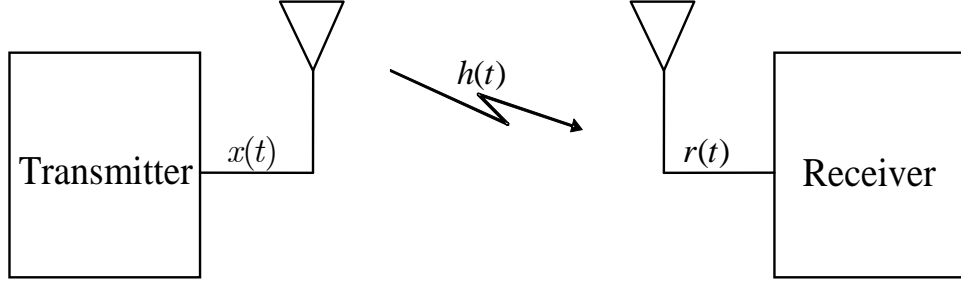


Figure 1 SISO System (After Ref. [7])

2. Single-Input Multiple-Output System

A single-input multiple-output (SIMO) system with one transmit antenna and multiple (J) receive antennas is illustrated in Figure 2.

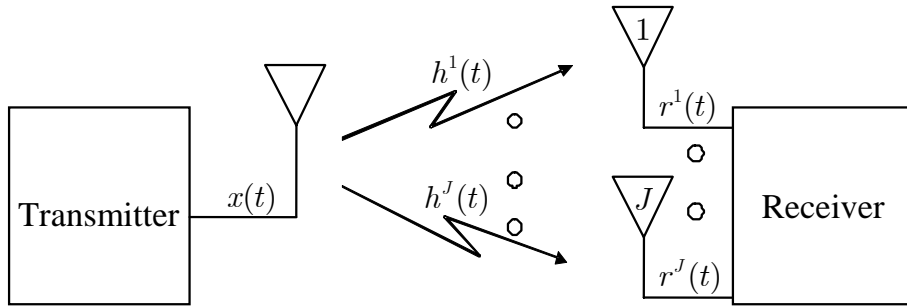


Figure 2 SIMO System (After Ref. [7])

The received signals at the receiver end can be represented as the set of linear equations

$$\begin{aligned} r^1(t) &= h^1(t)x(t) + n^1(t) \\ r^2(t) &= h^2(t)x(t) + n^2(t) \\ &\vdots \\ r^J(t) &= h^J(t)x(t) + n^J(t) \end{aligned} \tag{2.3}$$

where $r^j(t)$, $h^j(t)$ and $n^j(t)$, $j = 1, 2, 3, \dots, J$ represent the received signal, channel impulse response and noise, respectively, at the j^{th} receive antenna. If $x(t)$, $h(t)$ and $r(t)$ are sampled at the rate of one sample per symbol, then they can be represented as x , h , r . The received signal can also be represented in form of vectors.

$$\mathbf{x} = \begin{bmatrix} x^1 & x^2 & \dots & x^J \end{bmatrix}^T \quad \text{for} \quad x^1 = x^2 = \dots = x^J \quad (2.4)$$

$$\mathbf{h} = \begin{bmatrix} h^1 & h^2 & \dots & h^J \end{bmatrix}^T$$

$$\mathbf{n} = \begin{bmatrix} n^1 & n^2 & \dots & n^J \end{bmatrix}^T \quad (2.5)$$

Now, the received vector is represented as

$$\mathbf{r} = \mathbf{h} \cdot \mathbf{x} + \mathbf{n} \quad (2.6)$$

where \mathbf{x} , \mathbf{h} and \mathbf{n} are transmission, channel and noise vectors, respectively and operator '.' denotes element by element multiplication.

3. Multiple-Input Single-Output System

A multiple-input single-output (MISO) system with multiple (L) transmit antennas and one receive antenna is illustrated in Figure 3. The receive antenna receives a sum of all the signals transmitted by each antenna and can be represented as

$$r = h^1 x^1 + h^2 x^2 + \dots + h^L x^L + n \quad (2.7)$$

where x^l and h^l , $l = 1, 2, 3, \dots, L$ are the transmitted signal and channel response from transmit antenna l to the receive antenna and n is the AWGN. Equation (2.7) can also be written as

$$r = \sum_{l=1}^L h^l x^l + n. \quad (2.8)$$

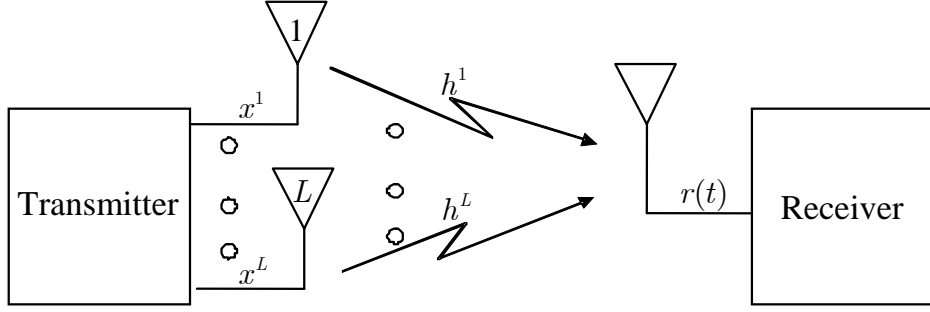


Figure 3 MISO System (After Ref. [7])

4. Multiple-Input Multiple-Output System

A multiple-input multiple-output (MIMO) system with multiple (L) transmit antennas and multiple (J) receive antennas is illustrated in Figure 4. MIMO systems are the focus of this thesis. Therefore, the MIMO model is discussed in detail in this section. The representation of the model is largely based on [1, 8]. For a faded channel, it is assumed that channel responses from each transmit antenna to each receive antenna are independent.

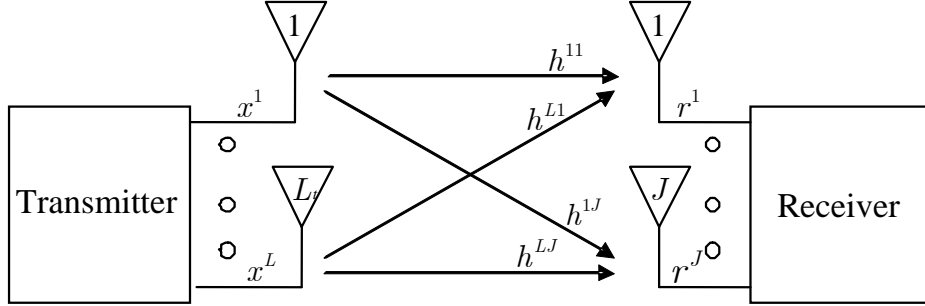


Figure 4 MIMO System (After Ref. [7])

The received signal at any receive antenna is the sum of all the signals transmitted by each transmit antenna passing through the respective channel and the AWGN.

$$\begin{aligned}
r^j &= h^{1j}x^1 + h^{2j}x^2 + \dots + h^{Lj}x^L + n^j \\
&= \begin{bmatrix} h^{1j} & h^{2j} \dots h^{Lj} \end{bmatrix} \begin{bmatrix} x^1 \\ x^2 \\ \vdots \\ x^L \end{bmatrix} + n^j.
\end{aligned} \tag{2.9}$$

h^{lj} is the channel response from transmit antenna l to receive antenna j where $l = 1, 2, 3, \dots, L$ and $j = 1, 2, 3, \dots, J$. The system therefore can be represented in matrix form as

$$\begin{bmatrix} r^1 \\ r^2 \\ \vdots \\ r^J \end{bmatrix} = \begin{bmatrix} h^{11} & h^{21} \dots h^{L1} \\ h^{21} & h^{22} \dots h^{L2} \\ \vdots & \vdots \quad \quad \vdots \\ h^{J1} & h^{J2} \dots h^{JL} \end{bmatrix} \begin{bmatrix} x^1 \\ x^2 \\ \vdots \\ x^L \end{bmatrix} + \begin{bmatrix} n^1 \\ n^2 \\ \vdots \\ n^J \end{bmatrix} \tag{2.10}$$

$$\mathbf{r} = \mathbf{H}\mathbf{x} + \mathbf{n} \tag{2.11}$$

where \mathbf{r} and \mathbf{n} represent the $J \times 1$ received signal and noise column vectors, \mathbf{H} is a $J \times L$ complex channel matrix and \mathbf{x} is the $L \times 1$ transmitted column matrix. [1]

All the elements in the channel matrix are considered independent identically distributed (IID) complex Gaussian random variables (GRVs), and similarly, the elements of the noise vector are also complex Gaussian random variables. According to information theory, the optimum distributions for transmitted signals are also Gaussian. Therefore, it is considered that all elements of \mathbf{x} are zero mean complex GRVs. Therefore, the covariance matrix of the transmitted signals is the same as the autocorrelation matrix and it is a diagonal matrix [1, 8]

$$\begin{aligned}
\mathbf{C}_{\mathbf{xx}} &= \mathbf{R}_{\mathbf{xx}} \\
\mathbf{R}_{\mathbf{xx}} &= \mathbf{E}[\mathbf{xx}^{*T}]
\end{aligned} \tag{2.12}$$

where \mathbf{x}^{*T} denotes the transpose and component-wise complex conjugate of the transmitted matrix \mathbf{x} . [1]

The total transmitted power, P , is the sum of all the diagonal elements of the autocorrelation matrix. To facilitate the analysis for the MIMO system, assume that all the transmit antennas transmit equal power [8].

$$P = E \left[\sum_{l=1}^L |x^l|^2 \right] = \sum_{l=1}^L E \left[|x^l|^2 \right] = \text{tr}(\mathbf{R}_{xx}) \quad (2.13)$$

$$P^l = E \left[|x^l|^2 \right] = \frac{P}{L} \quad (2.14)$$

where P^l is the average power transmitted from antenna l . An AWGN channel is considered, and according to information theory, the optimum distribution for the transmitted signal is also Gaussian [1]. Therefore, the elements of \mathbf{x} as stated in [1] are also considered independent and identically distributed (IID) Gaussian variables with zero mean. Then, the autocorrelation matrix can be written as

$$\mathbf{R}_{xx} = \frac{P}{L} \mathbf{I}_L \quad (2.15)$$

where \mathbf{I}_L is the identity matrix of size $L \times L$.

It is further assumed that the channel matrix is fixed at least for the duration of one symbol period and there is no attenuation due to path loss and no amplification due to antenna gain. In other words, each receive antenna receives the total transmitted power regardless of its branch. Thus, the normalization constraint for the elements of channel matrix \mathbf{H} for fixed coefficient can be represented as [1]

$$\sum_{l=1}^L |h^{jl}|^2 = L \quad \text{for } j = 1, 2, \dots, J. \quad (2.16)$$

For a faded channel, the channel matrix elements are random variables and the normalization constraint will apply to the expected value of Equation (2.16). This normalization constraint is required for a fair comparison with SISO systems with equal power transmitted [8]. It is also assumed that the channel impulse response at that time, referred to as the channel state information (CSI), is perfectly known at the receiver by sending training symbols. [1]

The elements of the noise vector \mathbf{n} are considered IID complex Gaussian random variables with zero mean and the variance of $\sigma_o^2/2$ for both real and imaginary parts. Independence of the noise elements and zero mean imply that the autocorrelation and covariance matrix are the same diagonal matrix. Therefore, the covariance matrix $\mathbf{C}_{\mathbf{nn}}$ of the noise vector can be represented as [1, 8]

$$\mathbf{C}_{\mathbf{nn}} = \mathbf{R}_{\mathbf{nn}} = \mathbb{E}[\mathbf{nn}^{*T}] \quad (2.17)$$

$$\mathbf{R}_{\mathbf{nn}} = \sigma_o^2 \mathbf{I}_L. \quad (2.18)$$

The average signal power at receive antenna j with assumed fixed channel coefficients can be given by [1, 8]

$$\begin{aligned} P_r^j &= \mathbb{E}[r^j r^{j*}] \\ &= \mathbb{E}\left[\sum_{l=1}^L h^{lj} x^l \sum_{m=1}^L h^{mj*} x^{m*}\right] \\ &= \mathbb{E}\left[\sum_{l=1}^L \sum_{m=1}^L h^{lj} x^l h^{mj*} x^{m*}\right] \\ &= \sum_{l=1}^L \sum_{m=1}^L h^{lj} h^{lj*} \mathbb{E}[x^l x^{l*}] \\ &= \sum_{l=1}^L |h^{lj}|^2 \mathbb{E}[|x^l|^2] \end{aligned} \quad (2.19)$$

where $(\cdot)^*$ denotes complex conjugate. Substitution of Equations (2.15) and (2.16) into Equation (2.19) yields

$$P_r^j = \sum_{l=1}^L |h^{lj}|^2 \mathbb{E}[|x^l|^2] = L \frac{P}{L} = P. \quad (2.20)$$

Then, the average signal-to-noise ratio (SNR) at each receive antenna, represented by γ , is given by [1, 8]

$$\gamma = \frac{P}{\sigma_o^2}. \quad (2.21)$$

Similarly, the autocorrelation matrix for the received signal can be represented as [8]

$$\mathbf{R}_{rr} = \mathbb{E}[\mathbf{r}\mathbf{r}^{*T}]. \quad (2.22)$$

$$\begin{aligned} \mathbf{R}_{rr} &= \mathbb{E}[(\mathbf{H}\mathbf{x} + \mathbf{n})(\mathbf{H}\mathbf{x} + \mathbf{n})^{*T}] \\ &= \mathbb{E}[(\mathbf{H}\mathbf{x} + \mathbf{n})((\mathbf{H}\mathbf{x})^{*T} + \mathbf{n}^{*T})] \\ &= \mathbb{E}[\mathbf{H}\mathbf{x}(\mathbf{H}\mathbf{x})^{*T} + \mathbf{H}\mathbf{x}\mathbf{n}^{*T} + \mathbf{n}(\mathbf{H}\mathbf{x})^{*T} + \mathbf{n}\mathbf{n}^{*T}] \\ &= \mathbb{E}[\mathbf{H}\mathbf{x}(\mathbf{H}\mathbf{x})^{*T}] + \mathbb{E}[\mathbf{H}\mathbf{x}\mathbf{n}^{*T}] + \mathbb{E}[(\mathbf{H}\mathbf{x})^{*T}\mathbf{n}] + \mathbb{E}[\mathbf{n}\mathbf{n}^{*T}]. \end{aligned} \quad (2.23)$$

By using the identity of transposition of a product of matrices [9] as follows

$$(\mathbf{H}\mathbf{x})^{*T} = \mathbf{x}^{*T}\mathbf{H}^{*T}. \quad (2.24)$$

Equation (2.23) can be written as

$$\mathbf{R}_{rr} = \mathbb{E}[\mathbf{H}\mathbf{x}\mathbf{x}^{*T}\mathbf{H}^{*T}] + \mathbb{E}[\mathbf{H}\mathbf{x}\mathbf{n}^{*T}] + \mathbb{E}[\mathbf{x}^{*T}\mathbf{H}^{*T}\mathbf{n}] + \mathbb{E}[\mathbf{n}\mathbf{n}^{*T}]. \quad (2.25)$$

If it is assumed that the channel coefficients are deterministic and signal matrix \mathbf{x} and noise matrix \mathbf{n} are independent with zero mean, Equation (2.25) yields

$$\begin{aligned} \mathbf{R}_{rr} &= \mathbf{H}\mathbb{E}[\mathbf{x}\mathbf{x}^{*T}]\mathbf{H}^{*T} + \mathbb{E}[\mathbf{n}\mathbf{n}^{*T}] \\ &= \mathbf{H}\mathbf{R}_{xx}\mathbf{H}^{*T} + \mathbf{R}_{nn}. \end{aligned} \quad (2.26)$$

B. SPACE TIME CODING

Space time coding is a technique to achieve higher diversity at the receiver end to mitigate multipath fading without increasing the transmitted power or bandwidth. Space time coding holds the promise to maximize the system capacity. The system capacity is defined in [1], “The maximum possible transmission rate such that the probability of error is arbitrarily small.” The capacity of SISO system is given by Shannon’s capacity equation [10]

$$\begin{aligned} C &= W \log_2(1 + SNR) \\ C &= W \log_2\left(1 + \frac{P}{\sigma^2}\right) \end{aligned} \quad (2.27)$$

where C , W , P and σ^2 represent capacity, bandwidth, average signal power and average noise power, respectively. The capacity of a MIMO system in a flat fading channel with perfect channel state information is given by [1]

$$C = W \log_2 \left(1 + LJ \frac{P}{\sigma^2} \right). \quad (2.28)$$

Space time coding techniques designed appropriately with MIMO systems have the potential to achieve the channel capacity in Equation (2.28). Space time coding provides the diversity both in time and space to achieve the higher performance at reduced transmitted power and without bandwidth expansion. Space time coding techniques can be classified into two main categories. The first category provides power efficiency without compromising the performance such as delay diversity, space-time block codes (STBC) and space-time turbo trellis codes (STTC). The other category, such as Bell Labs layered space-time technology (BLAST), increases the data rates with the use of bandwidth efficient modulation schemes [2].

The performance of a MIMO system can be further improved by applying forward error correction coding (FEC) with optimum interleaving at the cost of reduced data rate or increased bandwidth. FEC coding gain can be achieved without sacrificing the data rate or bandwidth by designing space time coding technique with higher rate modulation schemes. [1]

This thesis is focused on achieving multicarrier delay diversity gain. The incorporation of error control coding and interleaving is left for future work.

C. MULTICARRIER DELAY DIVERSITY IN MIMO SYSTEMS

The delay diversity technique was the first approach proposed for MIMO systems [2]. In this scheme, delayed versions of the same signal are transmitted by multiple antennas. This simple delay diversity was originally suggested for flat fading channels [11]. This scheme has the inherent problem of increasing frequency selectivity caused by the delay diversity. Full diversity cannot be achieved without equalization [12] and equalization for MIMO systems is very difficult due to the large number of channels. Thus, the receiver design becomes much more complicated. Orthogonal frequency division multiplexing (OFDM) with delay diversity is another approach to make good use of frequency selectivity of the delay diversity. The OFDM scheme with delay diversity has a limitation as an increase in the number of transmit antennas requires an increase in

the guard interval at the expense of bandwidth. If the guard interval is not as large as or larger than the delay spread of the channels, then it will cause inter-symbol interference (ISI) [12].

The OFDM scheme can be easily implemented by using the inverse discrete Fourier transform (IDFT), which can be efficiently computed by the inverse fast Fourier transform (IFFT). The same information can be translated back by the DFT operation. DFT and IDFT as defined in [13] are

$$\text{DFT}\{x[m]\} = X[k] = \sum_{n=0}^{N-1} x[n] e^{-i2\pi kn/N} \quad \text{for } k = 0, 1, 2, \dots, N-1 \quad (2.29)$$

$$\text{IDFT}\{X[k]\} = x[m] = \frac{1}{N} \sum_{k=0}^{N-1} X[k] e^{i2\pi km/N} \quad \text{for } m = 0, 1, 2, \dots, N-1. \quad (2.30)$$

Discrete Fourier transforms have a property that any circular shift in the time domain results in a phase shift in the frequency domain [13]

$$\text{DFT}\{x[(m-D)_N]\} = e^{-i2\pi kD/N} X[k] \quad \text{for } k = 0, 1, 2, \dots, N-1 \quad (2.31)$$

where D denotes the delay in the time index and $(n)_N$ denotes n modulo N . This cyclic delay property of the Fourier transforms can be used in an OFDM system design to induce diversity that can be exploited at the receiver end.

To overcome the problems of a simple time delay diversity scheme in a frequency selective fading channel for MIMO-OFDM systems, a new approach of cyclic delay diversity was suggested in [6]. This simple scheme does not require any additional guard interval with an increasing number of transmit antennas. The combination of cyclic delay diversity and OFDM in MIMO systems has been referred to as multicarrier delay diversity modulation (MDDM) in this thesis and this can be considered a special type of space-time coding. For a frequency selective channel, a cyclic guard interval (cyclic prefix) of duration G is added at the beginning of each OFDM symbol. This guard interval is greater than or equal to the maximum channel delay M to mitigate the intersymbol interference (ISI). The orthogonality of subcarriers is paramount for OFDM. The cyclic prefix converts a linear convolution channel into a circular convolution channel and the interference from the previous symbols will only affect the guard

interval. This restores the orthogonality at the receiver. Adding zeros as the guard interval can alleviate the interference between OFDM symbols. For a flat fading channel, the guard interval can be eliminated to increase the data rate. [2, 22]

The space time code for MDDM can be represented as [2]

$$\begin{pmatrix} x_{N-G} & x_{N-G+1} & \dots & x_{N-1} & x_0 & x_1 & x_2 & \dots & x_{N-1} \\ x_{N-G-1} & x_{N-G} & \dots & x_{N-2} & x_{N-1} & x_0 & x_1 & \dots & x_{N-2} \\ & & \cdot & & & & & & \\ & & \cdot & & & & & & \\ & & \cdot & & & & & & \\ \underbrace{x_{N-G-L+1} \ x_{N-G+2} \ \dots \ x_{N-L}}_{\text{cyclic guard interval}} & \underbrace{x_{N-L+1} \ x_{N-L+2} \ x_{N-L+3} \ \dots \ x_{N-L}}_{\text{data block}} & & & & & & & \end{pmatrix}_{L \times (N+G)} \quad (2.32)$$

where G is the length of the guard interval and N is the number of points in the IDFT.

The MDDM scheme has some advantages over space time block coding (STBC) and space time trellis coding (STTC). STBCs require all block codes be orthogonal and full rate transmission is not achievable for more than two transmit antennas. The complexity of STTC increases exponentially with the number of transmit antennas. STBCs and STTCs are fixed for a combination of transmit and receive antennas and they do not offer any flexibility in changing the number of antennas at either end. For each combination of the number of antennas, a new space-time code is required. These codes were designed for flat fading channels. For frequency selective channels, they cannot be used without equalization and other compensation techniques. However, the MDDM space time code can be used with any combination of transmit and receive antennas with little modification in the receiver design. The MDDM is based upon the OFDM modulation scheme. Therefore, orthogonal frequency division multiplexing fundamentals are discussed very briefly in the following sections. [1, 2]

D. ORTHOGONAL FREQUENCY DIVISION MULTIPLEXING

In conventional sequential data transmission over a single carrier, the data rate has a limit imposed by the availability of frequency spectrum and the delay spread of the channel. The bandwidth required is inversely proportional to the data symbol duration, which means that the highest achievable symbol rate is limited by the available bandwidth [16]. Considering a fixed delay spread of the channel, the ISI also increases

with the increase in the symbol rate as delayed copies of the symbols coming from the multipath can have significant overlap with the original symbol. The lessening of ISI will require equalization which further adds to the complexity of the system [17]. These problems can be mitigated by transmitting the data in parallel on multiple carriers with a reduced data rate on each carrier compared to the overall data rate. The reduced data rate will require reduced bandwidth which should not be more than the coherence bandwidth of the channel to avoid frequency selective fading. This multicarrier system can be designed by classical frequency division multiplexing (FDM) [1]. In this scheme, the carriers need to be well apart in frequency domain to avoid inter-carrier interference. Therefore, a guard frequency band is required between two consecutive subcarriers which makes this scheme highly inefficient in frequency spectrum utilization. This problem can be eliminated by using minimum-spaced orthogonal carriers. In OFDM, all carriers are allowed to overlap by maintaining orthogonality of all the subcarriers, which increases bandwidth efficiency [14]. The comparison of bandwidth efficiency for FDM and OFDM is illustrated in Figure 5.

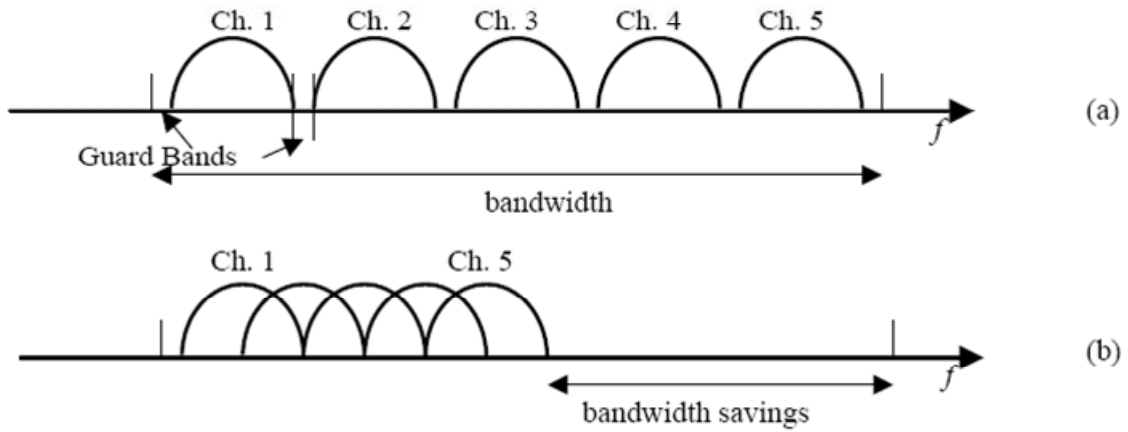


Figure 5 Frequency Spectrum of (a) FDM vs (b) OFDM (After Ref. [14])

In OFDM, to maintain the orthogonality of the subcarrier channels, the correlation between signals transmitted on subcarriers must be zero. Assume that the available bandwidth for the OFDM system is ΔW and it is to be divided in K subcarriers. The

input serial data stream is to be converted into K parallel data streams which are assigned to the K subcarriers [1]. The symbol duration of the input serial data is T_s' with serial data rate of $f_s' = 1/T_s'$. Therefore, if the number of parallel data streams is equal to the number of OFDM subcarriers, the symbol duration for OFDM will be

$$T_s = K T_s'. \quad (2.33)$$

Equation (2.33) indicates that the symbol duration of an OFDM signal is K times larger than that of single serial stream symbol duration. Therefore, the OFDM scheme has the inherited advantage over single carrier modulation techniques to mitigate ISI and frequency selectivity of the channel. The OFDM transmitted signal $S(t)$ can be written as

$$\begin{aligned} S(t) &= \sum_{m=0}^{K-1} A \{ d_{I_m} \cos(2\pi f_m t) - d_{Q_m} \sin(2\pi f_m t) \} \\ &= \sum_{m=0}^{K-1} a_m \left\{ \frac{d_{I_m}}{\sqrt{d_{I_m}^2 + d_{Q_m}^2}} \cos(2\pi f_m t) - \frac{d_{Q_m}}{\sqrt{d_{I_m}^2 + d_{Q_m}^2}} \sin(2\pi f_m t) \right\} \end{aligned} \quad (2.34)$$

where A is a constant, d_{I_m} , d_{Q_m} are the information-bearing components of the signal and $a_m = A \sqrt{(d_{I_m}^2 + d_{Q_m}^2)}$.

Using the trigonometric identity

$$\cos(\alpha + \beta) = \cos(\alpha) \cos(\beta) - \sin(\alpha) \sin(\beta) \quad (2.35)$$

$S(t)$ can be written as

$$\begin{aligned} S(t) &= \sum_{m=0}^{K-1} a_m \cos(2\pi f_m t + \theta_m) \\ &= \sum_{m=0}^{K-1} a_m \{ \cos(2\pi f_m t) \cos(\theta_m) - \sin(2\pi f_m t) \sin(\theta_m) \} \end{aligned} \quad (2.36)$$

where $\theta_m = \tan^{-1}\left(\frac{d_{Q_m}}{d_{I_m}}\right)$. The correlation between any two symbols transmitted on separate subcarriers, represented as R_{ij} , must be equal to zero to maintain the orthogonality of subcarriers [1].

$$\begin{aligned} R_{ij} &= \int_{-\infty}^{+\infty} s_i(t)s_j(t)dt \\ &= \int_0^{T_s} a_i \cos(2\pi f_i t + \theta_i t) a_j \cos(2\pi f_j t + \theta_j t) dt \end{aligned} \quad (2.37)$$

Using the trigonometric identity

$$\cos(\alpha)\cos(\beta) = \frac{1}{2}\cos(\alpha + \beta) + \frac{1}{2}\cos(\alpha - \beta). \quad (2.38)$$

Equation (2.37) can be written as

$$R_{ij} = \frac{a_i a_j}{2} \int_0^{T_s} \left(\cos(2\pi(f_i + f_j)t + (\theta_i + \theta_j)t) + \cos(2\pi(f_i - f_j)t + (\theta_i - \theta_j)t) \right) dt \quad (2.39)$$

where a_i , a_j , θ_i and θ_j are constant for the symbol duration.

For $2\pi(f_i + f_j) \gg \frac{1}{T_s}$, Equation (2.39) can be written as

$$R_{ij} = \frac{a_i a_j}{2} \int_0^{T_s} \cos(2\pi(f_i - f_j)t + (\theta_i - \theta_j)t) dt. \quad (2.40)$$

From Equation (2.40), $R_{ij} = 0$ if

$$\begin{aligned} (f_i - f_j)T_s &= M \text{ where } M \in \text{set of positive integers} \\ \Rightarrow f_i - f_j &= M / T_s. \end{aligned} \quad (2.41)$$

Therefore, minimum frequency separation between two consecutive subcarriers to maintain orthogonality must be

$$\Delta f = \frac{1}{T_s} = f_s \quad (2.42)$$

where f_s is the rate of OFDM symbols.

1. Generation of OFDM

From the earlier discussion of orthogonality in an OFDM signal, all subcarriers are orthogonal to one another and the center frequencies of any two subcarriers differ by a positive integer multiple of Δf . In spite of the overlapping of subcarrier frequency bands, the transmitted symbol can be recovered at the receiver end without any interference due to zero correlation of these subcarriers. In OFDM, serial data symbols are converted to parallel to form one OFDM symbol to be assigned to K subcarriers. Now, the bandpass signal can be represented as

$$S(t) = \sum_{m=0}^{K-1} A \left\{ d_{I_m} \cos(w_m t) - d_{Q_m} \sin(w_m t) \right\} \quad (2.43)$$

where the subcarrier frequencies $w_m = 2\pi f_m$ and $f_m = f_0 + m\Delta f$. The equation (2.43) can be written as

$$\begin{aligned} S(t) &= \text{Re} \left\{ \sum_{m=0}^{K-1} A(d_{I_m} + i d_{Q_m}) e^{i w_m t} \right\} \\ &= \text{Re} \left\{ \sum_{m=0}^{K-1} d[m] e^{i w_m t} \right\} \\ &= \text{Re} \left\{ \sum_{m=0}^{K-1} d[m] e^{i(2\pi(f_0 + m\Delta f)t)} \right\} \\ &= \text{Re} \left\{ \sum_{m=0}^{K-1} d[m] e^{i2\pi n \Delta f t} e^{i2\pi f_0 t} \right\} \\ &= \text{Re} \left\{ \sum_{m=0}^{K-1} \tilde{D}(t) e^{i2\pi f_0 t} \right\} \end{aligned} \quad (2.44)$$

where $d[m] = A d_{I_m} + i A d_{Q_m}$ and the complex envelope of the transmitted signal is denoted by

$$\tilde{D}(t) = \sum_{m=0}^{K-1} d[m] e^{i2\pi m \Delta f t}. \quad (2.45)$$

Matched filters or correlation demodulators can be used at the receiver end to recover the symbol for each subcarrier. Subsequently, for the implementation of this scheme, K modulators and K matched filters are required. As the number of subcarriers

increases, the complexity of the system also increases. For a large number of subcarriers, the complexity of the system makes it impractical. [1]

For making this scheme more practical, consider sampling the complex envelope signal \tilde{D} at the rate of K/T_s , i.e., the sampling interval is T_s/K . Now using Equation (2.42), Equation (2.45) can be represented as

$$\begin{aligned}\tilde{D}\left[\frac{MT_s}{K}\right] &= \sum_{m=0}^{K-1} d[m]e^{i2\pi m \Delta f MT_s / K} \\ &= \sum_{m=0}^{K-1} d[m]e^{i2\pi m MT_s / T_s K} \\ &= \sum_{m=0}^{K-1} d[m]e^{i2\pi m M / K}.\end{aligned}\tag{2.46}$$

Comparison of Equations (2.30) and (2.46) clearly yields that the right side of Equation (2.46) is the IDFT of $d[m]$ scaled by K .

$$\tilde{D} = K \text{IDFT}\{d[m]\}\tag{2.47}$$

Equation (2.47) facilitates the implementation of an OFDM system by taking the IDFT of the original data stream. Therefore, implementation of the OFDM scheme is completely digital. The complexity of the system is decreased as compared to the multi-oscillator based OFDM modulation technique. Even for large K , IDFT/DFT can be efficiently implemented by using fast Fourier transforms (FFT) which make computation much faster. [1]

Similarly, the receiver performs the FFT operation on the received signal to recover the original parallel data. Employing the FFT in the receiver drastically reduces the complexity as compared to employing coherent demodulators. The receiver can separate the subcarriers simply by using baseband signal processing techniques. These subcarrier signals can be integrated for the duration of the symbol period to produce decision variables for the estimation of the transmitted data.

2. Cyclic Guard Interval

As previously discussed, the OFDM modulation technique has the advantage of reducing the ISI caused by a multipath channel. This is achieved by converting serial data

at a high rate into parallel streams each at a lower data rate and increasing the symbol transmission duration on orthogonal carriers. In order to eliminate the ISI completely due to the time delay spread of the multipath channel, a guard interval is added before each OFDM symbol. The length of the guard interval is to be greater than the anticipated delay spread of the channel [1]. This guard interval insertion costs both in terms of power and data rate or bandwidth. If the length of the guard interval is less than the delay spread of the channel, then multiple delayed versions will induce ISI and inter-carrier interference by affecting the orthogonality of the subcarriers due to overlapping of different OFDM symbols [14]. Taking advantage of the cyclic nature of the DFT represented in Equation (2.31), the guard interval can be constructed by some cyclically shifted portion of the OFDM symbol. Therefore, it is referred to as a prefix in the literature. The addition of this cyclic guard interval has already been depicted in the space time code (Equation (2.32)). Additionally, this cyclic prefix also facilitates the synchronization of the carrier frequency and timing to obtain the orthogonality of the subcarriers [12]. The addition of the cyclic guard interval is illustrated in Figure 6.

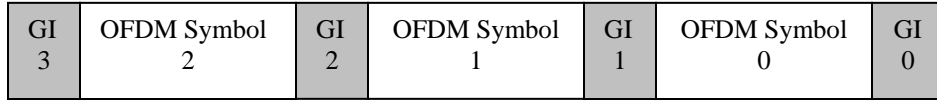


Figure 6 OFDM Symbols with Guard Intervals

E. THE MULTIPATH AND FADING CHANNEL

In terrestrial wireless communications, the line of sight (LOS) path for signal reception is often not available. The signal arriving at the receive antenna is comprised of many replicas of the signal coming from a number of reflectors and scatters present in the medium of transmission. This phenomenon is known as multipath. Even when the LOS path signal is present, the multipath components are usually also present. [15, 16]

In this section, a general view of the multipath channel is presented to understand its nature and a baseband equivalent model is derived for use in simulation. The MDDM technique will be tested in a multipath faded channel for performance analysis and evaluation.

In a multipath channel, the signal travels via several different paths before arriving at the receive antenna. Due to the different path lengths involved, the amplitude and phase of these received replicas are not the same. For example, if a short duration pulse is transmitted in a multipath channel, then a train of pulses of different amplitudes, phases and arrival times, will be received. As a result, the received signal can significantly vary in amplitude and phase and the spectral components of the signal are affected differently by the multipath faded channel. Therefore, the frequency response of the channel may not be flat over the entire bandwidth of the signal. Multipath components of the signal create time-spreading of the signal and cause intersymbol interference. [15, 16]

The channel conditions may not remain constant over time and the media composition (e.g., stratosphere, ionosphere) may also change. Furthermore, the number and position of the reflectors and scatters cannot be considered fixed. In mobile communications, due to the motion of transmitter and receiver, the multipath arrangements can never be assumed constant and Doppler shift in signal frequency proportional to the relative velocity is also observed. Therefore, the multipath fading channel is a time varying channel [15]. Time varying and time spreading aspects of the channel cannot be predicted or calculated precisely. For creating a good model of the channel, these parameters are measured, and based on these measured statistics, the channel can be characterized.

Doppler spread in the signal frequency describes the time varying nature of the channel. The coherence time is inversely proportional to the Doppler shift. The coherence time is the statistical measure over which the channel response does not change significantly. To characterize the channel, the coherence time is compared with the symbol duration. If the coherence time is less than the symbol durations, then the channel is called a fast fading channel. In the case of coherence time greater than the symbol duration, it is described as a slow fading channel. [15, 16]

The multipath delay spread is characterized by the coherence bandwidth. Coherence bandwidth has been defined in [17] as, “a statistical measure over which the frequency response of the channel is considered flat.” If the bandwidth of the signal is

greater than the coherence bandwidth of the channel, then different frequency components will be attenuated differently and the phase variations will also be nonlinear. This type of channel is said to be a frequency selective fading channel. If the coherence bandwidth of the channel is greater than the signal bandwidth, then all the frequency components will face flat fading with almost linear phase changes. This type of channel is said to be a frequency nonselective fading channel. [15, 16]

This fading channel can be modeled statistically as there are a large number of variables affecting the channel response. Most of these variables are random in nature and several probability distributions can be considered to model these random variables [16]. When there are a large number of reflectors and scatters in the physical channel, the cumulative effect of this large number of random variables, as per the central limit theorem, leads to a Gaussian process model for the channel response. In the case of no LOS component present, the process has zero mean with magnitude following the Rayleigh probability distribution and the phase is uniformly distributed on $[-\pi \text{ to } \pi]$. [15, 16]

1. Flat Rayleigh Fading Channel

A slow fading frequency nonselective channel was simulated to test the multicarrier delay diversity modulation scheme. The channel fading gain was kept fixed for the symbol duration to make it a slow fading channel. Considering the no line of sight (LOS) path case, a flat fading channel is usually simulated using a Rayleigh distribution for the magnitude of the channel response [16]. The Rayleigh distribution is a special case of the Ricean distribution with no line of sight component. The probability density function for a Rayleigh random variable can be derived from the Ricean probability density function as defined in [15]

$$f_{A_c}(a_c) = \frac{a_c}{\sigma^2} \exp\left(-\frac{(a_c^2 + \alpha^2)}{2\sigma^2}\right) I_0\left(\frac{\alpha a_c}{\sigma^2}\right) u(a_c) \quad (2.48)$$

where $I_0(\cdot)$ is the modified Bessel function of the first kind of zero order, $u(\cdot)$ is the unit step function and α^2 is the power in the LOS signal component and the average received signal power is

$$\overline{s^2(t)} = \overline{a_c^2} = \alpha^2 + 2\sigma^2 \quad (2.49)$$

$$u(a_c) = \begin{cases} 1 & a_c \geq 0 \\ 0 & a_c < 0. \end{cases} \quad (2.50)$$

For the Rayleigh distribution case, there is no line of sight component so $\alpha = 0$ and $I_0(0) = 1$. Using Equation (2.48), the Rayleigh probability density function can be represented as

$$f_{A_c}(a_c) = \frac{a_c}{\sigma^2} \exp\left(\frac{-a_c^2}{2\sigma^2}\right) u(a_c). \quad (2.51)$$

For the baseband simulation of a Rayleigh random variable, two zero mean independent real Gaussian random variables were summed as $X + jY$ [17]. The magnitude of this complex random quantity is the desired Rayleigh random variable and simulates the magnitude of the channel frequency response. The derivation of the proof that the complex sum of two zero mean Gaussian random variables has magnitude with Rayleigh distribution and phase uniformly distributed in $[-\pi, \pi]$ is largely based on [8].

Let X and Y be two zero mean independent identically distributed (IID) Gaussian random variables and their complex sum is represented by

$$Z = X + iY. \quad (2.52)$$

As Z is to simulate the frequency response of a Rayleigh flat fading channel, it can be written as

$$Z = h e^{i\theta} \quad (2.53)$$

$$V = |Z|^2 = X^2 + Y^2. \quad (2.54)$$

Since X and Y are zero mean IID Gaussian random variables (GRVs)

$$\overline{X} = \overline{Y} = 0 \quad (2.55)$$

$$\sigma_X^2 = \sigma_Y^2 = \sigma^2. \quad (2.56)$$

The random variable V is a sum of two squared zero mean GRVs and is called a central chi-squared random variable of degree 2. The probability density function for a central chi-squared random variable of degree n can be given as [16]

$$f_v(v) = \frac{1}{\sigma^n 2^{n/2} \Gamma\left(\frac{n}{2}\right)} v^{(n/2)-1} e^{-v/2\sigma^2} u(v) \quad (2.57)$$

where n is the number of independent variables and $\Gamma(\cdot)$ is the gamma function. For a central chi-squared random variable of degree two ($n = 2$), Equation (2.57) can be rewritten as

$$f_v(v) = \frac{1}{2\sigma^2 \Gamma(1)} e^{-v/2\sigma^2} u(v). \quad (2.58)$$

Since

$$\Gamma(1) = (1-1)! = 1, \quad (2.59)$$

[15], the probability density function of V as per Equation (2.58) can be written as

$$f_v(v) = \frac{1}{2\sigma^2} e^{-v/2\sigma^2} u(v). \quad (2.60)$$

The magnitude of the simulated Rayleigh flat faded channel frequency response can be written as

$$h = |Z| = \sqrt{V} \quad (2.61)$$

The probability density function for h can be obtained by transforming the probability density function of V given in Equation (2.58) according to [18]

$$f_H(h) = \frac{1}{|dh/dv|} f_v(v) \Big|_{v=h^2} \quad (2.62)$$

where

$$\frac{dh}{dv} = \frac{1}{2(v)^{1/2}}. \quad (2.63)$$

Substituting Equations (2.60) and (2.63) into Equation (2.62) yields

$$\begin{aligned} f_H(h) &= 2(h^2)^{1/2} \frac{1}{2\sigma^2} e^{-h^2/2\sigma^2} u(h) \\ f_H(h) &= \frac{h}{\sigma^2} e^{-h^2/2\sigma^2} u(h). \end{aligned} \quad (2.64)$$

Comparison of Equations (2.51) and (2.64) clearly indicates that the magnitude of the complex sum of two zero mean IID GRVs follows the Rayleigh distribution. The mean and variance of h as given in [18] are

$$\bar{h} = \sigma \sqrt{\frac{\pi}{2}} \quad (2.65)$$

$$\sigma_h^2 = \sigma^2 \left(2 - \frac{\pi}{2} \right). \quad (2.66)$$

Now, the probability distribution function for the phase, θ , of Z is to be derived.

The phase θ can be represented as [8]

$$\theta = \begin{cases} \tan^{-1}\left(\frac{Y}{X}\right) - \pi & \text{if } -\infty < X < 0 \text{ and } -\infty < Y \leq 0 & \text{(referred to as case A)} \\ \tan^{-1}\left(\frac{Y}{X}\right) & \text{if } 0 < X < \infty \text{ and } -\infty < Y < \infty & \text{(referred to as case B)} \\ \tan^{-1}\left(\frac{Y}{X}\right) + \pi & \text{if } -\infty < X < 0 \text{ and } 0 \leq Y < \infty & \text{(referred to as case C)} \end{cases} \quad (2.67)$$

Let the ratio of zero mean IID GRVs X and Y be defined as [8, 19]

$$R = \frac{Y}{X}. \quad (2.68)$$

The joint probability density function of X and Y can be written as

$$f_{XY}(x, y) = f_X(x)f_Y(y) = f_X(x)f_X(y) \quad (2.69)$$

where

$$f_X(x) = \frac{1}{\sqrt{2\pi\sigma^2}} e^{-x^2/2\sigma^2}. \quad (2.70)$$

For case A, $-\infty < X < 0$ and $-\infty < Y \leq 0$ which implies $-\pi \leq \theta \leq -\pi/2$. The conditional cumulative distribution function of R can be represented as [8, 19]

$$\begin{aligned} F_{R|A}(r) &= \Pr\{R < r|A\} = \Pr\left\{\frac{Y}{X} < r|A\right\} \\ &= \int_{-\infty}^0 \int_{rx}^0 f_{XY|A}(x, y) dy dx \\ &= 4 \int_{-\infty}^0 \int_{rx}^0 f_{XY}(x, y) dy dx \end{aligned} \quad (2.71)$$

where it is noted that

$$f_{XY|A}(x, y) = \begin{cases} 4f_{XY}(x, y) & \text{if } -\infty < x < 0 \text{ and } -\infty < y < 0 \\ 0 & \text{otherwise} \end{cases} \quad (2.72)$$

The conditional probability density function can be obtained by taking the derivative of the conditional cumulative distribution function with respect to random variable r [8, 19]

$$f_{R|A}(r) = \frac{dF_{R|A}(r)}{dr} = 4 \frac{d}{dr} \left[\int_{-\infty}^0 \int_{rx}^0 f_{XY}(x, y) dy dx \right]. \quad (2.73)$$

From Leibniz's rule [8, 19]

$$f_{R|A}(r) = 4 \int_{-\infty}^0 -x f_{XY}(x, rx) dx. \quad (2.74)$$

Substituting Equation (2.69) and (2.70) into Equation (2.74) yields [8, 19]

$$f_{R|A}(r) = -\frac{1}{\pi\sigma^2} \left[\int_{-\infty}^0 e^{-x^2 \left(\frac{1+r^2}{2\sigma^2} \right)} (2x) dx \right]. \quad (2.75)$$

Equation (2.75) can be represented as

$$f_{R|A}(r) = \frac{2}{\pi(1+r^2)} \quad 0 \leq r \leq \infty. \quad (2.76)$$

For case A,

$$\theta = \tan^{-1}(r) - \pi, \quad (2.77)$$

$$\left| \frac{d\theta}{dr} \right| = \frac{1}{1+r^2}. \quad (2.78)$$

The conditional probability density function of θ can be attained from Equation (2.76)

$$f_{\Theta|A}(\theta) = \frac{1}{|d\theta/dr|} f_{R|A}(r) \Big|_{r=\tan(\theta)} \quad (2.79)$$

$$f_{\Theta|A}(\theta) = (1+r^2) \frac{2}{\pi(1+r^2)} \Big|_{r=\tan(\theta)}. \quad (2.80)$$

Equation (2.80) can be written as

$$f_{\Theta|A}(\theta) = \frac{2}{\pi} \quad (2.81)$$

which implies

$$f_{\Theta}(\theta) = \frac{1}{2\pi} \quad \text{for } -\pi \leq \theta \leq \frac{-\pi}{2}. \quad (2.82)$$

Similarly for $0 < X \leq \infty, -\infty \leq Y \leq \infty$ and for $-\infty \leq X < 0, -\infty \leq Y \leq 0$, it can be proven [8] that

$$f_{\Theta|B}(\theta) = \frac{1}{\pi} \quad (2.83)$$

$$f_{\Theta|C}(\theta) = \frac{2}{\pi}. \quad (2.84)$$

Therefore, the unconditional probability density function for the phase θ can be written as

$$\begin{aligned} f_{\Theta}(\theta) &= f_{\Theta|A}(\theta) \Pr(A) + f_{\Theta|B}(\theta) \Pr(B) + f_{\Theta|C}(\theta) \Pr(C) \\ &= \frac{2}{\pi} \left(\frac{1}{4} \right) I_{\left(-\pi, -\frac{\pi}{2} \right]}(\theta) + \frac{1}{\pi} \left(\frac{1}{2} \right) I_{\left(-\frac{\pi}{2}, \frac{\pi}{2} \right]}(\theta) + \frac{2}{\pi} \left(\frac{1}{4} \right) I_{\left(\frac{\pi}{2}, \pi \right]}(\theta) \\ &= \begin{cases} \frac{1}{2\pi} & \text{if } -\pi < \theta \leq \pi \\ 0 & \text{otherwise} \end{cases} \end{aligned} \quad (2.85)$$

where $I(\cdot)$ is the indicator function defined as

$$I_A(x) \equiv \begin{cases} 1 & \text{if } x \in A \\ 0 & \text{otherwise} \end{cases} \quad (2.86)$$

In this section, it was proved that the complex sum of two zero mean IID GRVs gives a complex sum with Rayleigh distributed magnitude and uniformly distributed phase in $(-\pi, \pi]$. Therefore, this model can be used to simulate the frequency response of a multipath flat Rayleigh faded channel.

2. Maximal-Ratio Combining

As stated in previous sections, many wireless communication systems operate in multipath channels and the performance in a multipath channel is often reduced as compared to an AWGN channel. Diversity techniques can be employed to mitigate the effect of multipath. Diversity simply implies the transmission or reception of multiple copies of the same signal. Diversity can be achieved in time, frequency and space domains. It is assumed that all these diversity receptions are independent each with an independent channel response. [15]

For BPSK, the transmitted baseband symbols are defined as

$$\begin{aligned} x_0(t) &= Ae^0 = A & \text{for } 0 \leq t \leq T_c \\ x_1(t) &= Ae^{-i\pi} = -A & \text{for } 0 \leq t \leq T_c \end{aligned} \quad (2.87)$$

where T_c is the symbol duration in each time diversity and A is the peak amplitude of the BPSK signal. The energy for each time diversity reception, E , can be given as [16]

$$E = \int_0^{T_c} |x_k(t)|^2 dt = A^2 T_c \quad \text{for } k = 0, 1. \quad (2.88)$$

For time diversity, it is assumed that each received diversity signal passes through an independent faded channel and can be represented as

$$r_l(t) = h_l e^{i\theta_l} x_k(t) + n_l(t) \quad \text{for } 0 \leq t \leq T_c, k = 0, 1 \quad (2.89)$$

where l represents the number of the diversity reception and $n_l(t)$ is the complex valued AWGN with the circularly symmetric probability density function. The power spectral density function for $n_l(t)$ is

$$S_{nn}(f) = N_o \quad (2.90)$$

where the power spectral density functions for the real and imaginary components of $n_l(t)$ are

$$S_{\text{Re}[n]\text{Re}[n]}(f) = S_{\text{Im}[n]\text{Im}[n]}(f) = \frac{N_0}{2}. \quad (2.91)$$

For all the diversity receptions, the received signal can be written as

$$r(t) = \sum_{l=1}^L \left[h_l e^{-i\theta_l} x_k(t) + n_l(t) \right]. \quad (2.92)$$

The random variable $Y_{l,k}$ after the correlation receiver can be represented as [8]

$$Y_{l,k} = A \int_0^{T_c} (h_l e^{-i\theta_l} x_k(t) + n_l(t)) dt$$

$$Y_{l,k} = \begin{cases} A^2 T_c h_l e^{-i\theta_l} + N_l & \text{for } k=0 \\ -A^2 T_c h_l e^{-i\theta_l} + N_l & \text{for } k=1, \end{cases} \quad (2.93)$$

where N_l is a zero-mean complex Gaussian random variable with circularly symmetric probability density function which represents the noise component and can be given as

$$N_l = A \int_0^{T_c} n_l(t) dt. \quad (2.94)$$

Since the integrator is a filter with frequency response $H_{\text{int}}(f)$ and impulse response

$$h_{\text{int}}(t) = \begin{cases} 1 & \text{if } 0 \leq t < T_b \\ 0 & \text{otherwise.} \end{cases} \quad (2.95)$$

Then, the variance of N_l can be calculated using Paresval's Theorem and Equations (2.90) and (2.95)

$$\begin{aligned} \sigma_{N_l}^2 &\equiv E \left\{ |N_l|^2 \right\} = A^2 \int_{-\infty}^{+\infty} |H_{\text{int}}(f)|^2 S_m(f) df \\ &= A^2 \int_{-\infty}^{+\infty} h_{\text{int}}^2(t) N_0 df \\ &= A^2 N_0 T_b = EN_0 \end{aligned} \quad (2.96)$$

Substituting Equation (2.88) into Equation (2.93) yields

$$Y_{l,k} = \begin{cases} Eh_l e^{-i\theta_l} + N_l & \text{for } k = 0 \\ -Eh_l e^{-i\theta_l} + N_l & \text{for } k = 1. \end{cases} \quad (2.97)$$

It is assumed that the exact channel state information (CSI) is known at the receiver end. The complex conjugate of the CSI is multiplied by the random variables $Y_{l,k}$ to produce the random variables $Z_{l,k}$. Thus, the phase shift in the channel is compensated and the value of the mean of the random variables $Z_{l,k}$ is proportional to the signal power. Therefore, a strong received signal carries a larger weight than a weak received signal. All the diversity receptions are added to form the random variable Z_k . This optimum combiner is called the maximal ratio combiner (MRC) [16]. Figure 7 illustrates the MRC for BPSK with time diversity.

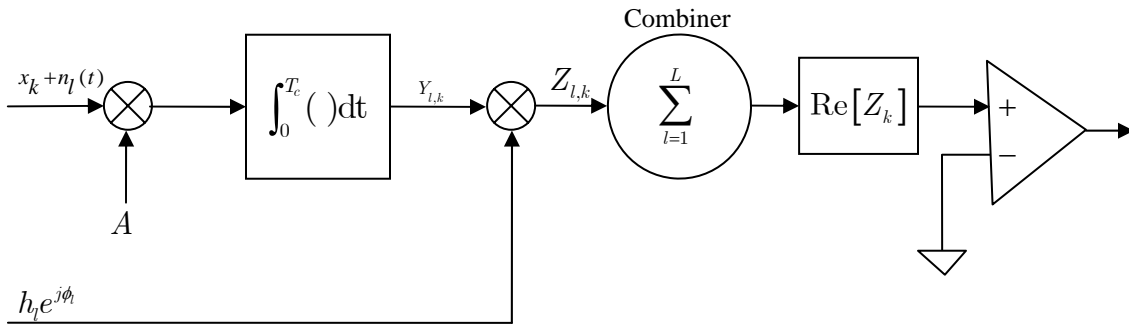


Figure 7 MRC for BPSK with Time Diversity (After Ref. [8, 15])

After maximal ratio combining, the random variable Z_k can be written as

$$Z_k = \begin{cases} \sum_{l=1}^L [Eh_l^2 + h_l e^{i\theta_l} N_l] & \text{for } k = 0 \\ -\sum_{l=1}^L [Eh_l^2 + h_l e^{i\theta_l} N_l] & \text{for } k = 1. \end{cases} \quad (2.98)$$

The real part of Z_k , denoted by $\zeta_k = \text{Re}\{Z_k\}$, is fed to the comparator for comparison with the predefined threshold level. For BPSK, if $\zeta_k > 0$, the receiver decides $k = 0$ was

transmitted. If $\zeta_k < 0$, the receiver decides $k = 1$ was transmitted. The decision variable ζ_k can be written as

$$\zeta_k = \text{Re}[Z_k] = \begin{cases} \sum_{l=1}^L \left(E h_l^2 + \text{Re} \left[h_l e^{i\theta_l} N_l \right] \right) & \text{for } k = 0 \\ -\sum_{l=1}^L \left(E h_l^2 + \text{Re} \left[h_l e^{i\theta_l} N_l \right] \right) & \text{for } k = 1. \end{cases} \quad (2.99)$$

From Equation (2.99), it is evident that the decision variable ζ_k is a Gaussian random variable with conditional mean (conditioned on the value of $\sum_{l=1}^L h_l^2$)

$$\overline{\zeta_k} = (-1)^k E \sum_{l=1}^L h_l^2. \quad (2.100)$$

Since the N_l 's are independent zero-mean complex Gaussian random variables with circularly symmetric probability density function and variance equal to EN_0 , the conditional variance of ζ_k can be expressed as:

$$\begin{aligned} \sigma_{\zeta}^2 &= \sigma_{\zeta_0}^2 = \sigma_{\zeta_1}^2 \\ &= \sum_{l=1}^L \text{Var} \left\{ \text{Re} \left(h_l e^{i\theta_l} N_l \right) \right\} \\ &= \sum_{l=1}^L h_l^2 \text{Var} \left\{ \text{Re} (N_l) \right\} \quad . \\ &= \frac{1}{2} \sum_{l=1}^L h_l^2 \text{Var} \{ N_l \} \\ &= \frac{EN_0}{2} \sum_{l=1}^L h_l^2 \end{aligned} \quad (2.101)$$

Assuming the probability of transmitting a “1” bit and a “0” bit are equal and using the fact that the conditional probabilities of bit error $P_{b|k}$ are equal due to the symmetry of the noise probability density function and the zero threshold, it is possible to calculate the conditional probability of bit error as:

$$\begin{aligned}
P_b &= \frac{1}{2} P_{b|0} + \frac{1}{2} P_{b|1} = P_{b|0} = \Pr\{\zeta_0 < 0\} \\
&= \Pr\left\{\frac{\zeta_0 - \bar{\zeta}_0}{\sigma_\zeta} < -\frac{\bar{\zeta}_0}{\sigma_\zeta}\right\} \\
&= \Pr\left\{\frac{\zeta_0 - \bar{\zeta}_0}{\sigma_\zeta} > \frac{\bar{\zeta}_0}{\sigma_\zeta}\right\} \\
&= Q\left(\frac{\bar{\zeta}_0}{\sigma_\zeta}\right) \\
&= Q\left(\sqrt{\frac{2E}{N_0} \sum_{l=1}^L h_l^2}\right).
\end{aligned} \tag{2.102}$$

Where $Q(x)$ is defined as [18]

$$Q(x) = \frac{1}{\sqrt{2\pi}} \int_x^\infty e^{-\frac{u^2}{2}} du. \tag{2.103}$$

Let γ be defined as

$$\gamma = \frac{E}{N_0} \sum_{l=1}^L h_l^2. \tag{2.104}$$

Substituting Equation (2.103) into (2.102), it is possible to rewrite the conditional probability of bit error as a probability of bit error conditioned on γ :

$$P_b(\gamma) = Q(\sqrt{2\gamma}). \tag{2.105}$$

The average probability of bit error can be obtained by taking the expectation of $P_b(\gamma)$ with respect to random variable γ [15, 16]. The average probability of bit error can be written as

$$\begin{aligned}
\overline{P_b} &= E[P_b(\gamma)] \\
&= \int_{-\infty}^{\infty} P_b(\gamma) f_\Gamma(\gamma) d\gamma
\end{aligned} \tag{2.106}$$

where $f_\Gamma(\gamma)$ is the probability density function for γ . Similarly, γ_l can be written as

$$\gamma_l = \frac{Eh_l^2}{N_0}. \quad (2.107)$$

The probability distribution function of h_l^2 was derived in the last section. Taking $h_l^2 = v_l$, Equation (2.60) can be represented as

$$f_{v_l}(v_l) = \frac{1}{2\sigma^2} e^{-v_l/2\sigma^2} u(v_l). \quad (2.108)$$

The average SNR per diversity reception can be written as

$$\begin{aligned} \bar{\gamma}_l &= E[\gamma_l] = E\left[\frac{Eh_l^2}{N_0}\right] \\ &= \frac{E}{N_0} E[h_l^2] = \frac{E}{N_0} E[v_l] \end{aligned} \quad (2.109)$$

The expectation can be evaluated as

$$\begin{aligned} E[v_l] &= \int_0^\infty v_l f_{v_l}(v_l) dv_l \\ &= \int_0^\infty v_l \frac{1}{2\sigma^2} e^{-v_l/2\sigma^2} dv_l = 2\sigma^2. \end{aligned} \quad (2.110)$$

Now the Equation (2.109) can be written as

$$\bar{\gamma}_l = \frac{2E\sigma^2}{N_0}. \quad (2.111)$$

The characteristic function of V_l can be written as [8, 16]

$$F_{V_l}(\omega) = \frac{1}{(1 - i2\sigma^2\omega)}. \quad (2.112)$$

If L IID random variables are added, then the probability density function of the sum is the L -fold convolution of the probability density function of the single random variable. Therefore, the characteristic function of the sum is the characteristic function of the single random variable raised to the power of L [16, 18]. Therefore, the characteristic

function for $V = \sum_{l=1}^L V_l$ is

$$F_V(\omega) = \frac{1}{(1 - i2\sigma^2\omega)^L}. \quad (2.113)$$

The probability density function of V is the inverse Fourier transform of the characteristic function and can be written as [8]

$$f_V(v) = \frac{v^{L-1}}{2^L \sigma^{2L} (L-1)!} e^{-v/2\sigma^2} u(v). \quad (2.114)$$

Consistent with Equation (2.104), it is possible to write

$$\gamma = \frac{Ev}{N_0} \quad (2.115)$$

and

$$\frac{d\gamma}{dv} = \frac{E}{N_0}. \quad (2.116)$$

Now, the probability distribution function for γ can be given as

$$f_\Gamma(\gamma) = \frac{1}{\frac{E}{N_0}} \frac{v^{L-1}}{2^L \sigma^{2L} (L-1)!} e^{-v/2\sigma^2} \bigg|_{v=\frac{\gamma}{E/N_0}} \quad (2.117)$$

$$f_\Gamma(\gamma) = \frac{\gamma^{L-1}}{\left(\frac{E2\sigma^2}{N_0}\right)^L (L-1)!} e^{-\frac{\gamma}{\frac{E2\sigma^2}{N_0}}}$$

Substituting Equation (2.111) into Equation (2.117) yields

$$f_\Gamma(\gamma) = \frac{\gamma^{L-1}}{(\bar{\gamma})^L (L-1)!} e^{-\frac{\gamma}{\bar{\gamma}}} u(\gamma). \quad (2.118)$$

Now, substituting Equation (2.105) and (2.118) into Equation (2.106), the average probability of bit error can be represented as [8]

$$\overline{P}_b = \int_0^\infty Q(\sqrt{2\gamma}) \frac{\gamma^{L-1}}{(\overline{\gamma}_l)^L (L-1)!} e^{-\frac{\gamma}{\overline{\gamma}_l}} d\gamma. \quad (2.119)$$

The solution for Equation (2.119) has been given in [16] as

$$\overline{P}_b = \left[\frac{(1-u)}{2} \right]^L \sum_{l=0}^{L-1} \binom{L-1+l}{l} \left[\frac{(1+u)}{2} \right]^l \quad (2.120)$$

where u is defined as

$$u = \sqrt{\frac{\overline{\gamma}}{1+\overline{\gamma}}}. \quad (2.121)$$

In time diversity, the total bit energy received is proportional to the number of diversity receptions and is represented as

$$E_b = LE \quad (2.122)$$

where L is the number of diversity reception and E is the energy per diversity reception. Substituting Equation (2.122) into Equation (2.109), $\overline{\gamma}_l$ can be written as

$$\overline{\gamma}_l = \frac{2E_b \sigma^2}{LN_o}. \quad (2.123)$$

Similarly, in the case of space diversity of order J as illustrated in Figure 8, each diversity reception is processed by a separate correlator. The integrating time period in each correlator is T_b . Therefore, the bit energy per diversity reception can be represented as

$$E = E_b \quad (2.124)$$

Now, the average SNR per diversity reception $\overline{\gamma}_l$ can be written as

$$\overline{\gamma}_l = \frac{2E_b \sigma^2}{N_0}. \quad (2.125)$$

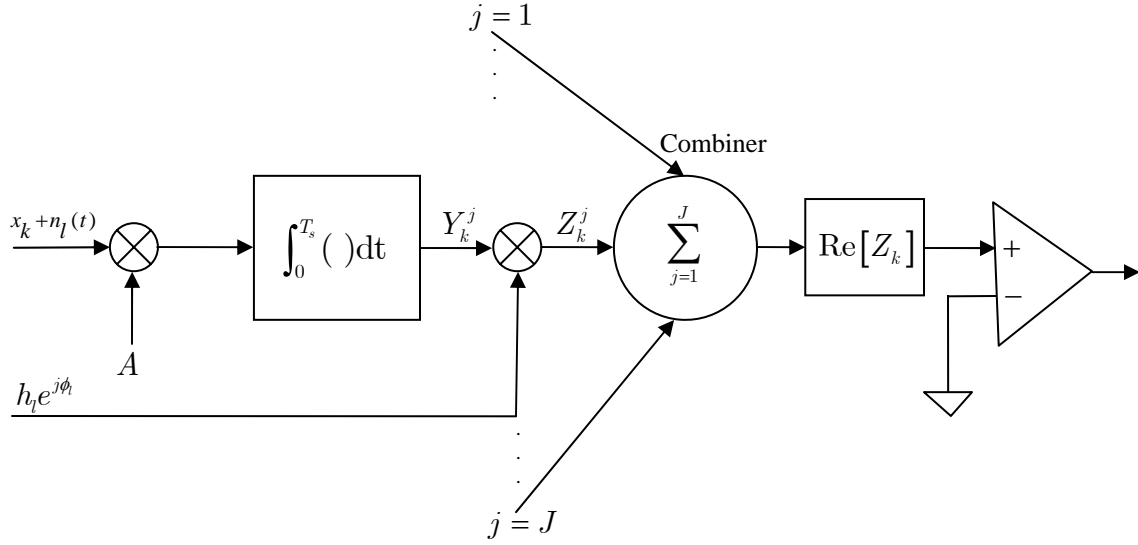


Figure 8 MRC for BPSK for Space Diversity (After Ref. [8, 15])

In this thesis, the performance of MDDM in MISO and MIMO systems is compared with the SISO system. In the case of the SISO system, there is no diversity and $L = 1$. Thus, the probability of bit error \overline{P}_b as per Equation (2.120) is given as [15, 16]

$$\overline{P}_b = \left[\frac{1-u}{2} \right]. \quad (2.126)$$

Substituting Equation (2.121) into Equation (2.126) yields

$$\overline{P}_b = \left[\frac{1}{2} \left(1 - \sqrt{\frac{\overline{\gamma}_l}{1 + \overline{\gamma}_l}} \right) \right]. \quad (2.127)$$

The probability of bit error for a BPSK MISO system in a multipath fading channel as given in Equation (2.127) will be compared with the simulated and theoretical probability of bit error for MDDM MISO and MIMO systems.

F. SUMMARY

In this chapter, the fundamentals of SISO, SIMO and MISO systems were introduced to facilitate better understanding of MIMO systems. To approach the maximum capacity of MIMO channels, space time codes can be designed in conjunction with the modulation techniques to incorporate diversity. Orthogonal frequency division

multiplexing (OFDM) can be used to mitigate the frequency selectivity of the channel. OFDM utilizes the discrete Fourier transform (DFT) of the baseband signal. The multicarrier cyclic delay diversity technique can be implemented by exploiting the cyclic shift property of the DFT. A baseband model for the flat Rayleigh fading channel was derived for simulation. Lastly, the MRC as an optimum diversity combining technique was discussed. The next chapter discusses the design of the simulated MDDM transmitters and receivers.

III. MULTICARRIER DELAY DIVERSITY MODULATION TRANSMITTER AND RECEIVER MODELS

This chapter introduces the implementation of the multicarrier delay diversity modulation scheme at the block level. The basic design of the transmitter and receiver is discussed briefly. In this thesis, the MDDM scheme is implemented using BPSK modulation. The inclusion of forward error correction (FEC) and higher bandwidth efficient modulation schemes can be considered for future work. The next chapter illustrates the simulation and analysis of the MDDM transmitter and receiver.

A. THE MULTICARRIER DELAY DIVERSITY MODULATION SCHEME

The scheme of implementing delay diversity with OFDM for MIMO systems was recommended for flat fading channels in [5]. The cyclic delay diversity approach with OFDM was suggested for the frequency selective fading channel in [6]. In this research, cyclic delay diversity with OFDM is investigated. The implementation of multicarrier delay diversity in MIMO systems has been discussed in the previous chapter. For modeling purposes, the MIMO configuration of two transmit and two receive antennas is discussed in this chapter. For simulation and analysis, the number of receive antennas varies from one to three. To facilitate better understanding and precise representation of signals from the transmit antenna to the receive antenna, the following notations will be used:

- X_k represents the BPSK symbol at k -th interval before the multicarrier delay diversity modulation and after demodulation
- X_k^l represents the BPSK symbol at k -th interval from the transmitting antenna l after multicarrier delay diversity delay modulation
- x_m^l represents the signal x to be transmitted from transmit antenna l in the m^{th} transmission interval,
- r_m^j represents the received signal at receive antenna j at the m^{th} time interval,
- h^{lj} represents the channel response from transmit antenna l to receive antenna j ,
- n^j represents the AWGN at receive antenna j , and
- asterisk $()^*$ represents the complex conjugate.

B. MDDM TRANSMITTER

The multicarrier delay diversity scheme will be simulated with binary phase shift keying modulation. A block diagram of the MDDM transmitter with two transmitting antennas is shown in Figure 9. The function of each block is explained briefly in the following discussion.

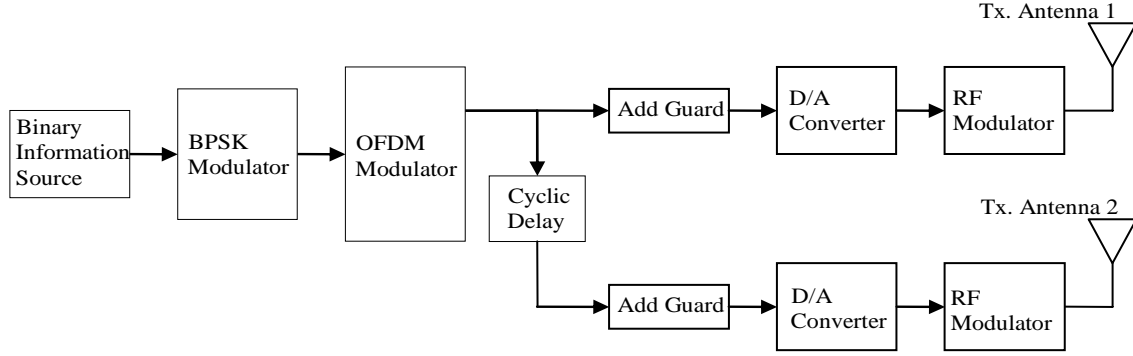


Figure 9 Block Diagram of MDDM Transmitter (After Ref. [2])

1. Binary Information Source and M PSK Modulator

The binary information source generates bits 0 and 1 with equal probabilities

$$\Pr[0] = \Pr[1] = 1/2. \quad (3.1)$$

Then, the bits are mapped to I and Q symbol coordinates by the M PSK modulator. The equivalent lowpass (i.e. complex envelope) M PSK symbols can be represented as

$$\tilde{X}_k(t) = A e^{j2\pi(m-1)/M} P_T(t) \quad \text{for } m = 1, 2, \dots, M \quad (3.2)$$

where A is the amplitude of the signal, M is the number of possible phases (for BPSK $M = 2$, for QPSK $M = 4$), T is the symbol duration, and $P_T(t)$ denotes

$$P_T(t) = \begin{cases} 1 & \text{for } 0 \leq t \leq T \\ 0 & \text{otherwise} \end{cases}. \quad (3.3)$$

2. OFDM Modulator

Mapped symbols are fed to the OFDM modulator block. In this block, first the serial input data stream is converted to parallel. Then, the IFFT operation is performed to

realize OFDM as discussed in the last chapter. The FFT size denotes the number of subcarriers. Figure 10 illustrates the OFDM modulator. [2]

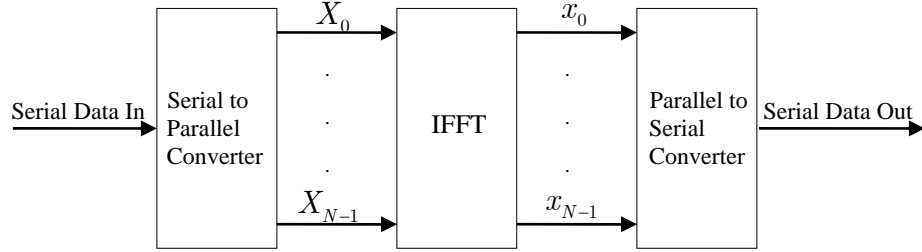


Figure 10 Orthogonal Frequency Division Multiplexing Modulator

In this thesis, the number of subcarriers is 256 to simulate OFDM, in accordance with the IEEE 802.16a standard. In this standard, three types of subcarriers are defined: data carriers for information symbol transmission, pilot carriers for the estimation of CSI and guard carriers (null carriers) placed on both sides of the frequency spectrum to avoid intercarrier interference from neighboring frequency bands. The assignment of the subcarriers in this thesis has been adopted from the IEEE 802.16a standard and given in Table 1. Figure 11 illustrates the subcarriers organization at the input of the IFFT block.

Size of FFT	256
# of information subcarriers	192
# of pilot subcarriers	8
# of null subcarriers (including the DC subcarrier)	56
# of lower frequency guard subcarriers	28
# of higher frequency guard subcarriers	27
Frequency indices of null subcarriers (including the DC subcarrier)	-128, -127, ..., -101, 0 +101, +102, ..., +127
Frequency indices of pilot subcarriers	1, 2, ..., 8

Table 1 Assignment of OFDM Subcarriers (After IEEE 802.16a standard, Ref. [20])

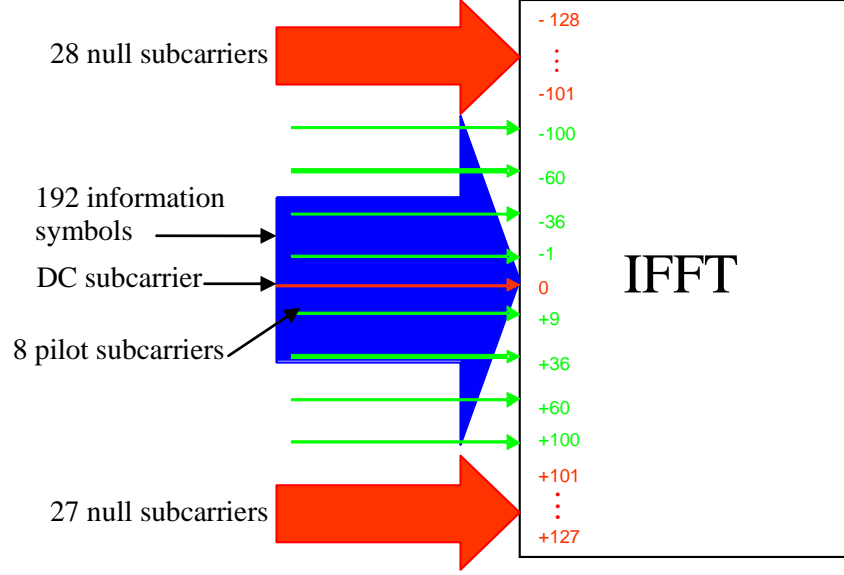


Figure 11 Assignment of Subcarriers at the Input of IFFT Block (After Ref. [20])

The output of the IFFT block can be represented according to the definition of Equation (2.30) as

$$x_m = \frac{1}{N} \sum_{k=0}^{N-1} X_k e^{j2\pi km / N} \quad \text{for } m = 0, 1, 2, \dots, 255 \quad (3.4)$$

where $N = 256$, and the index of the subcarrier is represented from 0 to 255 instead of -128 to 128 for convenience. After the IFFT operation, the OFDM sequence is converted from parallel to serial. [23]

3. Cyclic Delay Addition

After the IFFT operation, the symbols x_n are cyclically shifted to realize a cyclic delay of one information symbol period. For transmitting antenna 1, there is no delay and $D = 0$. For each subsequent antenna, the cyclic delay is increased one information symbol period. The signal after cyclic delay is given as

$$x_n^l = x_{(n-D)_N} \quad \text{where } l = 1, 2, \dots, L \quad \text{and} \quad D = l - 1 \quad (3.5)$$

4. Guard Interval (Cyclic Prefix) Addition

As discussed in the previous chapter, a guard interval at the beginning of each OFDM symbol is added to mitigate the effect of the multipath channel. The length of the

guard interval T_G , in the form of a cyclic prefix, is chosen to be greater than or equal to the anticipated delay spread of the channel. The addition of a guard interval is an overhead at the cost of data rate. The guard length is specified with respect to the OFDM symbol period T_s and is also referred to as guard ratio T_G / T_s . The addition of the guard interval has been illustrated in Figure 6. For example, in the IEEE 802.16 wireless standard, the guard ratio is chosen to be $1/32$. The FFT block size is 256. Therefore, the guard length is to be 8. The cyclic prefix constitutes the last eight samples of the IFFT output and it is concatenated to the beginning of the OFDM symbol sequence. Now, the sequence with added guard interval for each transmitting antenna can be represented as

$$\begin{aligned} x_{(n+G)}^1 &= [x[248] \ x[249] \ ...x[255] \ x[0] \ x[1] \ x[2] \ ...x[255]] \\ x_{(n+G)}^2 &= [x[247] \ x[248] \ ...x[254] \ x[255] \ x[0] \ x[1] \ ...x[254]]. \end{aligned} \quad (3.6)$$

5. Digital to Analog Conversion and RF Modulation

The IFFT operation, the cyclic delay operation and the guard interval operations are performed in the discrete time domain. For transmission purposes, these discrete symbols are converted to an analog signal using a digital to analog (D/A) converter. After digital to analog conversion, these symbols are continuous time baseband OFDM symbols. Then, these symbols are upconverted to the transmission radio frequency. After requisite amplification to the desired power level, these symbols are transmitted from the respective antennas. In this thesis, the simulation is performed at the discrete time baseband level and no digital to analog or RF modulation is implemented.

C. MDDM RECEIVER

The multicarrier delay diversity scheme can be employed with any number of receive antenna without changing the transmitted space time code. In this section, the receiver design for two receive antennas is discussed. It is assumed that the signals received at both receiving antennas are independent of each other due to independent channel responses and no antenna correlation. The MDDM receiver has almost the same structure as the MDDM transmitter but the operations are performed in reverse order. The MDDM receiver design is illustrated in Figure 12. At the receiving antenna, the cyclically time delayed OFDM symbols are received after passing through the channel with the AWGN and can be represented as

$$\begin{aligned}
r_{(n+G)}^1 &= A \left(h^{11} * x_{(n+G)}^1 + h^{21} * x_{(n+G)}^2 \right) + n^1 & \text{for } n = 0, 1, 2, \dots, N + G - 1 \\
r_{(n+G)}^2 &= A \left(h^{12} * x_{(n+G)}^1 + h^{22} * x_{(n+G)}^2 \right) + n^2 & \text{for } n = 0, 1, 2, \dots, N + G - 1
\end{aligned} \tag{3.7}$$

where $*$ represents circular convolution (due to the circular guard interval). [2]

After RF demodulation and analog to digital (A/D) conversion, the OFDM symbol received by each receiving antenna is in the discrete time domain. The guard interval added at the transmitter is removed. Then, this signal is fed to the OFDM demodulator as a baseband signal. In the OFDM demodulator block, the received OFDM symbol is converted from serial to parallel for the FFT operation. The OFDM demodulator is illustrated in Figure 13. After the FFT operation as defined in Equation (2.29), the signal can be represented as

$$R_k^j = \text{FFT} \{ r_n^j \} = \sum_{n=0}^{255} \left(\sum_{l=1}^2 (h^{lj} * x^l) + n^j \right) e^{j2\pi kn / 255} \quad \text{for } n = 0, 1, 2, \dots, 255. \tag{3.8}$$

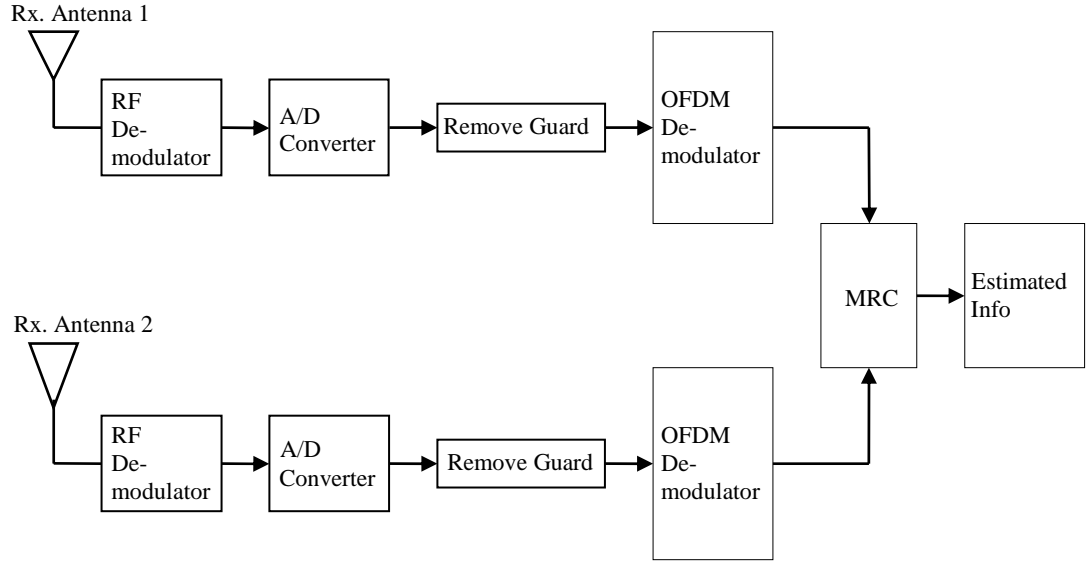


Figure 12 Block Diagram of MDDM Receiver

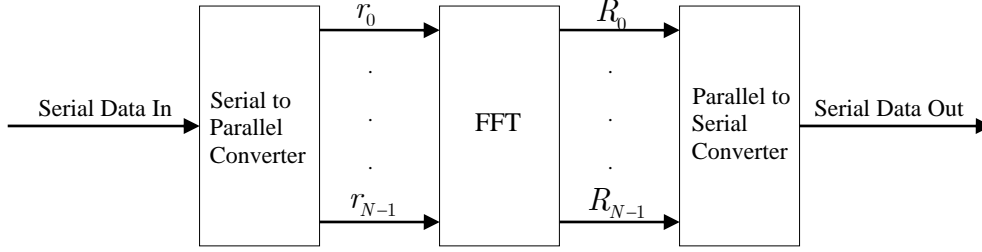


Figure 13 Orthogonal Frequency Division Multiplexing Demodulator

Using the linearity property of the discrete Fourier transform, Equation (3.8) can be represented as

$$\begin{aligned} R_k^1 &= H^{11}X_k^1 + H^{21}X_k^2 + N_k^1 & \text{for } k = 0, 1, 2, \dots, 255 \\ R_k^2 &= H^{12}X_k^1 + H^{22}X_k^2 + N_k^2 & \text{for } k = 0, 1, 2, \dots, 255 \end{aligned} \quad (3.9)$$

where H^{lj} is the frequency response of the channel from transmit antenna l to receive antenna j and N^j is the AWGN at receive antenna j in the frequency domain. Using the circular time shift property of the discrete Fourier transform as defined in Equation (2.31), Equation (3.9) can be written as

$$\begin{aligned} R_k^1 &= H^{11}X_k^1 + H^{21}X_k^1 e^{-i2\pi kD/N} + N^1 & \text{for } k = 0, 1, 2, \dots, 255 \\ R_k^2 &= H^{12}X_k^1 + H^{22}X_k^1 e^{-i2\pi kD/N} + N^2 & \text{for } k = 0, 1, 2, \dots, 255 \\ R_k^1 &= (H^{11} + H^{21}e^{-i2\pi kD/N})X_k^1 + N^1 & \text{for } k = 0, 1, 2, \dots, 255 \\ R_k^2 &= (H^{12} + H^{22}e^{-i2\pi kD/N})X_k^1 + N^2 & \text{for } k = 0, 1, 2, \dots, 25 \end{aligned} \quad (3.10)$$

where $D = 1$ is the cyclic time delay induced at transmit antenna two. Now, the effective channel response at the receive antenna j is defined as

$$H_k^j = H_k^{1j} + H_k^{2j} e^{-i2\pi k/N}. \quad (3.11)$$

Substituting Equation (3.11) into Equation (3.10), the signal at each receiving antenna can be written as

$$\begin{aligned} R_k^1 &= H_k^1 X_k^1 + N_k^1 \\ R_k^2 &= H_k^2 X_k^1 + N_k^2 \end{aligned} \quad (3.12)$$

Equation (3.12) shows clearly the space diversity receptions at the receiving end. They are combined by using the optimum maximal ratio combining receiver. MRC for space diversity has already been discussed in the previous chapter and illustrated in Figure 8. It is assumed that perfect CSI is known at the receiver end. In MRC, the received signal is multiplied with the complex conjugate of CSI and all diversity receptions are added to form the decision variable. The outputs of the integrators of the MRC for each diversity reception can be represented as

$$\begin{aligned} Y_k^1 &= A T_b H_k^1 X_k + N_k^{1'} \\ Y_k^2 &= A T_b H_k^2 X_k + N_k^{2'} \\ Y_k^1 &= \frac{E_b H_k^1 X_k}{A} + N_k^{1'} \\ Y_k^2 &= \frac{E_b H_k^2 X_k}{A} + N_k^{2'} \end{aligned} \quad (3.13)$$

where E_b is the average energy per bit, $N_k^{1'} = A T_b N_k^1$, and $N_k^{2'} = A T_b N_k^2$.

After the integrator stage, the random variable is multiplied by the complex conjugate of CSI and the resulting random variable can be represented as

$$\begin{aligned} Z_k^1 &= \frac{E_b H_k^1 (H_k^1)^* X_k}{A} + (H_k^1)^* N_k^{1'} \\ Z_k^2 &= \frac{E_b H_k^2 (H_k^2)^* X_k}{A} + (H_k^2)^* N_k^{2'} \\ Z_k^1 &= \frac{E_b |H_k^1|^2 X_k}{A} + (H_k^1)^* N_k^{1'} \\ Z_k^2 &= \frac{E_b |H_k^2|^2 X_k}{A} + (H_k^2)^* N_k^{2'} \end{aligned} \quad (3.14)$$

The decision variable Z_k at the output of combiner stage can be expressed as

$$\begin{aligned} Z_k &= Z_k^1 + Z_k^2 \\ Z_k &= E_b \left(|H_k^1|^2 + |H_k^2|^2 \right) \frac{X_k}{A} + (H_k^1)^* N_k^{1'} + (H_k^2)^* N_k^{2'} \end{aligned} \quad (3.15)$$

For the final decision of the estimated received data, the decision variable is compared with predetermined threshold levels. For the case of BPSK, the real part of Z_k is compared with a threshold level of zero to decide each received binary bit. [2, 15]

D. SUMMARY

This chapter discussed the designs of the MDDM transmitter and receiver at the block level. The function of each block was discussed with the representation of signals before and after each block operation. During the discussion, two assumptions were made, i.e., perfect knowledge of CSI at the receiver and constant channel response for the duration of the OFDM symbol. The next chapter analyzes the MDDM transmitter and receiver model for the AWGN channel with and without flat fading.

THIS PAGE INTENTIONALLY LEFT BLANK

IV. ANALYSIS AND SIMULATION OF MULTICARRIER DELAY DIVERSITY MODULATION SCHEME

In this chapter, the performance (bit error probability) analysis and simulation of MISO and MIMO systems with multicarrier delay diversity is presented. The MDDM transmitter and receiver as described in Chapter III were simulated in Matlab. The system is analyzed with an AWGN channel with and without Rayleigh fading. The analytical and simulated results are compared with a SISO BPSK system. To establish a fair comparison of the SISO system and the MIMO system with MDDM, the power transmitted for both systems is assumed equal. To facilitate better understanding and precise representation of signals from transmit to receive antenna, this thesis will adhere to the following notation:

- E_b represents the average energy per bit at the receiver of the SISO system,
- E_s represents the average energy per MIMO BPSK symbol per receiving antenna,
- T_s represents the OFDM symbol duration,
- T_s' represents the MIMO BPSK symbol duration and $T_s' = T_b$
- ζ_k represents the real part of decision variable Z_k .

Energy per bit is an important parameter for comparison and is defined as

$$E_b = \int_0^{T_b} |X_k|^2 dt = A^2 T_b \quad (4.1)$$

where k is the time index of the BPSK symbol (before serial to parallel and after parallel to serial conversions) and X_k is the BPSK modulated symbol as defined in Table 2.

Input bit at time k	Output Symbol X_k
0	A
1	$-A$

Table 2 BPSK Modulation Scheme (After Ref. [8])

For simulation and analysis, the amplitude $A = 1$ is maintained. Equation (4.1) shows that the energy per bit for BPSK modulation is the same for bit 0 and bit 1. Thus the transmitted power for the SISO system can be written as

$$P_{SISO} = \frac{E_b}{T_b} = A^2 \quad (4.2)$$

The probability of bit error P_b for a baseband equivalent SISO BPSK system in discrete domain for correlation demodulator can be represented as [15, 16]

$$P_b = Q\left(\frac{\bar{Z}^+}{\sigma_z}\right). \quad (4.3)$$

In this case \bar{Z}^+ is represented as

$$\bar{Z}^+ = A \quad (4.4)$$

and

$$\sigma_z^2 = \frac{N_0}{2T_b} \quad (4.5)$$

where $\frac{N_0}{2}$ represents the two sided noise power spectral density for the real part of the AWGN. Substituting Equation (4.4) and Equation (4.5) into Equation (4.3) yields,

$$P_b = Q\left(\frac{\sqrt{2T_b}A}{\sqrt{N_o}}\right) = Q\left(\sqrt{\frac{2E_b}{N_o}}\right). \quad (4.6)$$

The bit error probability of the SISO system as given by Equation (4.6) will serve as a benchmark for comparison of the MISO and MIMO systems with MDDM in the AWGN channel.

In this thesis the number of transmit antennas is two and both the transmit antennas transmit equal power. The total energy per bit transmitted for MISO and MIMO systems using BPSK symbols can be defined as

$$E_s' = P'T_s' \quad (4.7)$$

and

$$P_{SISO} = P_{MISO} = P_{MIMO} . \quad (4.8)$$

Therefore, the energy transmitted per antenna P' can be given as

$$P' = \frac{P_{SISO}}{L} = \frac{P_{SISO}}{2} . \quad (4.9)$$

Now, Equation (4.7) is rewritten as

$$\begin{aligned} E'_s &= P' T'_s = \frac{P_{SISO} T'_s}{2} \\ E'_s &= \frac{E_b}{2} . \end{aligned} \quad (4.10)$$

A. SIMULATION OF MDDM TRANSMITTER

The block diagram of the MDDM transmitter model is shown in Figure 9. The MDDM transmitter was simulated in MATLAB with equivalent baseband BPSK in the discrete time domain. The simulation was implemented with one sample for each BPSK symbol. The MDDM transmitter scheme, as mentioned in Chapter III with two transmitting antennas, was simulated without added guard interval, D/A converter and RF modulator blocks to facilitate the simulations. Equal power was transmitted from both the antennas. To achieve the same total power transmission as that of a single antenna BPSK transmitter, the signal at each branch of MIMO transmitter was multiplied with a gain factor of g for normalization. The transmitted energy per symbol for BPSK is same whether a binary 1 or 0 is transmitted. With the gain factor g the energy per symbol is represented as

$$E'_s = \int_0^{T'_s} |gX_k|^2 dt = g^2 A^2 T'_s . \quad (4.11)$$

Substituting Equation (4.10) into Equation (4.11) yields

$$\frac{P_{SISO} T'_s}{2} = g^2 A^2 T'_s . \quad (4.12)$$

Using Equation (4.2), Equation (4.12) can be rewritten as

$$\begin{aligned}
g^2 &= \frac{1}{2} \\
g &= \frac{1}{\sqrt{2}}.
\end{aligned} \tag{4.13}$$

The gain factor $g = 1/\sqrt{2}$ is maintained for all subsequent simulations to transmit the same power as that of a single antenna BPSK system. Thus the effective amplitude of the BPSK modulated signal for each antenna is given as

$$|X_k| = \frac{A}{\sqrt{2}} = \frac{1}{\sqrt{2}}. \tag{4.14}$$

B. SIMULATION OF MDDM RECIVER

The block diagram of the MDDM receiver model is shown in Figure 12. The MDDM receiver was also simulated in MATLAB with equivalent baseband BPSK in the discrete time domain. The MDDM receiver simulation was implemented as discussed in Chapter III except for the RF demodulator, the A/D converter and the Remove Guard blocks. The receiver was configured as a MISO system with only one receive antenna and as a MIMO system with two receive antennas and as a MIMO system with three receive antennas. After multicarrier delay diversity demodulation, the space diversity receptions of MIMO systems were combined by using the optimum MRC technique as discussed in Chapter II. After the BPSK correlation demodulator as illustrated in Figure 14, ζ_k (the real part of the random variable Z_k) was compared with the threshold level according to Table 3. For analysis and simulation purposes it is assumed that the transmitter and receiver frequencies are synchronized and, in the case of MIMO systems, all the diversity receptions are also synchronized.

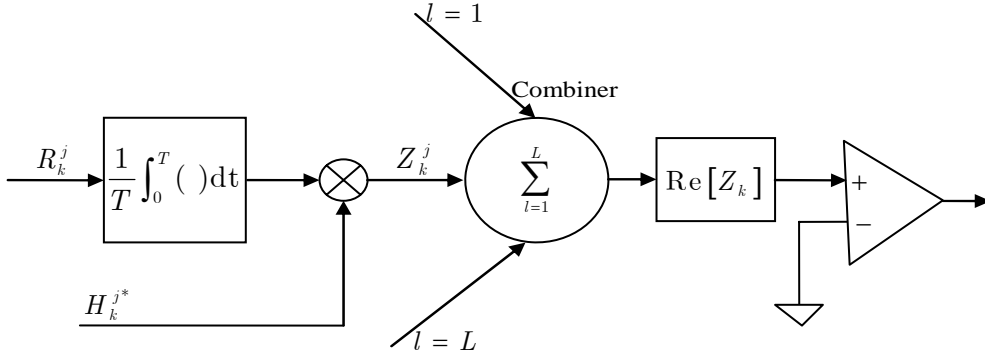


Figure 14 BPSK Correlation Demodulator for MIMO System with MDDM

	Output Binary Bit
$\zeta_k \geq 0$	0
$\zeta_k < 0$	1

Table 3 Demodulation of BPSK Signal (After Ref. [8]).

C. SIMULATION AND PERFORMANCE ANALYSIS OF MDDM IN AWGN

The performance of MDDM was first simulated and analyzed in AWGN only. In this simulation and analysis no fading is assumed. This means that each channel response coefficient h^{bj} equals one. A block diagram of the MIMO system in AWGN with three receiving antennas is illustrated in Figure 15. Both the MDDM transmitter and receiver are collapsed into one block each to facilitate presentation. In this simulation two gain blocks each with normalizing gain factor of g are shown at the outputs of the transmitter for each transmitting antenna. The AWGN channel blocks add white Gaussian noise to the signal at respective receiving antennas. The noise power is increased progressively with each simulation run to calculate the bit error rate at different signal to noise ratios. Bit error rate is calculated by comparing the input binary data stream at the input to the transmitter b_k and output binary data stream at the output of the receiver \hat{b}_k .

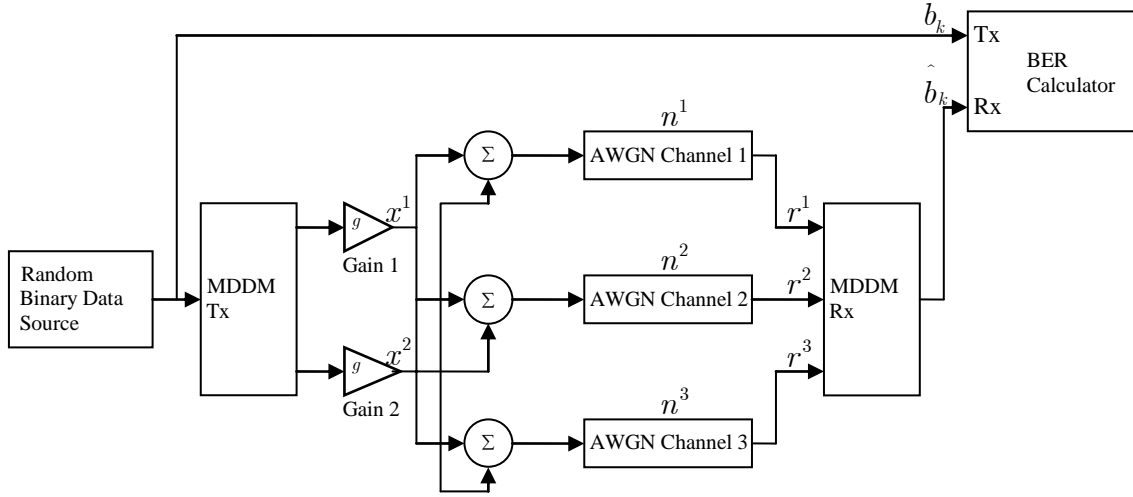


Figure 15 Simulation of MDDM MIMO System in AWGN

1. Performance Analysis of MISO System with Two Transmit and One Receive Antenna

At the receiving antenna, the received signal r_m at time m is given by

$$r_m = x_m^1 + x_m^2 + n_m. \quad (4.15)$$

where x_m^2 is a cyclically delayed signal and is given by Equation (3.5)

$$x_m^2 = x_{(m-1)_N}^1. \quad (4.16)$$

After the FFT operation, the received signal is written as

$$\text{FFT}[r_m] = \text{FFT}[x_m^1 + x_m^2 + n_m]. \quad (4.17)$$

Using the linearity property of the discrete Fourier transform [13], Equation (4.17) can be represented as

$$R_k = X_k^1 + X_k^2 + N_k. \quad (4.18)$$

Substituting Equation (2.31) and (4.16) into Equation (4.18) yields

$$\begin{aligned} R_k &= X_k^1 + X_k^1 e^{-j2\pi k/N} + N_k \\ R_k &= (1 + e^{-j2\pi k/N}) X_k^1 + N_k \end{aligned} \quad (4.19)$$

where N is the FFT size or the number of subcarriers, N_k is AWGN in the frequency domain and $(1 + e^{-j2\pi k/N})$ is the effective channel response for MDDM in AWGN channel. To facilitate the presentation, the phase angle ϕ_k is defined as

$$\phi_k = 2\pi k / N. \quad (4.20)$$

Multiplying Equation (4.19) by the complex conjugate of the effective channel response, the result is given by

$$Z_k = (1 + e^{-j\phi_k})(1 + e^{+j\phi_k})X_k^1 + (1 + e^{+j\phi_k})N_k. \quad (4.21)$$

Using Euler's identity

$$e^{j\theta} = \cos(\theta) + j \sin(\theta) \quad (4.22)$$

Equation (4.21) is rewritten as

$$Z_k = (2 + 2 \cos(\phi_k))X_k^1 + (1 + e^{+j\phi_k})N_k. \quad (4.23)$$

Equation (4.23) defines a complex Gaussian random variable Z_k due to AWGN. For demodulation of BPSK data, $\zeta_k = \text{Re}\{Z_k\}$ is compared with the threshold as given in Table 3. If correlation demodulator conditions are assumed then

$$\begin{aligned} E\{Z_k \mid "0" \text{ was transmitted}\} &= E\left\{\frac{1}{T_b} \int_0^{T_b} \left[\frac{A}{\sqrt{2}} (2 + 2 \cos \phi_k) + N_k (1 + e^{+j\phi_k}) \right] dt \right\} \\ &= [2 + 2 \cos(\phi_k)] \frac{A}{\sqrt{2}} \\ &= \sqrt{2} [1 + \cos(\phi_k)] A. \end{aligned} \quad (4.24)$$

Since this expected value is real, it follows that

$$\bar{\zeta}_k^+ = E\{\text{Re}\{Z_k\} \mid "0" \text{ was sent}\} = \sqrt{2} [1 + \cos(\phi_k)] A \quad (4.25)$$

The variance of $\zeta_k = \text{Re}\{Z_k\}$ is only due to the variance of real part of the noise component $(1 + e^{+j\phi_k})N_k$ [15, 16] and is represented by σ_ζ^2

$$\begin{aligned}\sigma_\zeta^2 &= \mathbb{E} \left\{ \left(\text{Re} \left[(1 + e^{+j\phi_k}) N_k \right] \right)^2 \right\} - \left(\mathbb{E} \left\{ \text{Re} \left[(1 + e^{+j\phi_k}) N_k \right] \right\} \right)^2 \\ \sigma_\zeta^2 &= \mathbb{E} \left\{ \left(\text{Re} \left[(1 + e^{+j\phi_k}) N_k \right] \right)^2 \right\}\end{aligned}\quad (4.26)$$

where $\mathbb{E} \{ \}$ represents the expected value. $\eta_k = \text{Re} \left[(1 + e^{+j\phi_k}) N_k \right]$ is the real part of a complex Gaussian random variable with zero mean. η_k and η_k^2 can be written as

$$\begin{aligned}\eta_k &= \text{Re} \left[(1 + e^{+j\phi_k}) N_k \right] = \frac{1}{2} \left((1 + e^{+j\phi_k}) N_k + (1 + e^{-j\phi_k}) N_k^* \right) \\ \eta_k^2 &= \left(\text{Re} \left[(1 + e^{+j\phi_k}) N_k \right] \right)^2 = \left(\frac{1}{2} \left((1 + e^{+j\phi_k}) N_k + (1 + e^{-j\phi_k}) N_k^* \right) \right)^2 \\ &= \frac{1}{4} \left((1 + e^{+j\phi_k})^2 N_k^2 + (1 + e^{-j\phi_k})^2 N_k^{*2} + 2(1 + e^{-j\phi_k})(1 + e^{+j\phi_k}) N_k N_k^* \right) \\ &= \frac{1}{4} \left((1 + e^{+j\phi_k})^2 N_k^2 + (1 + e^{-j\phi_k})^2 N_k^{*2} + 4(1 + \cos(\phi_k)) N_k N_k^* \right).\end{aligned}\quad (4.27)$$

where $()^*$ represents the complex conjugate. Substituting Equation (4.27) into Equation (4.26) gives

$$\begin{aligned}\sigma_\zeta^2 &= \mathbb{E} \left\{ \frac{1}{4} \left((1 + e^{+j\phi_k})^2 (N_k)^2 + (1 + e^{-j\phi_k})^2 (N_k^*)^2 + 4(1 + \cos(\phi_k)) N_k N_k^* \right) \right\} \\ &= \frac{1}{4} \left((1 + e^{+j\phi_k})^2 \mathbb{E} \left\{ (N_k)^2 \right\} + (1 + e^{-j\phi_k})^2 \mathbb{E} \left\{ (N_k^*)^2 \right\} + 4(1 + \cos(\phi_k)) \mathbb{E} \left\{ N_k N_k^* \right\} \right).\end{aligned}\quad (4.28)$$

As discussed earlier, N_k is a complex Gaussian random variable with zero mean, therefore

$$\mathbb{E} \left\{ (N_k)^2 \right\} = \mathbb{E} \left\{ (N_k^*)^2 \right\} = 0. \quad (4.29)$$

Substituting Equation (4.29) into Equation (4.28) gives

$$\sigma_\zeta^2 = [1 + \cos(\phi_k)] \mathbb{E} \left\{ N_k N_k^* \right\}. \quad (4.30)$$

Using Equation (2.29), N_k is given as

$$N_k = \sum_{m=0}^{N-1} n_m e^{-j2\pi km/N}. \quad (4.31)$$

Substituting Equation (4.31) into Equation (4.30) yields

$$\begin{aligned}
\sigma_\zeta^2 &= [1 + \cos(\phi_k)] E \left\{ \sum_{m=0}^{N-1} n_m e^{-j2\pi kn/N} \sum_{l=0}^{N-1} n_l^* e^{+j2\pi kl/N} \right\} \\
&= [1 + \cos(\phi_k)] \sum_{l=0}^{N-1} \sum_{m=0}^{N-1} E \{ n_l n_m^* \} e^{-j2\pi kl/N} e^{+j2\pi km/N} \\
&= [1 + \cos(\phi_k)] \sum_{l=0}^{N-1} \sum_{m=0}^{N-1} E \{ n_l n_m^* \} e^{-j2\pi k(l-m)/N}.
\end{aligned} \tag{4.32}$$

Samples of AWGN at different time instants are IID Gaussian random variables with zero mean. Therefore, they are uncorrelated and the variance can be represented as

$$\begin{aligned}
E \{ n_m n_p^* \} &= \begin{cases} E \{ n_m \} E \{ n_p^* \} & \text{if } m \neq p \\ E \{ |n_m|^2 \} & \text{if } m = p \end{cases} \\
&= \begin{cases} 0 & \text{if } m \neq p \\ \sigma_{n_m}^2 & \text{if } m = p. \end{cases}
\end{aligned} \tag{4.33}$$

Substituting Equation (4.33) into Equation (4.32) gives

$$\begin{aligned}
\sigma_\zeta^2 &= [1 + \cos(\phi_k)] \sum_{m=0}^{N-1} E \{ n_m n_m^* \} \\
&= [1 + \cos(\phi_k)] N \sigma_{n_m}^2
\end{aligned} \tag{4.34}$$

where $\sigma_{n_m}^2$ is the noise power of the OFDM symbol in the time domain before the FFT operation. If correlation demodulator conditions are assumed, the noise power for OFDM symbol durations is given by

$$\sigma_{n_m}^2 = \frac{N_o}{2} \int_{-\infty}^{\infty} |H(f)|^2 df \tag{4.35}$$

where $N_o/2$ (Watts per Hertz) is the power spectral density of the real part of noise and $H(f)$ is the frequency response of the integrator [15, 16]. Using Parseval's theorem [19], Equation (4.35) converts to

$$\begin{aligned}
\sigma_{n_m}^2 &= \frac{N_o}{2} \int_0^{T_s} |h[t]|^2 dt \\
&= \frac{N_o}{2} \int_0^{T_s} \frac{1}{T_s^2} dt \\
&= \frac{N_o}{2T_s}.
\end{aligned} \tag{4.36}$$

Substituting Equation (4.36) into Equation (4.34) gives

$$\sigma_\zeta^2 = \frac{[1 + \cos(\phi_k)] NN_o}{2T_s}. \tag{4.37}$$

Substituting, T_s from Equation (2.33) and since for BPSK $T_s' = T_b$, Equation (4.37) yields

$$\sigma_\zeta^2 = \frac{[1 + \cos(\phi_k)] NN_o}{2NT_b} = \frac{[1 + \cos(\phi_k)] N_o}{2T_b}. \tag{4.38}$$

Using Equations (4.24) and (4.38), the bit error probability P_b' conditioned on the value ϕ_k can be expressed as

$$\begin{aligned}
P_b' &= \Pr\{\zeta_k < 0 \mid \text{"0" was sent}\} \\
&= \Pr\left\{\frac{\zeta_k - \overline{\zeta_k^+}}{\sigma_{\zeta_k}} < -\frac{\overline{\zeta_k^+}}{\sigma_{\zeta_k}} \mid \text{"0"}\right\} \\
&= \Pr\left\{\frac{\zeta_k - \overline{\zeta_k^+}}{\sigma_{\zeta_k}} > \frac{\overline{\zeta_k^+}}{\sigma_{\zeta_k}} \mid \text{"0"}\right\} \\
&= Q\left(\frac{\overline{\zeta_k^+}}{\sigma_{\zeta_k}}\right) = Q\left(\frac{\sqrt{2}A(1 + \cos(\phi_k))}{\sqrt{[1 + \cos(\phi_k)] N_o / 2T_b}}\right) \\
&= Q\left(\frac{2A\sqrt{T_b [1 + \cos(\phi_k)]}}{\sqrt{N_o}}\right) = Q\left(2\sqrt{\frac{E_b [1 + \cos(\phi_k)]}{N_o}}\right).
\end{aligned} \tag{4.39}$$

The number of data symbols per OFDM frame is 192 as discussed in Chapter III. The indices of these data symbols are given as $k = 9, 10, \dots, 100, 156, 157, \dots, 255$. Thus, the average bit error probability P_b is given by

$$P_b = \frac{1}{192} \left(\sum_{k=9}^{100} Q \left(\sqrt{\frac{4[1 + \cos(\phi_k)] E_b}{N_o}} \right) + \sum_{k=156}^{255} Q \left(\sqrt{\frac{4[1 + \cos(\phi_k)] E_b}{N_o}} \right) \right). \quad (4.40)$$

The simulation was conducted with increasing E_b / N_o for 100,000 OFDM frames or 19.2 million data symbols per E_b / N_o value.

The simulated bit error rate (BER) for the MISO system is plotted in Figure 16 where $L = 2$ is the number of transmit antennas and $J = 1$ is the number of receive antennas. The theoretical probability of bit error as obtained in Equation (4.40) is also plotted. For comparison of performances, this figure also includes the theoretical probability of bit error for a baseband equivalent SISO system. The simulated results follow the theoretical results very closely. The MISO system with MDDM performs better than the SISO system for lower E_b / N_o values and the performance of the MISO system is poorer than that of SISO system for E_b / N_o greater than 6.5 dB.

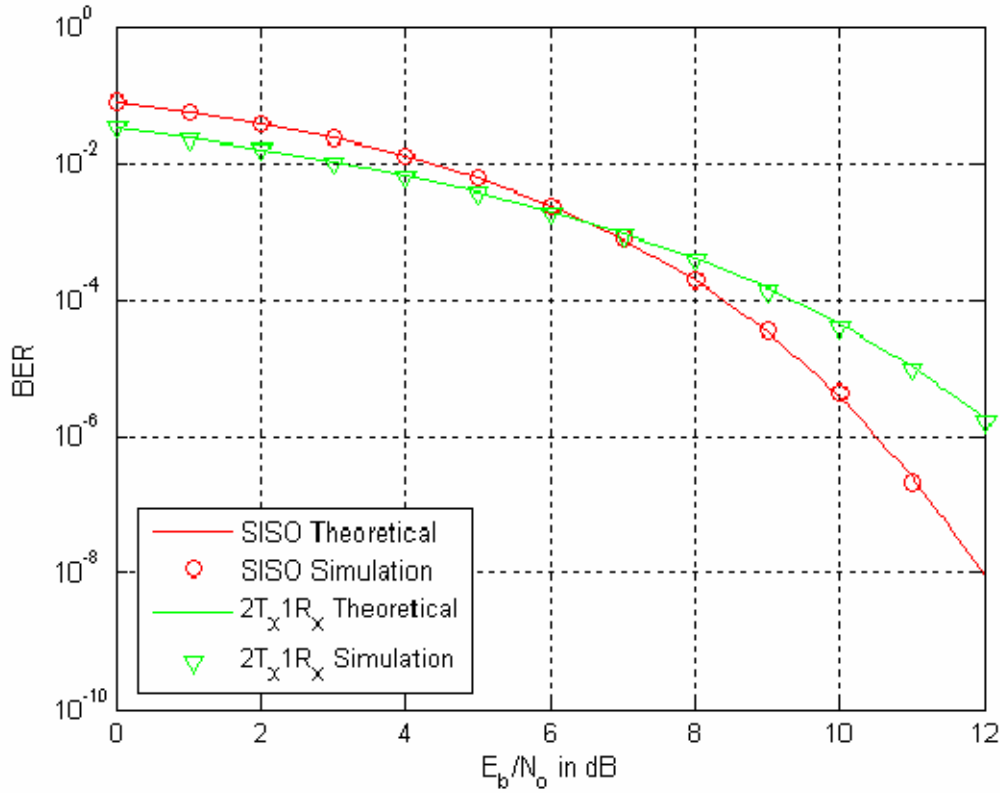


Figure 16 Results of MDDM MISO System in AWGN

2. Performance Analysis of MIMO System with Two Transmit and Two Receive Antennas

For the MDDM MIMO system with two receive antennas, it is assumed that the signal receptions at both the antennas are uncorrelated and signals are received at the same time without any relative delay. The received signals at both receive antennas are given by

$$\begin{aligned} r_m^1 &= x_m^1 + x_m^2 + n_m^1 \\ r_m^2 &= x_m^1 + x_m^2 + n_m^2. \end{aligned} \quad (4.41)$$

After the FFT operation the signals can be represented as

$$\begin{aligned} R_k^1 &= X_k^1 + X_k^2 + N_k^1 \\ R_k^2 &= X_k^1 + X_k^2 + N_k^2. \end{aligned} \quad (4.42)$$

Substituting Equation (2.31) and (4.19) into Equation (4.42) gives

$$\begin{aligned} R_k^1 &= X_k^1 + X_k^1 e^{-j2\pi k/N} + N_k^1 \\ R_k^2 &= X_k^1 + X_k^1 e^{-j2\pi k/N} + N_k^2 \\ R_k^1 &= (1 + e^{-j\phi_k}) X_k^1 + N_k^1 \\ R_k^2 &= (1 + e^{-j\phi_k}) X_k^1 + N_k^2. \end{aligned} \quad (4.43)$$

Following the derivation of Equation (4.23), Equation (4.43) converts to

$$\begin{aligned} Z_k^1 &= R_k^1(1 + e^{+j\phi_k}) = [2 + 2\cos(\phi_k)] X_k^1 + (1 + e^{+j\phi_k}) N_k^1 \\ Z_k^2 &= R_k^2(1 + e^{+j\phi_k}) = [2 + 2\cos(\phi_k)] X_k^1 + (1 + e^{+j\phi_k}) N_k^2. \end{aligned} \quad (4.44)$$

Now both space diversity receptions are combined to form random variable Z_k which is given by

$$\begin{aligned} Z_k &= Z_k^1 + Z_k^2 \\ &= [4 + 4\cos(\phi_k)] X_k^1 + (1 + e^{+j\phi_k}) N_k^1 + (1 + e^{+j\phi_k}) N_k^2 \\ &= 4[1 + \cos(\phi_k)] \frac{A}{\sqrt{2}} + (1 + e^{+j\phi_k}) N_k^1 + (1 + e^{+j\phi_k}) N_k^2 \\ &= 2\sqrt{2}A[1 + \cos(\phi_k)] + (1 + e^{+j\phi_k}) N_k^1 + (1 + e^{+j\phi_k}) N_k^2. \end{aligned} \quad (4.45)$$

If correlation demodulator conditions are assumed, then

$$\begin{aligned} E\{Z_k \mid \text{"0" was transmitted}\} &= E\left\{\frac{1}{T_b} \int_0^{T_b} Z_k dt\right\} \\ &= 2\sqrt{2}A(1 + \cos(\phi_k)). \end{aligned} \quad (4.46)$$

The variance of $\zeta_k = \text{Re}\{Z_k\}$ is only due to the variance of real part of noise components [15, 16]. Noise components at both receive antennas are IID Gaussian random variables. Therefore the total variance of the sum of two noise components is the sum of their individual variances [18]. The total noise variance is given as

$$\sigma_{\zeta_k}^2 = \sigma_{\zeta_k^1}^2 + \sigma_{\zeta_k^2}^2 \quad (4.47)$$

where $\zeta_k^1 = \text{Re}\{Z_k^1\}$ and $\zeta_k^2 = \text{Re}\{Z_k^2\}$. Following the derivation of noise variance derived in Equation (4.37), Equation (4.47) is represented as

$$\begin{aligned} \sigma_{\zeta_k}^2 &= \frac{[1 + \cos(\phi_k)]N_o}{2T_b} + \frac{[1 + \cos(\phi_k)]N_o}{2T_b} \\ &= \frac{[1 + \cos(\phi_k)]N_o}{T_b} \end{aligned} \quad (4.48)$$

and σ_{ζ_k} is given as

$$\sigma_{\zeta_k} = \sqrt{\frac{(1 + \cos(\phi_k))N_o}{T_b}}. \quad (4.49)$$

Following the derivation of Equation (4.39), the bit error probability P_b' conditioned on the value ϕ_k is given by

$$\begin{aligned} P_b' &= Q\left(\frac{2\sqrt{2}[1 + \cos(\phi_k)]A}{\sqrt{[1 + \cos(\phi_k)]N_o/T_b}}\right) \\ &= Q\left(\sqrt{\frac{8[1 + \cos(\phi_k)]A^2T_b}{N_o}}\right) \\ &= Q\left(\sqrt{\frac{8[1 + \cos(\phi_k)]E_b}{N_o}}\right). \end{aligned} \quad (4.50)$$

Following the derivation of Equation (4.40) the average probability of bit error P_b for a MDDM MIMO system with two transmit and two receiving antennas is given by

$$P_b = \frac{1}{192} \left(\sum_{k=9}^{100} Q \left(\sqrt{\frac{8(1 + \cos(\phi_k))E_b}{N_o}} \right) + \sum_{k=156}^{255} Q \left(\sqrt{\frac{8(1 + \cos(\phi_k))E_b}{N_o}} \right) \right). \quad (4.51)$$

The simulation was conducted for the same number of OFDM frames or data symbols as mentioned in the previous section. The simulated bit error rate (BER) for the MIMO system is plotted in Figure 17. The simulated results follow theoretical results very closely.

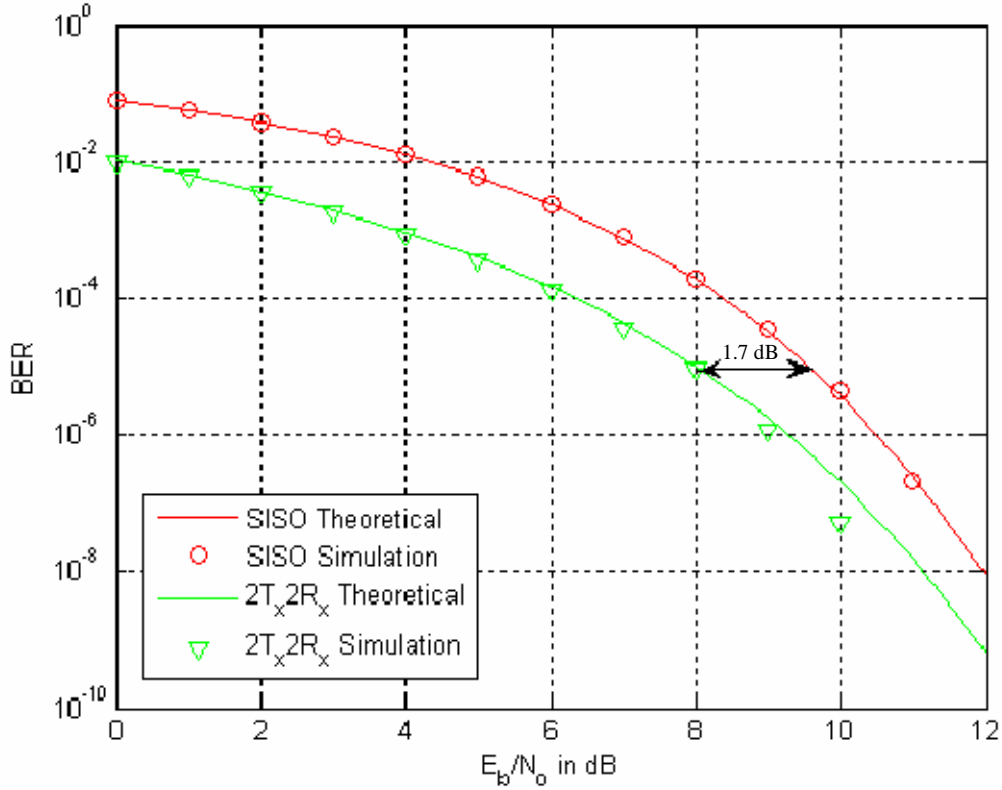


Figure 17 Results of MDDM MIMO System in AWGN

3. Performance Analysis of MIMO System with Two Transmit and Three Receive Antennas

Similarly, in this section, the performance analysis of MDDM MIMO system with two transmit and three receive antennas is discussed. Exploiting the symmetry of the receiver design, the derivation of results is mainly based on the results presented in the

last two sections. It is also assumed that the signal receptions at all antennas are uncorrelated and signals are received at the same time without any relative delay. The received signals at the three receive antennas are given by

$$\begin{aligned} r_m^1 &= x_m^1 + x_m^2 + n_m^1 \\ r_m^2 &= x_m^1 + x_m^2 + n_m^2 \\ r_m^3 &= x_m^1 + x_m^2 + n_m^3. \end{aligned} \quad (4.52)$$

After the FFT operation the signals are represented as

$$\begin{aligned} R_k^1 &= X_k^1 + X_k^2 + N_k^1 \\ R_k^2 &= X_k^1 + X_k^2 + N_k^2 \\ R_k^3 &= X_k^1 + X_k^2 + N_k^3. \end{aligned} \quad (4.53)$$

Based on the discussion in previous sections, the components of the variables from all the space diversity receptions are

$$\begin{aligned} Z_k^1 &= R_k^1(1 + e^{+j\phi_k}) = [2 + 2\cos(\phi_k)]X_k^1 + (1 + e^{+j\phi_k})N_k^1 \\ Z_k^2 &= R_k^2(1 + e^{+j\phi_k}) = [2 + 2\cos(\phi_k)]X_k^1 + (1 + e^{+j\phi_k})N_k^2 \\ Z_k^3 &= R_k^3(1 + e^{+j\phi_k}) = [2 + 2\cos(\phi_k)]X_k^1 + (1 + e^{+j\phi_k})N_k^3. \end{aligned} \quad (4.54)$$

Now all the space diversity receptions are combined to form random variable Z_k which is given by

$$\begin{aligned} Z_k &= Z_k^1 + Z_k^2 + Z_k^3 \\ &= 6[1 + \cos(\phi_k)]X_k^1 + (1 + e^{j\phi_k})N_k^1 + (1 + e^{j\phi_k})N_k^2 + (1 + e^{j\phi_k})N_k^3. \end{aligned} \quad (4.55)$$

If correlation demodulator conditions are assumed, then

$$\begin{aligned} E\{Z_k \mid "0" \text{ was transmitted}\} &= E\left\{\frac{1}{T_b} \int_0^{T_b} [2\sqrt{2}A(1 + \cos\phi_k) + N_k(1 + e^{+j\phi_k})] dt\right\} \\ &= 2\sqrt{2}A[1 + \cos(\phi_k)]. \end{aligned} \quad (4.56)$$

The variance of $\zeta_k = \text{Re}\{Z_k\}$ is only due to the variance of real part of noise components [15, 16]. Noise components at all the receive antennas are IID Gaussian

random variables. Therefore the total variance of the sum of three noise components is the sum of their individual variances [18]. The total noise variance is given as

$$\sigma_{\zeta_k}^2 = \sigma_{\zeta_k^1}^2 + \sigma_{\zeta_k^2}^2 + \sigma_{\zeta_k^3}^2 \quad (4.57)$$

where $\zeta_k^1 = \text{Re}\{Z_k^1\}$, $\zeta_k^2 = \text{Re}\{Z_k^2\}$ and $\zeta_k^3 = \text{Re}\{Z_k^3\}$. Following the derivation of noise variance derived in Equation (4.37), Equation (4.57) is represented as

$$\sigma_{\zeta_k}^2 = \frac{3[1 + \cos(\phi_k)]N_o}{2T_b} \quad (4.58)$$

and σ_{ζ_k} is

$$\sigma_{\zeta_k} = \sqrt{\frac{3[1 + \cos(\phi_k)]N_o}{2T_b}}. \quad (4.59)$$

Following the derivation of Equation (4.39), the bit error probability P_b' conditioned on the value ϕ_k is given by

$$\begin{aligned} P_b' &= Q\left(\frac{3\sqrt{2}[1 + \cos(\phi_k)]A}{\sqrt{3[1 + \cos(\phi_k)]N_o / 2T_b}}\right) \\ &= Q\left(\sqrt{\frac{12[1 + \cos(\phi_k)]A^2T_b}{N_o}}\right) \\ &= Q\left(\sqrt{\frac{12[1 + \cos(\phi_k)]E_b}{N_o}}\right). \end{aligned} \quad (4.60)$$

The average probability of bit error P_b for this case can be obtained by

$$P_b = \frac{1}{192} \left(\sum_{k=9}^{100} Q\left(\sqrt{\frac{12[1 + \cos(\phi_k)]E_b}{N_o}}\right) + \sum_{k=156}^{255} Q\left(\sqrt{\frac{12[1 + \cos(\phi_k)]E_b}{N_o}}\right) \right). \quad (4.61)$$

The simulation was conducted for the same number of OFDM frames or data symbols as mentioned in the previous section. The simulated bit error rate (BER) for the MIMO system is plotted in Figure 18. The simulated results follow theoretical results very closely.

A comparison of Equations (4.40), (4.51) and (4.61) clearly reveals that the improvement factor increases linearly with increasing number of receiving antenna. Thus, the average probability of bit error in AWGN channel for MDDM scheme discussed in this thesis with J receiving antenna can be represented in general form as

$$P_b = \frac{1}{192} \left(\sum_{k=9}^{100} Q \left(\sqrt{\frac{4J(1 + \cos(\phi_k))E_b}{N_o}} \right) + \sum_{k=156}^{255} Q \left(\sqrt{\frac{4J(1 + \cos(\phi_k))E_b}{N_o}} \right) \right). \quad (4.62)$$

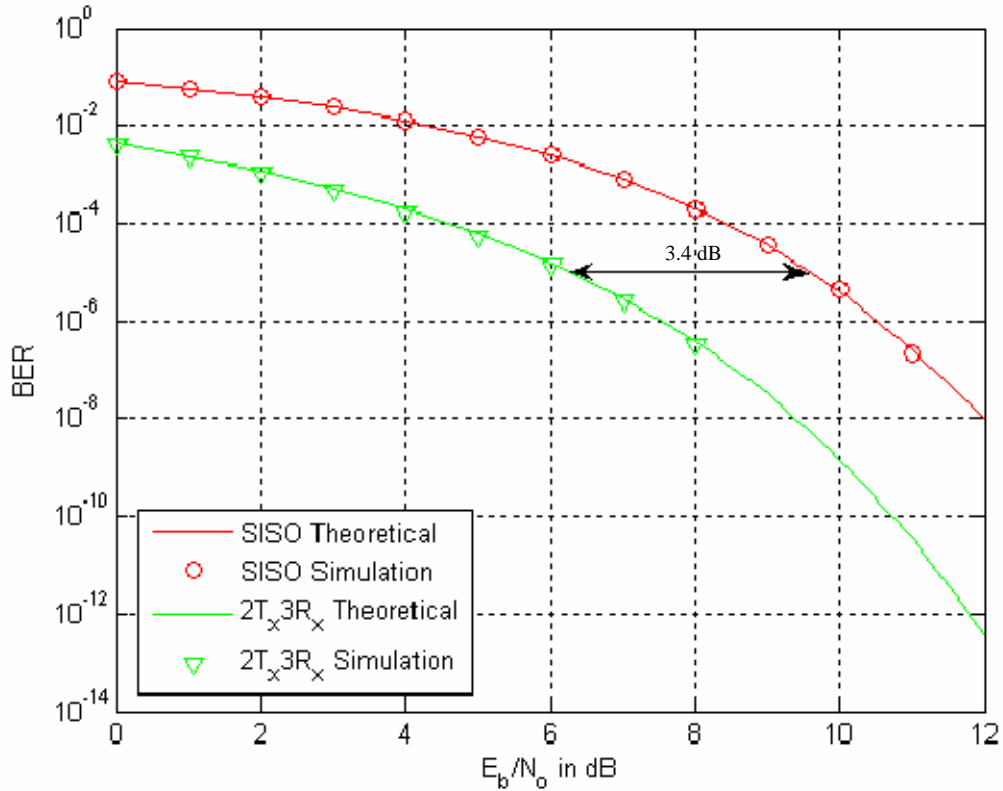


Figure 18 Results of MDDM MIMO System in AWGN

D. SIMULATION AND PERFORMANCE ANALYSIS OF MDDM IN A MULTIPATH FADING CHANNEL

Next, the MDDM scheme was simulated and analyzed with the effect of a slow fading frequency nonselective channel. The multipath model for the slow Rayleigh fading channel was discussed in Chapter II. A multipath fading channel is inserted in Figure 15 from each transmit antenna to each receive antenna. A block diagram of the MIMO

system with slow fading frequency nonselective channel plus AWGN is illustrated in Figure 19. It is assumed that the each channel frequency response remains constant for an OFDM symbol duration. Therefore the channel is slow fading. The simulated channel response is the complex sum of two IID Gaussian random sources. The block model of channel response is illustrated in Figure 20. In simulation, each channel response is multiplied with the transmitted signal from the respective antenna and input to the AWGN block of respective receive antenna.

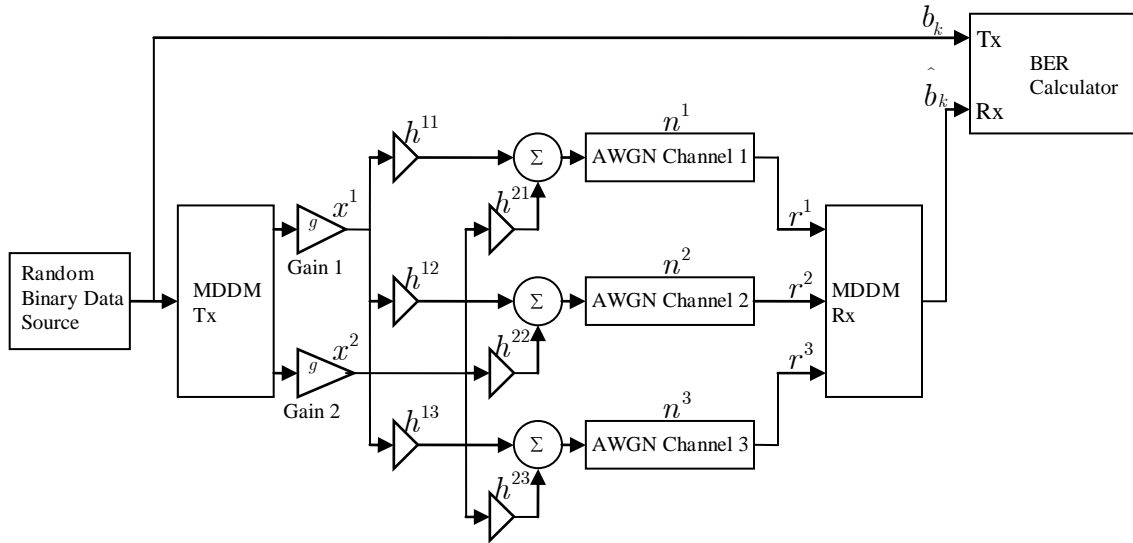


Figure 19 Simulation of MDDM MIMO System in Multipath

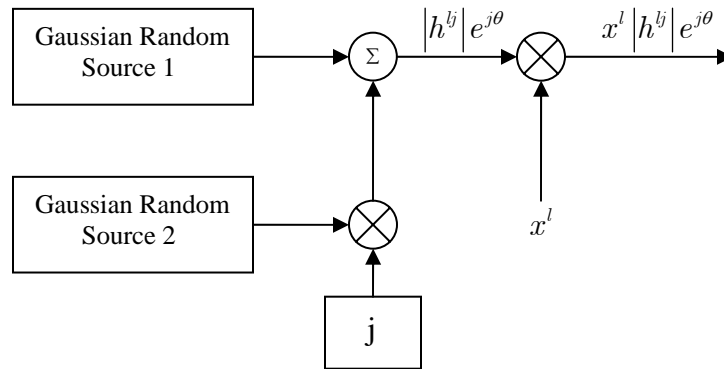


Figure 20 Simulation of Channel Response

Each Gaussian random source generates a zero mean random variable. In this simulation model, the variance of each Gaussian source is equal and is set to a value such that the variance of the complex sum of these Gaussian random sources is one. Using Equation (2.52), the channel response from transmit antenna l to receive antenna j is represented as

$$\begin{aligned} h^{lj} &= |h^{lj}| e^{j\theta_{lj}} \\ &= X + jY \end{aligned} \quad (4.63)$$

where X and Y are IID Gaussian random variables with zero mean and equal variance. The variance of the complex sum can be given as

$$\begin{aligned} \sigma_{h^{lj}}^2 &= E \{ h^{lj} h^{lj*} \} - \left(|E \{ h^{lj} \}| \right)^2 \\ &= E \{ (X + jY)(X + jY)^* \} \\ &= E \{ X^2 + Y^2 \} \\ &= \sigma_X^2 + \sigma_Y^2 \\ &= 1. \end{aligned} \quad (4.64)$$

Thus the variance of each Gaussian random source was set as

$$\sigma_X^2 = \sigma_Y^2 = 1/2. \quad (4.65)$$

1. Performance Analysis of MISO System with Two Transmit and One Receive Antenna

At the receive antenna, the signal r_m is written as

$$r_m = h^{11}x_m^1 + h^{21}x_m^2 + n_m. \quad (4.66)$$

where h^{11} and h^{21} are channel responses from transmit antenna 1 and 2 to the receive antenna respectively. These channel responses are assumed independent. After the FFT operation, the signal is written as

$$\text{FFT}[r_m] = \text{FFT}[h^{11}x_m^1 + h^{21}x_m^2 + n_m]. \quad (4.67)$$

All the channel responses are considered constant for the duration of an OFDM symbol for the slow fading channel. Now, Equation (4.67) can be written as

$$R_k = h^{11}X_k^1 + h^{21}X_k^2 + N_k. \quad (4.68)$$

Substituting Equation (2.31) , (4.16) and (4.20) into Equation (4.68) yields

$$\begin{aligned} R_k &= h^{11} X_k^1 + h^{21} X_k^1 e^{-j\phi_k} + N_k \\ R_k &= (h^{11} + h^{21} e^{-j\phi_k}) X_k^1 + N_k \end{aligned} \quad (4.69)$$

where N_k is AWGN in the frequency domain and $(h^{11} + h^{21} e^{-j\phi_k})$ is the effective channel response for the MDDM in the multipath channel. In Equation (4.69) h^{21} is a random variable with Rayleigh distributed amplitude and phase uniformly distributed on $(-\pi, \pi]$. Thus, multiplying h^{21} by $e^{-j\phi_k}$ does not change the statistics of the random variable and their product is represented as $h^{21'}$. Now, the effective channel response can be written as

$$H^1 = h^{11} + h^{21'} \quad (4.70)$$

Using the MRC receiver as shown in Figure 14, Equation (4.69) is multiplied by the complex conjugate of the effective channel response and the random variable Z_k is represented as

$$Z_k = H^1 H^{1*} X_k^1 + H^{1*} N_k. \quad (4.71)$$

Now, Equation (4.71) can be written as

$$\begin{aligned} Z_k &= |H^1|^2 X_k^1 + H^{1*} N_k \\ &= (h^{11} + h^{21'}) (h^{11} + h^{21'})^* X_k^1 + (h^{11} + h^{21'})^* N_k \\ &= (|h^{11}|^2 + |h^{21'}|^2 + 2(h_I^{11} h_I^{21'} + h_Q^{11} h_Q^{21'})) X_k^1 + (h^{11} + h^{21'})^* N_k \end{aligned} \quad (4.72)$$

where $h^{ij} = h_I^{ij} + j h_Q^{ij}$, i.e. h_I^{ij} and h_Q^{ij} are the inphase and quadrature components of the respective channel responses.

For a fixed set of channel responses Equation (4.72) represents a complex Gaussian random variable Z_k due to AWGN [16]. To demodulate the BPSK signal, the real part of the decision variable Z_k , $\zeta_k = \text{Re}\{Z_k\}$, is compared with a threshold as given in Table 3. If correlation demodulator conditions are assumed, then

$$\begin{aligned}
\overline{\zeta_k^+} &= E \{ \text{Re} \{ Z_k \} \mid \text{"0" was transmitted} \} \\
&= E \left\{ \frac{1}{T_b} \int_0^{T_b} \left[|h^{11}|^2 + |h^{21}|^2 + 2(h_I^{11}h_I^{21} + h_Q^{11}h_Q^{21})X_k^1 + (h^{11} + h^{21})^* N_k \right] dt \right\} \quad (4.73) \\
&= \left[|h^{11}|^2 + |h^{21}|^2 + 2(h_I^{11}h_I^{21} + h_Q^{11}h_Q^{21}) \right] \frac{A}{\sqrt{2}}
\end{aligned}$$

The variance of ζ_k is only due to the variance of real part of the noise component $H^{1*} N_k$ [15, 16] and is represented as

$$\begin{aligned}
\sigma_{\zeta_k}^2 &= E \left\{ \left(\text{Re} [H^{1*} N_k] \right)^2 \right\} - \left(E \{ \text{Re} [H^{1*} N_k] \} \right)^2 \\
&= E \left\{ \left(\text{Re} [H^{1*} N_k] \right)^2 \right\} \quad (4.74)
\end{aligned}$$

where $E \{ \}$ represents the expected value. η_k is the real part of noise component with zero mean which can be written as

$$\eta_k = \text{Re} [H^{1*} N_k] = \frac{1}{2} (H^{1*} N_k + H^1 N_k^*) \quad (4.75)$$

And

$$\begin{aligned}
\eta_k^2 &= \left(\text{Re} [H^{1*} N_k] \right)^2 = \left(\frac{1}{2} (H^{1*} N_k + H^1 N_k^*) \right)^2 \\
&= \frac{1}{4} \left((H^{1*})^2 N_k^2 + (H^1)^2 (N_k^*)^2 + 2H^1 H^{1*} N_k N_k^* \right) \quad (4.76) \\
&= \frac{1}{4} \left((H^{1*})^2 N_k^2 + (H^1)^2 (N_k^*)^2 + 2|H^1|^2 N_k N_k^* \right).
\end{aligned}$$

Substituting Equation (4.74) into Equation (4.75) yields

$$\begin{aligned}
\sigma_{\zeta_k}^2 &= E \left\{ \frac{1}{4} \left((H^{1*})^2 N_k^2 + (H^1)^2 (N_k^*)^2 + 2|H^1|^2 N_k N_k^* \right) \right\} \\
&= \frac{1}{4} \left((H^{1*})^2 E \{ (N_k)^2 \} + (H^1)^2 E \{ (N_k^*)^2 \} + 2|H^1|^2 E \{ N_k N_k^* \} \right). \quad (4.77)
\end{aligned}$$

N_k is a complex Gaussian random variable with zero mean, therefore

$$E \{ (N_k)^2 \} = E \{ (N_k^*)^2 \} = 0. \quad (4.78)$$

Substituting Equation (4.78) into Equation (4.77) yields

$$\begin{aligned}
\sigma_{\zeta_k}^2 &= \frac{2}{4} |H^1|^2 \mathbb{E}\{N_k N_k^*\} \\
&= \frac{1}{2} \left(|h^{11}|^2 + |h^{21'}|^2 + 2(h_I^{11} h_I^{21'} + h_Q^{11} h_Q^{21'}) \right) \mathbb{E}\{N_k N_k^*\}.
\end{aligned} \tag{4.79}$$

Now, Equation (4.79) can be written as

$$\begin{aligned}
\sigma_{\zeta_k}^2 &= \frac{1}{2} \left[|h^{11}|^2 + |h^{21'}|^2 + 2(h_I^{11} h_I^{21'} + h_Q^{11} h_Q^{21'}) \right] \frac{N_o}{2T_b} \\
\sigma_{\zeta_k} &= \sqrt{\left[|h^{11}|^2 + |h^{21'}|^2 + 2(h_I^{11} h_I^{21'} + h_Q^{11} h_Q^{21'}) \right] \frac{N_o}{4T_b}}.
\end{aligned} \tag{4.80}$$

Now, the conditional bit error probability can be represented as

$$\begin{aligned}
P'_b &= \Pr\{\zeta_k < 0 \mid \text{"0" was sent}\} \\
&= \Pr\left\{ \frac{\zeta_k - \overline{\zeta_k^+}}{\sigma_{\zeta_k}} < -\frac{\overline{\zeta_k^+}}{\sigma_{\zeta_k}} \mid \text{"0"} \right\} \\
&= \Pr\left\{ \frac{\zeta_k - \overline{\zeta_k^+}}{\sigma_{\zeta_k}} > \frac{\overline{\zeta_k^+}}{\sigma_{\zeta_k}} \mid \text{"0"} \right\} \\
&= Q\left(\frac{\overline{\zeta_k^+}}{\sigma_{\zeta_k}} \right) \\
&= Q\left(\frac{\left(|h^{11}|^2 + |h^{21'}|^2 + 2(h_I^{11} h_I^{21'} + h_Q^{11} h_Q^{21'}) \right) A / \sqrt{2}}{\sqrt{\left(|h^{11}|^2 + |h^{21'}|^2 + 2(h_I^{11} h_I^{21'} + h_Q^{11} h_Q^{21'}) \right) N_o / 4T_b}} \right) \\
&= Q\left(\sqrt{\frac{2A^2 T_b \left(|h^{11}|^2 + |h^{21'}|^2 + 2(h_I^{11} h_I^{21'} + h_Q^{11} h_Q^{21'}) \right)}{N_o}} \right)
\end{aligned} \tag{4.81}$$

or

$$P'_b(\beta_1) = Q\left(\sqrt{\frac{2E_b \beta_1}{N_o}} \right) \tag{4.82}$$

where β_1 is given as

$$\beta_1 = |h^{11}|^2 + |h^{21'}|^2 + 2(h_I^{11} h_I^{21'} + h_Q^{11} h_Q^{21'}). \tag{4.83}$$

Equation (4.82) depicts the bit error probability of a MDDM MISO system conditioned on the random variable β_1 . The performance of an MDDM MISO system over a

frequency nonselective, slowly fading Rayleigh channel with MRC can be obtained by taking the average of the conditional bit error probability over all possible values of the random variable β_1 . Now, the unconditional bit error probability can be given as

$$\begin{aligned} P_b &= \int_0^{\infty} P_b(\beta_1) f_{\beta_1}(\beta_1) d\beta_1 \\ &= \int_0^{\infty} Q\left(\sqrt{2E_b\beta_1 / N_o}\right) f_{\beta_1}(\beta_1) d\beta_1 \end{aligned} \quad (4.84)$$

where $f_{\beta_1}(\beta_1)$ is the probability density function for β_1 .

The random variable β_1 as defined in Equation (4.83) is a sum of two central chi squared random variables of degree two, $|h^{11}|^2$ and $|h^{21'}|^2$, and two products of Gaussian random variables, $2h_t^{11}h_t^{21'}$ and $2h_q^{11}h_q^{21'}$. These central chi squared random variables and Gaussian random variables are also correlated. The probability density function of the random variable β_1 and integral of Equation (4.84) were computed numerically.

The random variable β_1 was generated in Matlab by taking one million samples each of channel response h^{11} and $h^{21'}$. The effective channel response was multiplied by its complex conjugate. The distribution of β_1 over its range was obtained by evaluating a histogram of 500 equally spaced bins with the help of the Matlab function *hist*. The distribution of the data was interpolated by cubic spline data interpolation with the help of the Matlab function *spline*. After data interpolation, this data distribution curve was normalized to make the total area under the distribution curve equal to one. Then, the probability over all possible values was interpolated by using the Matlab function *spline*. At the end, the average probability of bit error was computed numerically over all the possible values of the random variable β_1 . The Matlab code is presented in Appendix B. [21]

The simulated and the numerically computed theoretical results of a MISO system over frequency nonselective slowly fading Rayleigh channel are shown in Figure 21. For the comparison of the performances, the theoretical bit error rate (BER) of the BPSK SISO system as obtained in Equation (2.127) is also plotted along with the bit error probability obtained from the simulation. The simulated results are close to the

theoretical results for lower values of E_b/N_o and for higher values of E_b/N_o the theoretical results are more optimistic. This may be due to the use of the Matlab function *spline* to interpolate the probability distribution function of the random variable β_1 . Further analysis could be carried out to determine the causes of this deviation. It was not investigated further in this work. Figure 21 clearly shows that the performance of the MDDM MISO system is better than the SISO system.

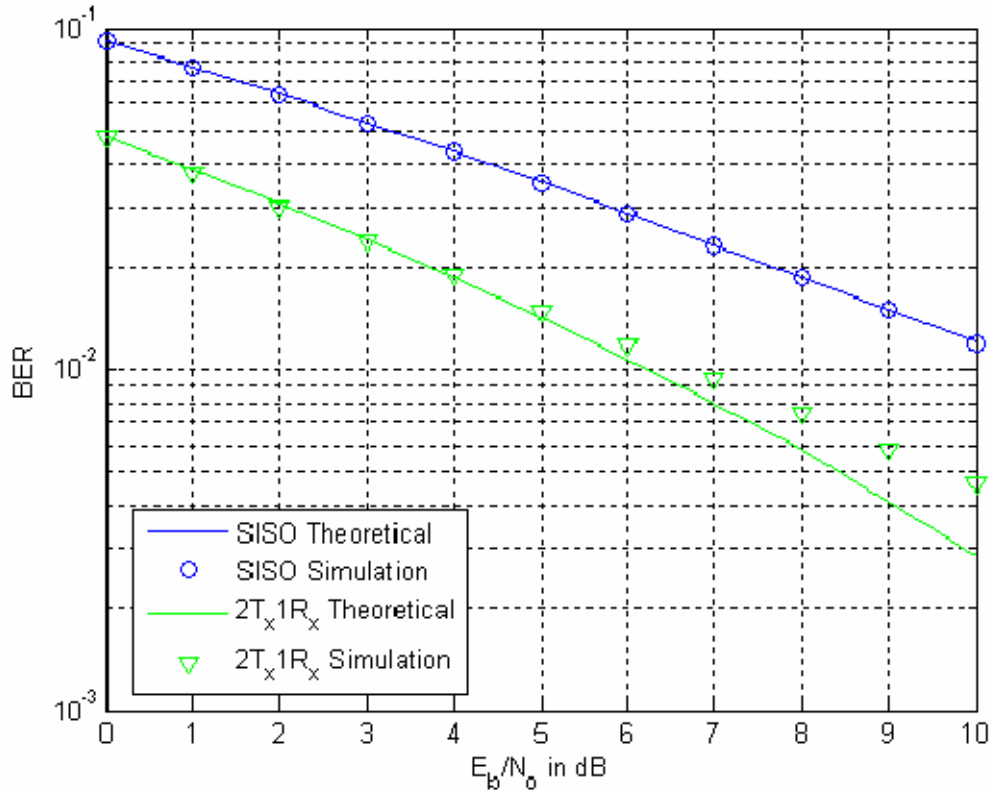


Figure 21 Results of MDDM MISO System in Slow Rayleigh Fading Channel

2. Performance Analysis of MIMO System with Two Transmit and Two Receive Antennas

In this section, the performance analysis of a MIMO system with two transmit and two receive antennas is presented. The simulation model and analysis are mainly based on the previous section. At each of the receive antennas, the received signals are given by

$$\begin{aligned} r_m^1 &= h^{11}x_m^1 + h^{21}x_m^2 + n_m^1 \\ r_m^2 &= h^{12}x_m^1 + h^{22}x_m^2 + n_m^2. \end{aligned} \quad (4.85)$$

where h^{lj} represents channel response from transmit antenna l to receive antenna j and r_m^j is the received signal at receive antenna j . It is considered that all the channel responses are independent and the reception of the signals at both the antennas is uncorrelated. After the FFT operation the signals are represented as

$$\begin{aligned}\text{FFT}[r_m^1] &= \text{FFT}[h^{11}x_m^1 + h^{21}x_m^2 + n_m^1] \\ \text{FFT}[r_m^2] &= \text{FFT}[h^{12}x_m^1 + h^{22}x_m^2 + n_m^2].\end{aligned}\tag{4.86}$$

All the channel responses are considered constant for the duration of an OFDM symbol. Now, Equation (4.86) can be written as

$$\begin{aligned}R_k^1 &= h^{11}X_k^1 + h^{21}X_k^2 + N_k^1 \\ R_k^2 &= h^{12}X_k^1 + h^{22}X_k^2 + N_k^2.\end{aligned}\tag{4.87}$$

Substituting Equations (2.31), (4.16) and (4.20) into Equations (4.87) yields

$$\begin{aligned}R_k^1 &= h^{11}X_k^1 + h^{21}X_k^1e^{-j\phi_k} + N_k^1 \\ R_k^2 &= h^{12}X_k^1 + h^{22}X_k^1e^{-j\phi_k} + N_k^2 \\ R_k^1 &= (h^{11} + h^{21}e^{-j\phi_k})X_k^1 + N_k^1 \\ R_k^2 &= (h^{12} + h^{22}e^{-j\phi_k})X_k^1 + N_k^2\end{aligned}\tag{4.88}$$

where N_k^j is AWGN in the frequency domain at receive antenna j , $(h^{11} + h^{21}e^{-j\phi_k})$ is the effective channel response at receive antenna 1 and $(h^{12} + h^{22}e^{-j\phi_k})$ is the effective channel response at receive antenna 2. In Equation (4.88), all h^{lj} ($l = 1, 2$ and $j = 1, 2$) are random variables with Rayleigh distributed amplitude and phase uniformly distributed on $(-\pi, \pi]$. Thus, multiplying h^{21} and h^{22} by $e^{-j\phi_k}$ does not change the statistics of both the random variables and their respective products are represented as $h^{21'} = h^{21}e^{-j\phi_k}$ and $h^{22'} = h^{22}e^{-j\phi_k}$. Now, the effective channel responses are written as

$$\begin{aligned}H^1 &= h^{11} + h^{21'} \\ H^2 &= h^{12} + h^{22'}.\end{aligned}\tag{4.89}$$

Using the MRC receiver as shown in Figure 14, Equation (4.88) is multiplied by the complex conjugate of the effective channel response and the random variables for respective diversity receptions are given by

$$\begin{aligned}
Z_k^1 &= H^1 H^{1*} X_k^1 + H^{1*} N_k^1 \\
Z_k^2 &= H^2 H^{2*} X_k^1 + H^{2*} N_k^2 \\
Z_k^1 &= |H^1|^2 X_k^1 + H^{1*} N_k^1 \\
Z_k^2 &= |H^2|^2 X_k^1 + H^{2*} N_k^2.
\end{aligned} \tag{4.90}$$

Now Equations (4.90) can be expressed as

$$\begin{aligned}
Z_k^1 &= \left(|h^{11}|^2 + |h^{21}|^2 + 2(h_I^{11} h_I^{21} + h_Q^{11} h_Q^{21}) \right) X_k^1 + (h^{11} + h^{21})^* N_k^1 \\
Z_k^2 &= \left(|h^{12}|^2 + |h^{22}|^2 + 2(h_I^{12} h_I^{22} + h_Q^{12} h_Q^{22}) \right) X_k^1 + (h^{12} + h^{22})^* N_k^2
\end{aligned} \tag{4.91}$$

where $h_I^{lj} = \text{Re}\{h^{lj}\}$ and $h_Q^{lj} = \text{Im}\{h^{lj}\}$ are the inphase and quadrature components of the respective channel responses.

After combining both the space diversity receptions in the MRC receiver the decision variable Z_k is given as

$$\begin{aligned}
Z_k &= Z_k^1 + Z_k^2 \\
&= |H^1|^2 X_k^1 + |H^2|^2 X_k^1 + H^{1*} N_k^1 + H^{2*} N_k^2 \\
&= \left(|H^1|^2 + |H^2|^2 \right) X_k^1 + H^{1*} N_k^1 + H^{2*} N_k^2.
\end{aligned} \tag{4.92}$$

For a fixed set of channel responses Equation (4.92) represents a complex Gaussian random variable Z_k due to AWGN [16]. To demodulate the BPSK signal, the real part of the decision variable Z_k , $\zeta_k = \text{Re}\{Z_k\}$, is compared with a threshold as given in Table 3. If correlation demodulator conditions are assumed, then

$$\begin{aligned}
\overline{\zeta_k^+} &= \mathbb{E} \left\{ \text{Re} \{ Z_k \} \mid \text{"0" was transmitted} \right\} \\
&= \mathbb{E} \left\{ \frac{1}{T_b} \int_0^{T_b} \left[\left(|H^1|^2 + |H^2|^2 \right) X_k^1 + H^{1*} N_k^1 + H^{2*} N_k^2 \right] dt \right\} \\
&= \frac{A}{\sqrt{2}} \left[|h^{11}|^2 + |h^{21}|^2 + 2 \left(h_I^{11} h_I^{21'} + h_Q^{11} h_Q^{21'} \right) + |h^{12}|^2 + |h^{22}|^2 + 2 \left(h_I^{12} h_I^{22'} + h_Q^{12} h_Q^{22'} \right) \right] \\
&= \frac{A\beta_2}{\sqrt{2}}
\end{aligned} \tag{4.93}$$

where

$$\begin{aligned}
\beta_2 &= |h^{11}|^2 + |h^{21}|^2 + |h^{12}|^2 + |h^{22}|^2 + 2 \left(h_I^{11} h_I^{21'} + h_Q^{11} h_Q^{21'} \right) + \\
&\quad 2 \left(h_I^{12} h_I^{22'} + h_Q^{12} h_Q^{22'} \right).
\end{aligned} \tag{4.94}$$

The variance of ζ_k is only due to the variance of real part of the noise components $H^{1*} N_k^1$ and $H^{2*} N_k^2$ [15, 16]. Noise components at both the receive antennas N_k^1 and N_k^2 are IID complex Gaussian random variables. Thus, the variance of their sum is the sum of their individual variances and is given as

$$\sigma_{\zeta_k}^2 = \sigma_{\zeta_k^1}^2 + \sigma_{\zeta_k^2}^2. \tag{4.95}$$

Following the results derived in the previous section from Equation (4.74) to (4.80), $\sigma_{\zeta_k}^2$ can be expressed as

$$\begin{aligned}
\sigma_{\zeta_k}^2 &= \frac{1}{2} |H^1|^2 \mathbb{E} \{ N_k^1 N_k^{1*} \} + \frac{1}{2} |H^2|^2 \mathbb{E} \{ N_k^2 N_k^{2*} \} \\
&= \frac{N_0}{4T_b} \left[|h^{11}|^2 + |h^{21}|^2 + 2 \left(h_I^{11} h_I^{21'} + h_Q^{11} h_Q^{21'} \right) + \right. \\
&\quad \left. |h^{12}|^2 + |h^{22}|^2 + 2 \left(h_I^{12} h_I^{22'} + h_Q^{12} h_Q^{22'} \right) \right].
\end{aligned} \tag{4.96}$$

Substituting Equation (4.94) into Equation (4.96) yeilds

$$\begin{aligned}
\sigma_{\zeta_k}^2 &= \frac{N_0 \beta_2}{4T_b} \\
\sigma_{\zeta_k} &= \sqrt{\frac{N_0 \beta_2}{4T_b}}.
\end{aligned} \tag{4.97}$$

Now, substituting Equation (4.93) and (4.97) into Equation (4.3), the conditional bit error probability is represented as

$$\begin{aligned}
P_b(\beta_2) &= Q\left(\frac{A\beta_2 / \sqrt{2}}{\sqrt{\beta_2 N_o / 4T_b}}\right) \\
&= Q\left(\sqrt{\frac{2E_b\beta_2}{N_o}}\right).
\end{aligned} \tag{4.98}$$

Equation (4.98) represents the bit error probability of an MDDM MIMO system with two transmit antennas and two receive antennas conditioned on a random variable β_2 . The performance of the MDDM MIMO system over a frequency nonselective slowly fading Rayleigh channel with MRC can be obtained by taking the average of the conditional bit error probability over all possible values of random variable β_2 . Now the unconditional bit error probability can be given as

$$\begin{aligned}
P_b &= \int_0^{\infty} P_b(\beta_2) f_{\beta_2}(\beta_2) d\beta_2 \\
&= \int_0^{\infty} Q\left(\sqrt{2E_b\beta_2 / N_o}\right) f_{\beta_2}(\beta_2) d\beta_2
\end{aligned} \tag{4.99}$$

where $f_{\beta_2}(\beta_2)$ is the probability density function for β_2 .

The random variable β_2 as defined in Equation (4.94) is a sum of central chi squared random variables of degree two and products of Gaussian random variables. The central chi squared random variables and Gaussian random variables are also correlated. The probability density function of the random variable β_2 and integral of Equation (4.99) were computed numerically, using the same algorithm as discussed in previous section.

The simulated and the numerically computed theoretical results of the MIMO system with two transmit antennas and two receive antennas over a frequency nonselective slowly fading Rayleigh channel are shown in Figure 22. For the comparison of the performances, this figure also includes the theoretical and the simulated bit error probability of a BPSK SISO system. The simulation results, for low E_b / N_o values, deviate slightly from the theoretical results. The theoretical results are more optimistic for low E_b / N_o . The reason for this slight deviation may be the same as discussed in the previous section, however, this was not investigated in this work.

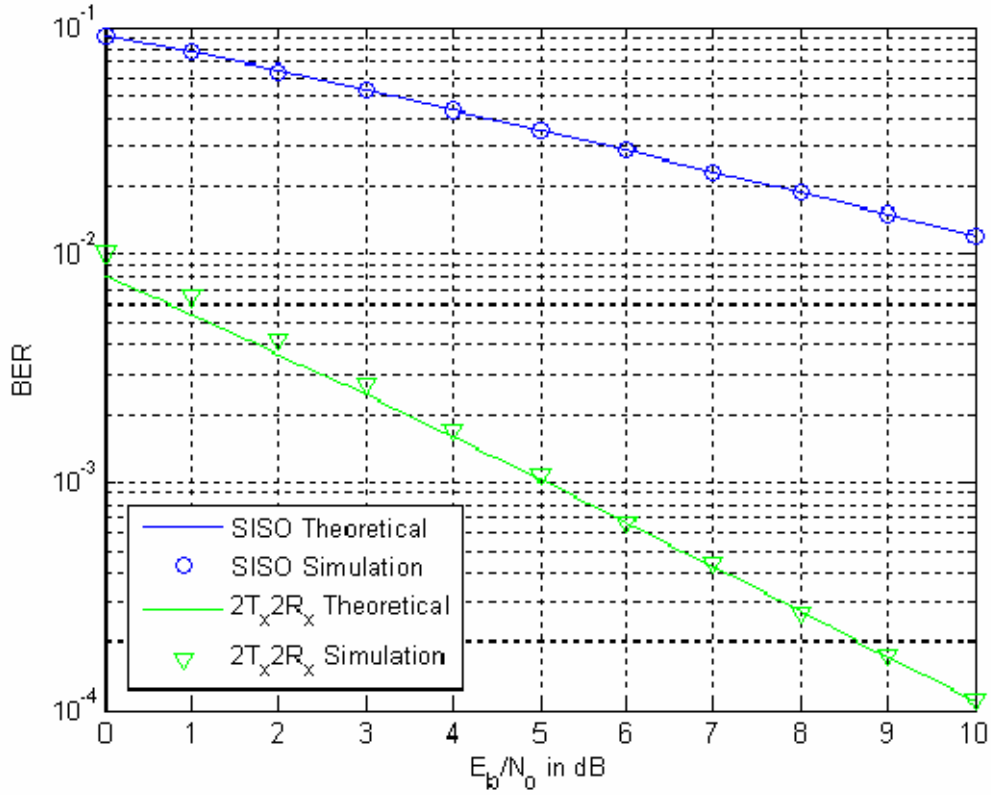


Figure 22 Results of MDDM MIMO System in Slow Rayleigh Fading Channel

3. Performance Analysis of MIMO System with Two Transmit and Three Receive Antennas

In this section the performance analysis of a MIMO system with two transmit and three receive antennas is presented. The scheme for building the simulation model and the analysis is the same as discussed in last two sections. At the receive antennas, the received signals are given by

$$\begin{aligned}
 r_m^1 &= h^{11}x_m^1 + h^{21}x_m^2 + n_m^1 \\
 r_m^2 &= h^{12}x_m^1 + h^{22}x_m^2 + n_m^2 \\
 r_m^3 &= h^{13}x_m^1 + h^{23}x_m^2 + n_m^3.
 \end{aligned} \tag{4.100}$$

After the FFT operation the signals are written as

$$\begin{aligned}
\text{FFT}[r_m^1] &= \text{FFT}[h^{11}x_m^1 + h^{21}x_m^2 + n_m^1] \\
\text{FFT}[r_m^2] &= \text{FFT}[h^{12}x_m^1 + h^{22}x_m^2 + n_m^2] \\
\text{FFT}[r_m^3] &= \text{FFT}[h^{13}x_m^1 + h^{23}x_m^2 + n_m^3].
\end{aligned} \tag{4.101}$$

All the channel responses are considered fixed for the duration of an OFDM symbol. Now, Equation (4.101) can be written as

$$\begin{aligned}
R_k^1 &= h^{11}X_k^1 + h^{21}X_k^2 + N_k^1 \\
R_k^2 &= h^{12}X_k^1 + h^{22}X_k^2 + N_k^2 \\
R_k^3 &= h^{13}X_k^1 + h^{23}X_k^2 + N_k^3.
\end{aligned} \tag{4.102}$$

Substituting Equations (2.31), (4.16) and (4.20) into Equations (4.102) yields

$$\begin{aligned}
R_k^1 &= h^{11}X_k^1 + h^{21}X_k^1e^{-j\phi_k} + N_k^1 \\
R_k^2 &= h^{12}X_k^1 + h^{22}X_k^1e^{-j\phi_k} + N_k^2 \\
R_k^3 &= h^{13}X_k^1 + h^{23}X_k^1e^{-j\phi_k} + N_k^3 \\
R_k^1 &= (h^{11} + h^{21}e^{-j\phi_k})X_k^1 + N_k^1 \\
R_k^2 &= (h^{12} + h^{22}e^{-j\phi_k})X_k^1 + N_k^2 \\
R_k^3 &= (h^{13} + h^{23}e^{-j\phi_k})X_k^1 + N_k^3
\end{aligned} \tag{4.103}$$

where N_k is AWGN in the frequency domain. $(h^{11} + h^{21}e^{-j\phi_k})$, $(h^{12} + h^{22}e^{-j\phi_k})$ and $(h^{13} + h^{23}e^{-j\phi_k})$ are the effective channel responses at receive antennas 1, 2 and 3 respectively. In Equation (4.103), all h^{lj} ($l = 1, 2$ and $j = 1, 2, 3$) are random variables with Rayleigh distributed amplitude and phase uniformly distributed in $(-\pi, \pi]$. Thus, multiplying h^{21} , h^{22} and h^{23} by $e^{-j\phi_k}$ does not change the statistics of these random variables and their respective products are represented as $h^{21'} = h^{21}e^{-j\phi_k}$, $h^{22'} = h^{22}e^{-j\phi_k}$ and $h^{23'} = h^{23}e^{-j\phi_k}$. Now, the effective channel responses are given as

$$\begin{aligned}
H^1 &= h^{11} + h^{21'} \\
H^2 &= h^{12} + h^{22'} \\
H^3 &= h^{13} + h^{23'}.
\end{aligned} \tag{4.104}$$

Using MRC receiver as shown in Figure 14, Equation (4.88) is multiplied by the complex conjugate of the effective channel response and the random variable Z_k^j at respective diversity receptions are written as

$$\begin{aligned}
Z_k^1 &= H^1 H^{1*} X_k^1 + H^{1*} N_k^1 \\
Z_k^2 &= H^2 H^{2*} X_k^1 + H^{2*} N_k^2 \\
Z_k^3 &= H^3 H^{3*} X_k^1 + H^{3*} N_k^3 \\
Z_k^1 &= |H^1|^2 X_k^1 + H^{1*} N_k^1 \\
Z_k^2 &= |H^2|^2 X_k^1 + H^{2*} N_k^2 \\
Z_k^3 &= |H^3|^2 X_k^1 + H^{3*} N_k^3.
\end{aligned} \tag{4.105}$$

Now, Equations (4.105) can be represented as

$$\begin{aligned}
Z_k^1 &= \left[|h^{11}|^2 + |h^{21}|^2 + 2(h_I^{11}h_I^{21} + h_Q^{11}h_Q^{21}) \right] X_k^1 + (h^{11} + h^{21})^* N_k^1 \\
Z_k^2 &= \left[|h^{12}|^2 + |h^{22}|^2 + 2(h_I^{12}h_I^{22} + h_Q^{12}h_Q^{22}) \right] X_k^1 + (h^{12} + h^{22})^* N_k^2 \\
Z_k^3 &= \left[|h^{13}|^2 + |h^{23}|^2 + 2(h_I^{13}h_I^{23} + h_Q^{13}h_Q^{23}) \right] X_k^1 + (h^{13} + h^{23})^* N_k^3
\end{aligned} \tag{4.106}$$

where $h_I^{lj} = \text{Re}\{h^{lj}\}$ and $h_Q^{lj} = \text{Im}\{h^{lj}\}$ are the inphase and quadrature components of the respective channel responses.

After combining all the space diversity receptions in the MRC receiver the decision variable Z_k is given as

$$\begin{aligned}
Z_k &= Z_k^1 + Z_k^2 + Z_k^3 \\
&= |H^1|^2 X_k^1 + |H^2|^2 X_k^1 + |H^3|^2 X_k^1 + H^{1*} N_k^1 + H^{2*} N_k^2 + H^{3*} N_k^3 \\
&= \left(|H^1|^2 + |H^2|^2 + |H^3|^2 \right) X_k^1 + H^{1*} N_k^1 + H^{2*} N_k^2 + H^{3*} N_k^3.
\end{aligned} \tag{4.107}$$

For a fixed set of channel responses Equation (4.107) represents a complex Gaussian random variable Z_k due to AWGN [16]. To demodulate the BPSK signal, the real part of the decision variable Z_k , $\zeta_k = \text{Re}\{Z_k\}$, is compared with a threshold as given in Table 3. If correlation demodulator conditions are assumed, then

$$\begin{aligned}
\overline{\zeta_k^+} &= \text{E} \{ \text{Re} \{ Z_k \} \mid \text{"0" was transmitted} \} \\
&= \text{E} \left\{ \frac{1}{T_b} \int_0^{T_b} \left[\left(|H^1|^2 + |H^2|^2 + |H^3|^2 \right) X_k^1 + H^{1*} N_k^1 + H^{2*} N_k^2 + H^{3*} N_k^3 \right] dt \right\} \\
&= \left(|H^1|^2 + |H^2|^2 + |H^3|^2 \right) X_k^1 \\
&= \frac{A}{\sqrt{2}} \left[|h^{11}|^2 + |h^{21}|^2 + 2(h_I^{11} h_I^{21'} + h_Q^{11} h_Q^{21'}) + |h^{12}|^2 + |h^{22}|^2 + \right. \\
&\quad \left. 2(h_I^{12} h_I^{22'} + h_Q^{12} h_Q^{22'}) + |h^{13}|^2 + |h^{23}|^2 + 2(h_I^{13} h_I^{23'} + h_Q^{13} h_Q^{23'}) \right] \\
&= \frac{A\beta_3}{\sqrt{2}}
\end{aligned} \tag{4.108}$$

where

$$\begin{aligned}
\beta_3 &= |h^{11}|^2 + |h^{21}|^2 + |h^{12}|^2 + |h^{22}|^2 + |h^{13}|^2 + |h^{23}|^2 + 2(h_I^{11} h_I^{21'} + h_Q^{11} h_Q^{21'}) + \\
&\quad 2(h_I^{12} h_I^{22'} + h_Q^{12} h_Q^{22'}) + 2(h_I^{13} h_I^{23'} + h_Q^{13} h_Q^{23'}).
\end{aligned} \tag{4.109}$$

The variance of ζ_k is only due to the variance of real part of the noise components $H^{1*} N_k^1$, $H^{2*} N_k^2$ and $H^{3*} N_k^3$ [15, 16]. Noise components at all the receiving antennas N_k^1 , N_k^2 and N_k^3 are IID complex Gaussian random variables. Thus, the variance of their sum is the sum of their individual variances and is represented as

$$\sigma_{\zeta_k}^2 = \sigma_{\zeta_k^1}^2 + \sigma_{\zeta_k^2}^2 + \sigma_{\zeta_k^3}^2. \tag{4.110}$$

Following the results derived in previous section from Equation (4.74) to (4.80), $\sigma_{\zeta_k}^2$ can be written as

$$\begin{aligned}
\sigma_{\zeta_k}^2 &= \frac{1}{2} \left(|H^1|^2 \text{E} \{ N_k^1 N_k^{1*} \} + |H^2|^2 \text{E} \{ N_k^2 N_k^{2*} \} + |H^3|^2 \text{E} \{ N_k^3 N_k^{3*} \} \right) \\
&= \frac{N_0}{4T_b} \left[|h^{11}|^2 + |h^{21}|^2 + 2(h_I^{11} h_I^{21'} + h_Q^{11} h_Q^{21'}) + |h^{12}|^2 + |h^{22}|^2 + \right. \\
&\quad \left. 2(h_I^{12} h_I^{22'} + h_Q^{12} h_Q^{22'}) + |h^{13}|^2 + |h^{23}|^2 + 2(h_I^{13} h_I^{23'} + h_Q^{13} h_Q^{23'}) \right].
\end{aligned} \tag{4.111}$$

Substituting Equation (4.109) into Equation (4.111) yields

$$\begin{aligned}
\sigma_{\zeta_k}^2 &= \frac{N_0 \beta_3}{4T_b} \\
\sigma_{\zeta_k} &= \sqrt{\frac{N_0 \beta_3}{4T_b}}.
\end{aligned} \tag{4.112}$$

Now, substituting Equation (4.108) and (4.112) into Equation (4.3), the conditional bit error probability is written as

$$\begin{aligned} P_b(\beta_3) &= Q\left(\frac{A\beta_3/\sqrt{2}}{\sqrt{\beta_3 N_o/4T_b}}\right) \\ &= Q\left(\sqrt{\frac{2E_b\beta_3}{N_o}}\right) \end{aligned} \quad (4.113)$$

Equation (4.113) shows the bit error probability of the MDDM MIMO system with two transmit antennas and three receive antennas conditioned on the random variable β_3 . The performance of the MDDM MIMO system over a frequency nonselective, slowly fading Rayleigh channel with MRC can be obtained by taking the average of the conditional bit error probability over all possible values of random variable β_3 . Now, unconditional bit error probability can be represented as

$$\begin{aligned} P_b &= \int_0^{\infty} P_b(\beta_3) f_{B_3}(\beta_3) d\beta_3 \\ &= \int_0^{\infty} Q\left(\sqrt{2E_b\beta_3/N_o}\right) f_{B_3}(\beta_3) d\beta_3 \end{aligned} \quad (4.114)$$

where $f_{B_3}(\beta_3)$ is the probability density function for β_3 .

The random variable β_3 as defined in Equation (4.109) is also a sum of central chi squared random variables of degree two and products of Gaussian random variables. The central chi squared random variables and the Gaussian random variables are also correlated. The probability density function of the random variable β_3 and integral of Equation (4.99) were computed numerically, using the same algorithm as discussed in previous section.

The simulated and the numerically computed theoretical results of the MIMO system (with 2 transmit antennas and 3 receive antennas) over a frequency nonselective slowly fading Rayleigh channel are shown in Figure 23. For comparison of the performances, this figure also includes the theoretical and the simulated bit error probability for a BPSK SISO system. This figure shows that for low E_b/N_o values the theoretical results are more optimistic and for high E_b/N_o values, the simulation results

are more optimistic. This deviation of simulation results from the theoretical results may also be due to the reasons as discussed in previous sections. Further analysis can be carried out to investigate the exact causes of this trend as a future work; this was not investigated further in this work.

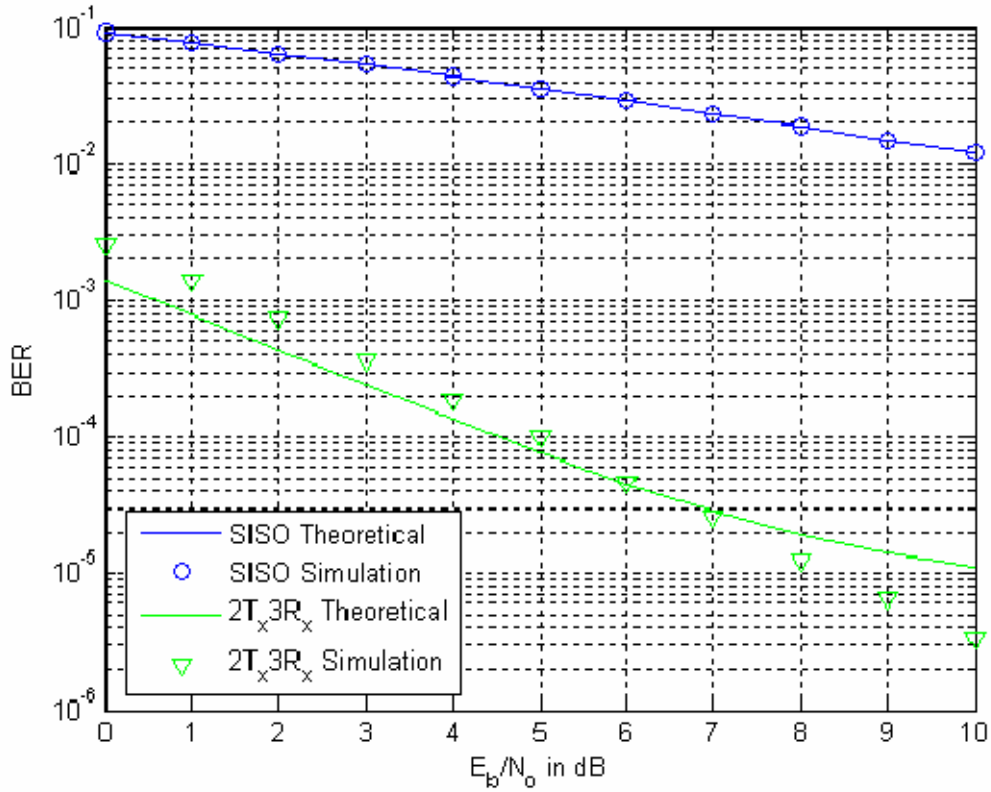


Figure 23 Results of MDDM MIMO System in Slow Rayleigh Fading Channel

E. SUMMARY

In this chapter, the MDDM MISO and MIMO systems as discussed in Chapter III were examined with the AWGN channel with and without slow Rayleigh fading. These systems were simulated in Matlab and the theoretical results were shown in comparison with the simulated results. The simulated results follow the theoretical results closely. In the next chapter the results of the thesis are summarized and areas for follow on work are presented.

V. CONCLUSION

The goal of this thesis was to design and analyze a MIMO system with multicarrier delay diversity modulation. MDDM was incorporated with orthogonal frequency division multiplexing and cyclic delay diversity. A MISO system and MIMO systems were designed using the MDDM. They were simulated in Matlab with BPSK and were tested in a progressive manner, first in an AWGN channel and then in a multipath fading channel with AWGN. The BER performance of these systems was analyzed and compared with the performance of the simulated systems. The simulated performance results and theoretical analysis results were compared with the conventional SISO system performance.

A. RESULTS

The simulated MDDM MISO and MIMO systems achieved BER performance results consistent with the theoretical analysis in an AWGN channel with and without multipath fading. The performance metric of bit error probability versus E_b / N_o (energy per bit to noise power spectral density ratio) was used. To establish a fair comparison, the transmitted power and data rate for SISO, MISO and MIMO systems were equal. The comparison of performances in AWGN showed that the MDDM MISO system performed better than the SISO system for low E_b / N_o with up to a 6.5 dB performance gain and performed worse for higher E_b / N_o values. The performances of the MDDM MIMO systems were better than that of SISO system for all values of E_b / N_o . MIMO systems with two receive antennas and three receive antennas, outperformed a SISO system by 1.7 dB and 3.4 dB performance gain. In a multipath fading channel with AWGN, MISO and MIMO systems were able to achieve significant advantage over a SISO system. The improvement in performances of the MDDM MISO and MIMO systems over the SISO system can be exploited for military and civilian applications.

B. RECOMMENDATION FOR FUTURE RESEARCH

There are four areas identified for future research. First, the MDDM MIMO system performance can be analyzed in different fading conditions as described by another fading model in place of the slow frequency nonselective Rayleigh fading

channel. Good choices for alternate fading models include slow Ricean frequency nonselective fading, slow Nakagami frequency nonselective fading, and various forms of frequency selective fading.

In addition to the analysis performed in this thesis, higher order modulation schemes in lieu of BPSK, i.e., M PSK and M QAM, can be incorporated and analyzed to evaluate the performance of the MDDM MIMO systems.

Next, forward error correction (FEC) coding with interleaving can be incorporated into the MDDM MIMO system with a maximum likelihood sequence estimation receiver. The performance can be analyzed theoretically and compared with simulated performance.

Lastly, the MIMO system analysis herein assumes perfect CSI at the receiver. If this information about the channel can be extracted at the receiver, then it can be sent to the transmitter. The transmitter can use CSI to more efficiently transmit power to the receiver through channels that are less faded than others. Techniques that control the transmitter can be investigated and performance of the system analyzed.

APPENDIX MATLAB CODES

This appendix includes the Matlab code for simulating the MDDM scheme in an AWGN channel with and without frequency nonselective Rayleigh fading. This also includes the theoretically computed results for the BER performance of the MDDM.

A. SIMULATION OF THE MDDM IN AN AWGN CHANNEL

```
%***** MDDM Simulation with AWGN only *****

clear all
num_frame = 100000;
fftsize = 256;           % Number of subcarriers
data_size = 192;         % Data symbol in an OFDM frame
t_data = data_size*num_frame; % Total number of data for the simulation
hfc = 27;                % high frequency carriers
lfc = 28;                % low frequency carriers
pilot=ones(1,8);         % All pilot sybmols set to ones
dc_comp = 0;             % DC component not transmitted

for n=1:fftsize
    p_shift(n,1)=exp(i*2*pi*(n-1)/fftsize); % Phase shift due to cyclic delay
end                                           % afer fft operation

EbNo_dB=0:12;
for nn=1:length(EbNo_dB)
    SNR=EbNo_dB(nn)+ 3; % converting SNR to EbNo
    t_err_SISO=0; t_err_2T1R=0; t_err_2T2R=0; t_err_2T3R=0;
    BER=0; totalerr=0;
    %***** Simulating input data and BPSK modulation *****
    for mm =1:num_frame
        r = rand(1,data_size);
        for m=1:data_size
            if r(1,m)< 0.5
                info(1,m)=0; symbol(1,m)=1;
            else
                info(1,m)=1; symbol(1,m)=-1;
            end
        end
    end
    %***** Creating OFDM Block *****
    Pre_IFFT_blk=[ dc_comp  pilot symbol(1:92)  zeros(1,(hfc+lfc))  symbol(93:data_size)];
```

```

%***** Simulating Trnasmitted signal*****
txsig1 = ifft((Pre_IFFT_blk).'); % taking IFFT after S/P coversion
txsig2 = circshift(txsig1,1); % adding Cyclic Delay Diversity
Tx_signal = 1/sqrt(2)*(txsig1+txsig2);
%***** Simulating Receivs *****
Rx_sig = awgn(symbol,SNR,'measured'); % Received signal for SISO BPSK
Rx_sig_1 = awgn(Tx_signal,SNR,'measured'); % Received signal by Ant. 1
Rx_sig_2 = awgn(Tx_signal,SNR,'measured'); % Received signal by Ant. 2
Rx_sig_3 = awgn(Tx_signal,SNR,'measured'); % Received signal by Ant. 3
Rx_2T1R = fft(Rx_sig_1); % 2 Tx 1 Rx Antennas
Rx_2T2R = fft(Rx_sig_1+Rx_sig_2); % 2 Tx 2 Rx Antennas
Rx_2T3R = fft(Rx_sig_1+Rx_sig_2+Rx_sig_3); % 2 Tx 3 Rx Antennas
Rx_data_2T1R =(Rx_2T1R.*(1+p_shift));
Rx_data_2T2R =(Rx_2T2R.*(1+p_shift));
Rx_data_2T3R =(Rx_2T3R.*(1+p_shift));
Rx_data_2T1R =(Rx_data_2T1R).'; % converting P/S
Rx_data_2T2R =(Rx_data_2T2R).';
Rx_data_2T3R =(Rx_data_2T3R).';
% Extracing received data from ofdm block
Rx_info_2T1R = [Rx_data_2T1R(10:101) Rx_data_2T1R(157:fftsize)];
Rx_info_2T2R = [Rx_data_2T2R(10:101) Rx_data_2T2R(157:fftsize)];
Rx_info_2T3R = [Rx_data_2T3R(10:101) Rx_data_2T3R(157:fftsize)];
%***** Demodulating BPSK signal *****
for k=1:data_size
    if real(Rx_sig(1,k)) > 0 % demodulating SISO info
        R_info(1,k)=0;
    else R_info(1,k)=1;
    end
    if real(Rx_info_2T1R(1,k)) > 0 % demodulating 2T1R info
        R_info_2T1R(1,k)=0;
    else R_info_2T1R(1,k)=1;
    end
    if real(Rx_info_2T2R(1,k)) > 0 % demodulating 2T2R info
        R_info_2T2R(1,k)=0;
    else R_info_2T2R(1,k)=1;
    end
    if real(Rx_info_2T3R(1,k)) > 0 % demodulating 2T3R info

```

```

        R_info_2T3R(1,k)=0;
    else R_info_2T3R(1,k)=1;
    end
end
end
%***** Probability of bit error Pb *****
err_SISO = length(find(info-R_info));    % calculating errors
err_2T1R = length(find(info-R_info_2T1R));
err_2T2R = length(find(info-R_info_2T2R));
err_2T3R = length(find(info-R_info_2T3R));
t_err_SISO = t_err_SISO+err_SISO; % Calculating total errors
t_err_2T1R = t_err_2T1R+err_2T1R;
t_err_2T2R = t_err_2T2R+err_2T2R;
t_err_2T3R = t_err_2T3R+err_2T3R;
end
Pb_SISO(nn) = t_err_SISO/t_data; %calculating BER
Pb_2T1R(nn) = t_err_2T1R/t_data;
Pb_2T2R(nn) = t_err_2T2R/t_data;
Pb_2T3R(nn) = t_err_2T3R/t_data;
end
save MDDM_AWGN_R EbNo_dB Pb_SISO Pb_2T1R Pb_2T2R Pb_2T3R
load Theo_AWGN_R
figure
semilogy(EbNo_dB,Pb_SISO_T,'k',EbNo_dB, Pb_2T1R_T,'r',EbNo_dB, Pb_2T2R_T,...
    'b',EbNo_dB, Pb_2T3R_T,'g',EbNo_dB,Pb_SISO,'ko', EbNo_dB,Pb_2T1R,'rv',...
    EbNo_dB,Pb_2T2R,'b*',EbNo_dB,Pb_2T3R,'gd')
grid on
xlabel('E_b/N_o in dB')
ylabel('P_b')
legend('SISO_T','2T1R_T','2T2R_T','2T3R_T',...
    'SISO_S','2T1R_S','2T2R_S','2T3R_S')
title('Comparison of Theoretical and Simulated Results')

```

B. COMPUTING THEORETICAL BER OF THE MDDM IN AN AWGN CHANNEL

```

%***** Theoretical BER in AWGN Channel *****
clear all
phase = linspace(0,2*pi*255/256,256);
phi = [phase(10:101) phase(157:256)];

```

```

comp = (1+cos(phi));
EbNo_dB=0:12;
EbNo=10.^(EbNo_dB/10);
for n = 1:length(EbNo)
    temp = EbNo(n);
    for k=1:length(phi)
        Q2T1R(k,n) = 0.5*erfc(sqrt(2*temp*comp(k)));
        Q2T2R(k,n) = 0.5*erfc(sqrt(4*temp*comp(k)));
        Q2T3R(k,n) = 0.5*erfc(sqrt(6*temp*comp(k)));
    end
end
%***** Theoretical BPSK *****
Pb_SISO_T=0.5*erfc(sqrt(EbNo));
Pb_2T1R_T = 1/length(phi)*sum(Q2T1R);
Pb_2T2R_T = 1/length(phi)*sum(Q2T2R);
Pb_2T3R_T = 1/length(phi)*sum(Q2T3R);
save Theo_AWGN_R EbNo_dB Pb_SISO_T Pb_2T1R_T Pb_2T2R_T Pb_2T3R_T
load MDDM_AWGN_R
figure
semilogy(EbNo_dB,Pb_SISO_T,'k',EbNo_dB, Pb_2T1R_T,'r',EbNo_dB,...
Pb_2T2R_T,'b',EbNo_dB, Pb_2T3R_T,'g',EbNo_dB,Pb_SISO,'ko',...
EbNo_dB,Pb_2T1R,'rv', EbNo_dB,Pb_2T2R,'b*',EbNo_dB,Pb_2T3R,'gd')
grid on
xlabel('E_b/N_o in dB')
ylabel('P_b')
legend('SISO_T','2T1R_T','2T2R_T','2T3R_T','SISO_S','2T1R_S','2T2R_S','2T3R_S')
title('Copmarison of Theoretical and Simulated Resulsts')

```

C. SIMULATION OF THE MDDM IN FREQUENCY NONSELECTIVE SLOW FADING RAYLEIGH CHANNEL

```

%* Simulation of MDDM MISO and MIMO Systems in Frequency Nonselective Slow
% Fading Rayleigh Channel
% RAYLEIGH FADING CHANNEL
clear all
num_frame=100000;
fftsize=256; % Number of subcarriers
data_size=192; % Data symbol in one frame
t_data = data_size*num_frame; % Total number of data for the simulation

```

```

hfc = 27;           % high frequency carriers
lfc = 28;           % low frequency carriers
pilot=ones(1,8);    % All pilot sybmols set to ones
dc_comp = 0;        % DC component not transmitted
for n=1:fftsize
    p_shift(n,1)=exp(-i*2*pi*(n-1)/fftsize); % Phase shift due to cyclic delay
end                % afer fft operation
EbNo_dB=0:10;
for nn=1:length(EbNo_dB)
    SNR=EbNo_dB(nn)+3;
    t_err_SISO_F=0;   t_err_2T1R_F=0;   t_err_2T2R_F=0;   t_err_2T3R_F=0;
    BER=0;   totalerr=0;
    %***** Simulating input data and BPSK modulation *****
    for mm =1:num_frame
        r=rand(1,data_size);
        for m=1:data_size
            if r(1,m)< 0.5
                info(1,m)=0;   symbol(1,m)=1;
            else
                info(1,m)=1;   symbol(1,m)=-1;
            end
        end
    end
    %***** Creating OFDM Block *****
    Pre_IFFT_blk=[ dc_comp   pilot symbol(1:92) zeros(1,(hfc+lfc))...
        symbol(93:data_size)];
    %***** Simulating Trnasmit signal*****
    txsig1= 1/sqrt(2)*ifft((Pre_IFFT_blk).'); % taking IFFT after S/P coversion
    txsig2=circshift(txsig1,1);
    %***** Simulating Received signal%%%%%%%%%%%%
    % Frequency Responses of Channels
    h=1/sqrt(2)*(randn(1,data_size)+j*randn(1,data_size)); % SISO system channel
    h_11=1/sqrt(2)*(randn(1)+j*randn(1)); % Tx Ant. 1 to Rx Ant. 1
    h_21=1/sqrt(2)*(randn(1)+j*randn(1)); %Freq. Response of Chan. T.A.2 to R.A.1
    h_12=1/sqrt(2)*(randn(1)+j*randn(1)); %Freq. Response of Chan. T.A.1 to R.A.2
    h_22=1/sqrt(2)*(randn(1)+j*randn(1)); %Freq. Response of Chan. T.A.2 to R.A.2
    h_13=1/sqrt(2)*(randn(1)+j*randn(1)); %Freq. Response of Chan. T.A.1 to R.A.3
    h_23=1/sqrt(2)*(randn(1)+j*randn(1)); %Freq. Response of Chan. T.A.2 to R.A.3

```

```

H_1=h_11+h_21*p_shift; % Composite channel response at R.A. 1
H_2=h_12+h_22*p_shift; % Composite channel response at R.A. 2
H_3=h_13+h_23*p_shift; % Composite channel response at R.A. 3
%***** Simulating Receivers *****
Rx_sig = awgn(symbol.*h,SNR,'measured'); % Received signal for SISO BPSK
Rx_sig_1=awgn((txsig1*h_11+txsig2*h_21),SNR,'measured');
% simulating Ant.# 1 received signal with rayleigh flat fading channel
Rx_sig_2=awgn((txsig1*h_12+txsig2*h_22),SNR,'measured');
% simulating Ant.# 2 received signal with rayleigh flat fading channel
Rx_sig_3=awgn((txsig1*h_13+txsig2*h_23),SNR,'measured');
% simulating Ant.# 2 received signal with rayleigh flat fading channel
fft_sig_1=fft(Rx_sig_1);
fft_sig_2=fft(Rx_sig_2);
fft_sig_3=fft(Rx_sig_3);
%Simulating MRC Receiver
Vk_SISO=Rx_sig.*conj(h); %SISO system reception with CSI
Vk_1=fft_sig_1.*conj(H_1); %Antenna 1 diversity reception
Vk_2=fft_sig_2.*conj(H_2); %Antenna 2 diversity reception
Vk_3=fft_sig_3.*conj(H_3); %Antenna 3 diversity reception
% Combining all space diversity receptions
Zk_2T1R=real((Vk_1).'); %Decision variable of MISO (2T1R) and P/S conversion
Zk_2T2R=real((Vk_1+Vk_2).'); %Decision variable of MIMO (2T2R) and P/S conversion
Zk_2T3R=real((Vk_1+Vk_2+Vk_3).'); %Decision variable of MIMO (2T3R) and P/S conversion
% Extracing real part of decision variable from ofdm block
Rx_info_2T1R_F = [Zk_2T1R(10:101) Zk_2T1R(157:fftsize)];
Rx_info_2T2R_F = [Zk_2T2R(10:101) Zk_2T2R(157:fftsize)];
Rx_info_2T3R_F = [Zk_2T3R(10:101) Zk_2T3R(157:fftsize)];
Rx_info_SISO_F=real(Vk_SISO); %BPSK SISO System received data
%***** Demodulating BPSK signal *****
for k=1:data_size
    if Rx_info_SISO_F(1,k) > 0 % demodulating SISO info
        R_info_SISO_F(1,k)=0;
    else R_info_SISO_F(1,k)=1;
    end
    if Rx_info_2T1R_F(1,k) > 0 % demodulating 2T1R info
        R_info_2T1R_F(1,k)=0;
    else R_info_2T1R_F(1,k)=1;

```

```

end
if Rx_info_2T2R_F(1,k) > 0    % demodulating 2T2R info
    R_info_2T2R_F(1,k)=0;
else R_info_2T2R_F(1,k)=1;
end
if Rx_info_2T3R_F(1,k) > 0    % demodulating 2T3R info
    R_info_2T3R_F(1,k)=0;
else R_info_2T3R_F(1,k)=1;
end
end
%%***** Probability of bit error Pb *****
err_SISO_F = length(find(info-R_info_SISO_F));    % calculating errors
err_2T1R_F = length(find(info-R_info_2T1R_F));
err_2T2R_F = length(find(info-R_info_2T2R_F));
err_2T3R_F = length(find(info-R_info_2T3R_F));
t_err_SISO_F = t_err_SISO_F+err_SISO_F;    % Calculating total errors
t_err_2T1R_F = t_err_2T1R_F+err_2T1R_F;
t_err_2T2R_F = t_err_2T2R_F+err_2T2R_F;
t_err_2T3R_F = t_err_2T3R_F+err_2T3R_F;
end
Pb_SISO_F(nn) = t_err_SISO_F/t_data;    %calculating BER
Pb_2T1R_F(nn) = t_err_2T1R_F/t_data;
Pb_2T2R_F(nn) = t_err_2T2R_F/t_data;
Pb_2T3R_F(nn) = t_err_2T3R_F/t_data;
end
save MDDM_SRF_R EbNo_dB Pb_SISO_F Pb_2T1R_F Pb_2T2R_F Pb_2T3R_F
load Theo_SRF_R
figure
semilogy(EbNo_dB,Pb_SISO_F_T,'k',EbNo_dB, Pb_2T1R_F_T,'r',EbNo_dB,...
    Pb_2T2R_F_T,'b',EbNo_dB, Pb_2T3R_F_T,'g',EbNo_dB,Pb_SISO_F,'ko',...
    EbNo_dB,Pb_2T1R_F,'rv', EbNo_dB,Pb_2T2R_F,'b*',EbNo_dB,Pb_2T3R_F,'gd')
grid on
xlabel('E_b/N_o in dB')
ylabel('P_b')
legend('SISO_T','2T1R_T','2T2R_T','2T3R_T','SISO_S','2T1R_S','2T2R_S','2T3R_S')
title('Copmarison of Theoretical and Simulated Resulsts')

```


D. COMPUTING THEORETICAL BER OF THE MDDM IN FREQUENCY NONSELECTIVE SLOW FADING RAYLEIGH CHANNEL

% Calculating Theoretical Results By Numerical Methods

global W X N

EbNo_dB = 0:10;

EbNo = 10.^(EbNo_dB/10);

% creating independent channel responses

h_11=1/sqrt(2)*(randn(1,10^6)+j*randn(1,10^6)); % Tx Ant. 1 to Rx Ant.1

h_21=1/sqrt(2)*(randn(1,10^6)+j*randn(1,10^6)); % T.A.2 to R.A.1

h_12=1/sqrt(2)*(randn(1,10^6)+j*randn(1,10^6)); % T.A.1 to R.A.2

h_22=1/sqrt(2)*(randn(1,10^6)+j*randn(1,10^6)); % T.A.2 to R.A.2

h_13=1/sqrt(2)*(randn(1,10^6)+j*randn(1,10^6)); % T.A.1 to R.A.3

h_23=1/sqrt(2)*(randn(1,10^6)+j*randn(1,10^6)); % T.A.2 to R.A.3

H_1=h_11+h_21; %*p_shift; % Effective channel response at R.A. 1

H_2=h_12+h_22; %*p_shift; % Effective channel response at R.A. 2

H_3=h_13+h_23; %*p_shift; % Effective channel response at R.A. 3

% creating random variables Beta

Beta_1=((H_1).*conj(H_1));

Beta_2=((H_1).*conj(H_1))+((H_2).*conj(H_2));

Beta_3=((H_1).*conj(H_1))+((H_2).*conj(H_2))+((H_3).*conj(H_3));

[N1 X1]=hist(Beta_1,500);

[N2 X2]=hist(Beta_2,500);

[N3 X3]=hist(Beta_3,500);

% Theoretical BER for SISO

x = sqrt(2*EbNo./(1+2*EbNo));

Pb_SISO_F_T = 0.5*(1-x);

% Estimating PDF Beta_1 and Calculating Theoretical BER for 2T1R

X=X1; N=N1;

W=quad(@Func_Est_Cur,min(X1),max(X1)); % Normalizing factor for PDF

Pr_Beta_1 = quad(@Func_pdf_Beta,min(X1), max(X1))

dBeta_1=(min(X1):0.0001:max(X1));

for i=1:length(EbNo)

Q_2Beta_1 = 0.5*erfc(sqrt(2*EbNo(i)*dBeta_1));

Pb_2T1R_F_T(i) = sum(Q_2Beta_1.*abs(Func_pdf_Beta(dBeta_1)))*0.0001;

end

% Estimating PDF Beta_2 and Calculating Theoretical BER for 2T2R

X=X2; N=N2;

```

W=quad(@Func_Est_Cur,min(X2),max(X2)); % Normalizing factor for PDF
Pr_Beta_2 = quad(@Func_pdf_Beta,min(X2), max(X2))
dBeta_2=(0:0.0001:max(X2));
for i=1:length(EbNo)
    Q_2Beta_2 = 0.5*erfc(sqrt(2*EbNo(i)*dBeta_2));
    Pb_2T2R_F_T(i) = sum(Q_2Beta_2.*abs(Func_pdf_Beta(dBeta_2)))*0.0001;
end
% Estimating PDF Beta_3 and Calculating Theoretical BER for 2T3R
X=X3; N=N3;
W=quad(@Func_Est_Cur,min(X3),max(X3)); % Normalizing factor for PDF
Pr_Beta_3 = quad(@Func_pdf_Beta,min(X3), max(X3))
dBeta_3=(0:0.0001:max(X3));
for i=1:length(EbNo)
    Q_2Beta_3 = 0.5*erfc(sqrt(2*EbNo(i)*dBeta_3));
    Pb_2T3R_F_T(i) = sum(Q_2Beta_3.*abs(Func_pdf_Beta(dBeta_3)))*0.0001;
end
save Theo_SRF_R EbNo_dB Pb_SISO_F_T Pb_2T1R_F_T Pb_2T2R_F_T Pb_2T3R_F_T
load MDDM_SRF_R
figure
semilogy(EbNo_dB,Pb_SISO_F_T,'k',EbNo_dB, Pb_2T1R_F_T,'r',EbNo_dB, ...
    Pb_2T2R_F_T,'b',EbNo_dB, Pb_2T3R_F_T,'g',EbNo_dB,Pb_SISO_F,'ko',...
    EbNo_dB,Pb_2T1R_F,'rv', EbNo_dB,Pb_2T2R_F,'b*',EbNo_dB,Pb_2T3R_F,'gd')
grid on
xlabel('E_b/N_o in dB')
ylabel('P_b')
legend('SISO_T','2T1R_T','2T2R_T','2T3R_T','SISO_S','2T1R_S','2T2R_S','2T3R_S')
title('Comparison of Theoretical and Simulated Results')

```

E. FUNCTIONS TO INTERPOLATE PROBABILITY DISTRIBUTION FUNCTIONS

```

function y = Func_Est_Cur(x);

%Title    : Estimation of Data Distribution of Random Variable Beeta
%Author   : Muhammad Shahid, Naval Post Graduate School, September 2005
%-----
% y = Func_Est_Cur(x)
%-----
%Input    : Random variabel Beeta
%Output   : Estimated Data Distribution of Beeta

```

```

%-----
global W X N
y=spline(X,N,x);
    function PDF = Func_pdf_Beta(b_2);
%Title    : Interpolation of PDF of Random Variable Beeta
%Author   : Muhammad Shahid, Naval Post Graduate School, September 2005
%-----
% PDF = Func_pdf_Beta(b_2);
%-----
%Input    : Random variabel Beeta
%Output   : PDF of Beeta
%-----
global W X N
PDF=spline(X,N,b_2)/W;

```

LIST OF REFERENCES

- [1] Branka Vucetic and Jinhong Yuan, “*Space-Time Coding.*” John Wiley & Sons, West Sussex, England, 2003.
- [2] Jun Tan, Gordon L. Stuber, “Multicarrier Delay Diversity Modulation for OFDM Systems.” IEEE Transactions on Wireless Communications, Vol. 3, No. 5, September 2004. pp. 1756-1763.
- [3] A. Wittneben, “A new bandwidth efficient transmit antenna modulation diversity scheme for linear digital modulation.” in Proc. IEEE Int. Conf. Communications, 1993, pp. 1630-1634.
- [4] N. Seshadri and J. H. Winters, “Two signaling schemes for improving the error performance of frequency-division-duplex (FDD) transmission systems using transmitter antenna diversity.” Int J. Wireless Inform. Networks, vol. 1, No. 1, pp. 24-47, January 1994.
- [5] S. Kaiser, “Spatial transmit diversity techniques for broadband OFDM systems.” in Proc. IEEE GLOBECOM, San Francisco, California, November 2000, pp. 1824-1828.
- [6] A. Dammann and S. Kaiser, “Standard conformable antenna diversity techniques for OFDM and its application to the DVB-T system.” in Proc. IEEE GLOBECOM, San Antonio, Texas, November 2001, pp. 3100-3105.
- [7] A. Paulraj, R. Nabar and D. Gore, “Introduction to Space Time Wireless Communications.” Cambridge University Press, Cambridge, United Kingdom, 2003.
- [8] Michael J. Turpin, “An Investigation of a Multiple-Input Multiple-Output Communication System with the Alamouti Space-Time Code.” Master’s Thesis, Naval Postgraduate School, Monterey, California, June 2004.

- [9] Erwin Kreyszig, "Advanced Engineering Mathematics, Fourth Edition." John Wiley & Sons, New York, 1979.
- [10] Bernard Sklar, "Digital Communications Fundamentals and Applications." Second Edition, Prentice Hall, Upper Saddle River, New Jersey, 2002.
- [11] Meixia Tao and Toger S. Cheng, "Spade Code Design in Delay Diversity Transmission for PSK modulation." Vehicular Technology Conference, 2002. Proceedings. IEEE 56th Volume 1, 24-28 Sept. 2002, pp. 444-448, vol. 1.
- [12] Gerhaud Bauch and Javed Shamim Malik, "Orthogonal Frequency Division Multiple Access with Cyclic Delay Diversity." ITG Workshop on Smart Antennas, 2004, pp. 17-24.
- [13] Roberto Cristi, "Modern Digital Signal Processing." Brooks/Cole-Thomson Learning, Pacific Grove, California USA, 2004.
- [14] Patrick A. Count, "Performance Analysis of OFDM in Frequency Selective, Slowly Fading Nakagami Channel." Master's Thesis, Naval Postgraduate School, Monterey, California, June 2001.
- [15] Clark Robertson, "EC4550 Digital Communications Systems Lecture Notes." Naval Postgraduate School, Monterey, California 2004 (unpublished).
- [16] John G. Proakis, "Digital Communications." Fourth Edition, McGraw Hill, New York, 2001.
- [17] Theodore S. Rappaport, "Wireless Communications Principles and Practice." Second Edition, Prentice Hall PTR, Upper Saddle River, New Jersey, 2002.
- [18] Charles W. Therrien, Murali Tummala, "Probability for Electrical and Computer Engineers." CRC Press, Washington, D.C. 2004.
- [19] Peyton Z. Peebles Jr., "Probability, Random Variables and Random Signal Principles." Fourth Edition, McGraw-Hill, New York, 2001.

- [20] Halil Derya Saglam, "Simulation Performance of Multiple-input Multiple-output System Employing Single-carrier Modulation and Orthogonal Frequency Division Multiplexing." Master's Thesis, Naval Postgraduate School, Monterey, California, December 2004.
- [21] Matlab Helpfile, The Math Works, Inc., Version 7.0.4.365 (R14) Service Pack 2, Natick, Massachusetts, 29 January 2005.
- [22] Fredrik Kristensen, Peter Nilson and Anders Olsson, "A Generic Transmitter for Wireless OFDM Transmitter." The 14th IEEE 2003 International Symposium on Personal, Indoor and Mobile Radio Communication Proceedings.
- [23] IEEE Std. 802.16-2001, IEEE Standard for Local and Metropolitan area networks Part 16: Air Interface for Fixed Broadband Wireless Access Systems.

THIS PAGE INTENTIONALLY LEFT BLANK

INITIAL DISTRIBUTION LIST

1. Defense Technical Information Center
Ft. Belvoir, Virginia
2. Dudley Knox Library
Naval Postgraduate School
Monterey, California
3. Chairman, Code EC
Electrical and Computer Engineering Department
Naval Postgraduate School
Monterey, California
4. Frank Kragh, Code EC/Kh
Electrical and Computer Engineering Department
Naval Postgraduate School
Monterey, California
5. Tri Ha, Code EC/Ha
Electrical and Computer Engineering Department
Naval Postgraduate School
Monterey, California
6. Clark Robertson, Code EC/Rc
Electrical and Computer Engineering Department
Naval Postgraduate School
Monterey, California
7. Muhammad Shahid
Pakistan Air Force